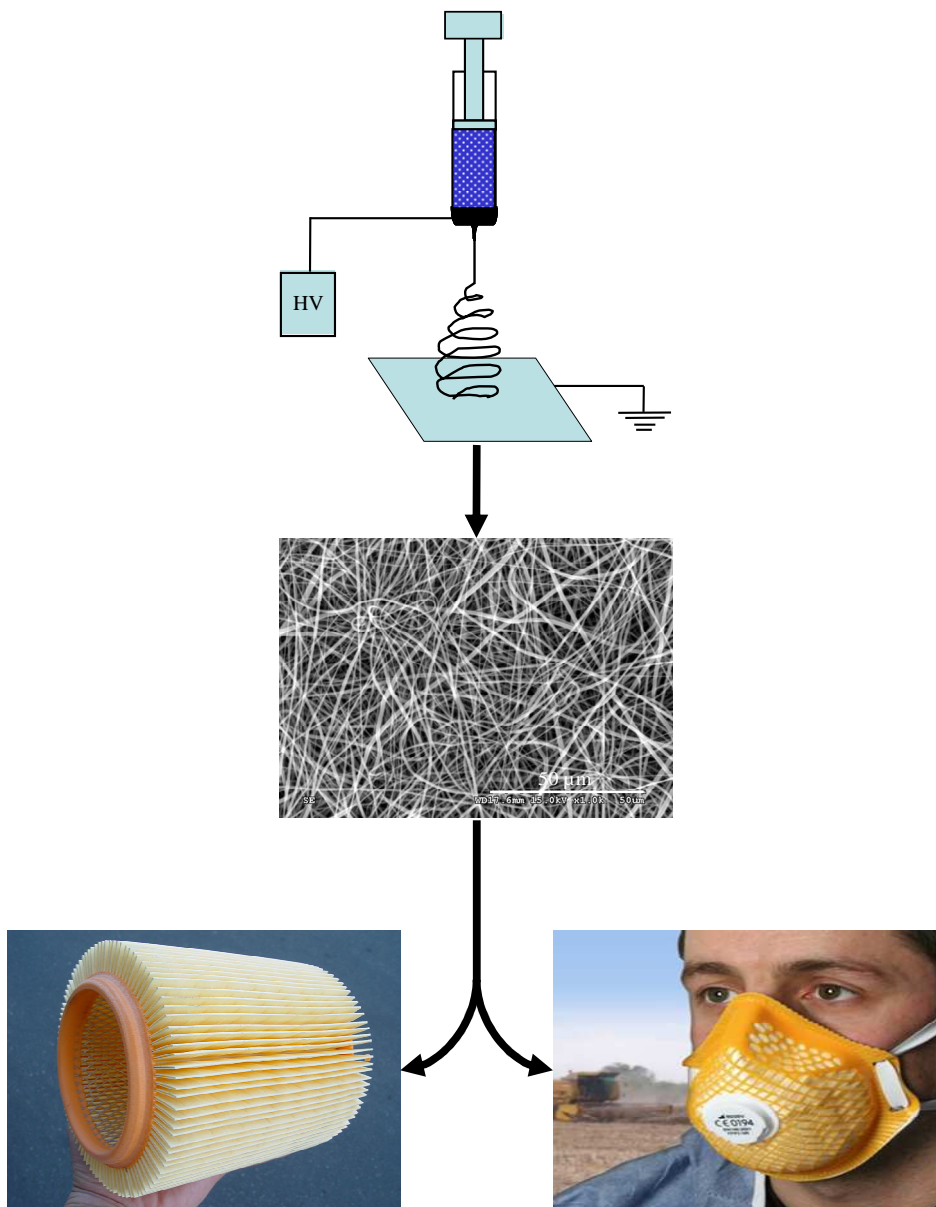


Melt Electrospinning of Thermoplastic Polymers

Ibrahim Hassounah



Melt Electrospinning of Thermoplastic Polymers

Von der Fakultät für Mathematik, Informatik und Naturwissenschaften
der RWTH Aachen University zur Erlangung des akademischen Grades eines
Doktors der Naturwissenschaften genehmigte Dissertation

vorgelegt von

M. Sc. Chemistry

Ibrahim Hassounah

aus Al-Lod, Palästina

Berichter: Universitätsprofessor Dr. rer. nat. Martin Möller
 Universitätsprofessor Dr. rer. nat. Alexander Böker

Tag der mündlichen Prüfung: 13. Februar 2012

Diese Dissertation ist auf den Internetseiten der Hochschulbibliothek online verfügbar.

“...You have to combine the elements that come out with those going on, so that each convex element, in the full light, is matched by the concave one, that is, a shadow; the luminous element must be accurate in detail because it is what stand out: the one in the shade can be without detail....”

Antonio Gaudí, 25.06.1852 – 10.06.1926

Architect

Acknowledgment

At the beginning, I am thanking Allah, the merciful god, who gave me the power, motivation and patience to do my PhD work and to perform this thesis. Without his help and his mercy, I would not be able to perform this work and to write this thesis.

I want to express my gratitude to my parents and my family, who encouraged and motivate me to improve my career through completion of my studies in PhD level.

I would like to thank Prof. Dr. Martin Möller, who gave me a great chance and the possibility to work in this thesis at DWI.

I am grateful to Dr. Helga Thomas for her strong scientific supervision and guiding me during my thesis research at DWI. As well as, her efforts to appear this thesis into the existence are gratefully acknowledged. This thesis would not have been possible unless her support.

I am sincerely and heartily grateful to Dr. Karola Schäfer, who supported me at the beginning of my thesis and who helped me to perform all documentary work at the registration office at RWTH-Aachen. Without her help, I would loss more time performing the documentary work. As well as, for her help in explaining me the thesis topic and the aim of the research work.

I am heartily thankful to Ph.D. Dirk Grafahrend for useful discussions in the field of melt electrospinning and for the training on melt electrospinning process. His efforts for supplying the ideas, suggestions and materials as well as for intensive correction of my thesis are also gratefully thankful. He is also acknowledged for his organizing of the work trip to Grenoble, where I got a great opportunity to learn new things and new technologies there.

I want also to express my gratitude to Prof. Dr. Crisian Popescu, Dr. Helmut Keul, Dr. Ahmed Mourran and Dr. Xiaomin Zhu for their useful discussions of my topic which give me motivation and a great chance to understand some ambiguous points in my thesis.

I would like also to thank Fuat Topuz, Karl-Heinz Heffels, Dr. Kristina Klinkhammer and Dr. Priya Garg for their great efforts in intensive corrections and criticizing of my thesis.

I am also grateful to Dr. Walter Tillmann for IR-analysis, Stephan Rütten and Dr. Kim-Hô Phan for SEM and ESEM analysis, Dr. Karin Peter and Markus Nobis for supplying me the accessories of Brabender twin extruder and DSM twin extruder and Wilfred Stephens for manufacturing of parts of melt electrospinning device and melt electrospinning lab scale machine.

I would like also to extent my gratitude to Philip Jungbecker and Christoph Hacker from ITA and Richard Rothe from IEM for their cooperation in this thesis work and for scaling up of the melt electrospinning process and for their design of the lab scale melt electrospinning machine.

For the friendly environment at DWI I would like to thank with a great pleasure Konstantina Dyankova, Smriti Singh, Dr. Heidrun Keul, Jörg Meyer, Michael Scharpf, Dr. Michael Erberich, Dr. Janis Lejnieks, Dr. Cristian Vaida, Metodi Bozukov, Nina Keusgen, Firat Özdemir, Dr. Alexandra Mendrek, Dr. Sebastian Mendrek, Dr. Yungchun He, Hailin Wang, Dr. Throsten Anders, Dr. Petra Mela, Dr. Irene Colicchio, Markus Kettel, Dr. Nikolay Belov, Dr. Sanja Perinović, Matthias Deschesne, Ramona Kloss, Qizheng Dou, Silwia Skudlarek, Marian Skudlarek, Zoltán Szekeres, Dr. Mohammed Salama, Dr. Ahmed Hassabo, Dr. Amina Mohammed, Mohammed Roman, Tsolomon Narangerel, Dora Alves, Silvia Meilhammer, Petra Esser, Dr. Susana Prieto, Dr. Josef Föhles, Dr. Miran Yu, Yasmin Yazici, Thomas Wormann, Nguyễn T.D. Thanh, Dr. Artur Henke, Marco Bakes, Kristina Bruellhoff, Dr. Julia Llexia Calvet, Nebia Greving, Juliana Kurniadi, Ramona Ronge, Dr. Dragos Popescu, Dr. Reza Najjar, Dr. Rostislav Vinokur, Artem Davidenko, Dr. Marga Lensen, Dr. Claudia Cesa and Jingbo Wang.

Last but not the least; I would like to acknowledge Expedition Exchange Inc. and Spaldings Ltd. for allowing me to use their pictures on the cover page of my thesis.

Finally, I offer my regards and blessings to all of those who supported me in any respect during the completion of my studies.

Table of content

| | |
|-----------------------------------------------------------------------------|----|
| Acknowledgment | 5 |
| Table of content..... | 7 |
| Symbols and abbreviations..... | 13 |
| List of Publications..... | 16 |
| Summary | 18 |
| Zusammenfassung..... | 19 |
| Chapter 1: Introduction to electrospinning..... | 20 |
| 1 Introduction | 20 |
| 2 References | 24 |
| Chapter 2: State of the art..... | 26 |
| 1 Electrospinning..... | 26 |
| 1.1 History..... | 26 |
| 1.2 Electrospinning process..... | 28 |
| 1.3 Developing of instabilities in electrospun polymer jets..... | 29 |
| 1.4 Solution electrospinning and melt electrospinning | 31 |
| 2 References | 33 |
| Chapter 3: Influence of melt viscosity on melt electrospinning process..... | 37 |

| | | |
|-------|----------------------------------------------------------------|----|
| 1 | Abstract | 37 |
| 2 | Introduction | 38 |
| 2.1 | Parameters affecting melt viscosity..... | 38 |
| 2.1.1 | Effect of molecular parameters | 39 |
| 2.1.2 | Effect of external parameters | 39 |
| 2.2 | Viscosity measurement | 40 |
| 2.3 | Control of melt viscosity | 41 |
| 3 | Experimental | 43 |
| 3.1 | Electrospinning..... | 43 |
| 3.2 | Materials..... | 45 |
| 3.2.1 | Isotactic polypropylene | 45 |
| 3.2.2 | Preparation of polypropylene blends..... | 45 |
| 3.2.3 | Additives | 45 |
| 3.3 | Characterization methods..... | 47 |
| 3.4 | Results and discussion..... | 47 |
| 3.4.1 | Influence of melt temperature | 47 |
| 3.4.2 | Influence of molecular weight..... | 49 |
| 3.4.3 | Polypropylene with bimodal molecular weight distribution | 50 |
| 3.4.4 | Influence of molecular structure | 52 |
| 3.4.5 | Effect of slipping agents..... | 54 |

| | | |
|-------------------------------------------------------------------------------------------------------------|------------------------------------------------------------------------|----|
| 3.4.5.1 | Influence of type of slipping agent..... | 54 |
| 3.4.5.2 | Effect of slipping agent concentration | 55 |
| 3.4.6 | Influence of viscosity breaking agents | 58 |
| 3.4.6.1 | Type of viscosity breaking agent | 58 |
| 3.4.6.2 | Effect of degradation time and amount of viscosity breaking agent..... | 60 |
| 4 | Summary | 62 |
| 5 | References | 63 |
| Chapter 4: The Influence of ambient and processing parameters on melt electrospinning of polypropylene..... | | |
| 65 | | |
| 1 | Abstract | 65 |
| 2 | Introduction | 66 |
| 2.1 | Influence of the heat gradient..... | 67 |
| 2.2 | Influence of the electric field strength..... | 67 |
| 2.3 | Influence of the flow rate | 69 |
| 2.4 | Effect of the distance between electrodes | 69 |
| 2.5 | Influence of the needle diameter | 70 |
| 2.6 | Influence of the spinning environment..... | 71 |
| 2.7 | Effect of the rotation speed | 71 |
| 3 | Experimental | 72 |
| 3.1 | Electrospinning..... | 72 |
| 3.2 | Materials..... | 74 |

| | |
|------------------------------------------------------------------------------------------|----|
| Table of content | 10 |
| <hr/> | |
| 3.2.1 Polypropylene..... | 74 |
| 3.2.2 Synthesis of sodium stearate and preparation of viscosity breaking agent..... | 74 |
| 3.2.3 Preparation of the samples | 74 |
| 3.3 Characterization methods..... | 74 |
| 3.4 Results and discussion..... | 75 |
| 3.4.1 Influence of spinneret design | 75 |
| 3.4.2 Effect of heat gradient | 77 |
| 3.4.3 Influence of electric field strength | 80 |
| 3.4.4 Influence of flow rate | 82 |
| 3.4.5 Influence of the distance between electrodes..... | 83 |
| 3.4.6 Influence of needle diameter | 84 |
| 3.4.7 Influence of polarity | 85 |
| 3.4.8 Influence of humidity | 88 |
| 3.4.9 Influence of rotation speed..... | 89 |
| 4 Summary | 91 |
| 5 References | 92 |
| Chapter 5: Nucleation and crystallization of melt electrospun polypropylene fibers | 94 |
| 1 Abstract | 94 |
| 2 Introduction | 95 |
| 2.1 Polypropylene degradation and polymer chain scission regulation..... | 96 |

| | |
|---------------------------------------------------------------|---------------------------------------------------------|
| Table of content | 11 |
| <hr/> | |
| 2.2 | Nucleation and crystallization in polypropylene..... 98 |
| 3 | Experimental 100 |
| 3.1 | Electrospinning..... 100 |
| 3.2 | Materials..... 101 |
| 3.2.1 | Polypropylene..... 101 |
| 3.2.2 | Nucleating agents 101 |
| 3.2.3 | Synthesis of sodium stearate 102 |
| 3.2.4 | Preparation of the samples 102 |
| 3.3 | Characterization methods..... 102 |
| 3.4 | Results and discussion..... 102 |
| 3.4.1 | Influence of nucleating agent 102 |
| 3.4.2 | Influence of nucleating agents concentration..... 106 |
| 3.4.3 | Influence of nucleating agent type 109 |
| 4 | Summary 112 |
| 5 | References 113 |
| Appendix: Work package with electrospinning machine 116 | |
| 1 | Introduction 116 |
| 2 | Experimental 118 |
| 2.1 | Electrospinning..... 118 |
| 2.2 | Materials and preparation of the sample 119 |

| | |
|-------------------------------------------------|-----|
| Table of content | 12 |
| <hr/> | |
| 2.3 Characterization methods | 119 |
| 3 Results and discussion..... | 119 |
| 3.1 Effect of electric field strength..... | 119 |
| 3.2 Effect of flow rate | 120 |
| 3.3 Effect of distance between electrodes | 124 |
| 4 Summary | 126 |
| Curriculum Vitae..... | 127 |

Symbols and abbreviations

| | |
|-----------|-------------------------------------------------------------------------|
| CRPP | Controlled rheology polypropylene |
| DSC | Dynamic scanning calorimetry |
| DWI | DWI at the RWTH Aachen University e.V. |
| EFS | Electric field strength |
| F (aero) | Aerodynamic force |
| F (elect) | Electrical force |
| F (grav) | Force of gravity |
| F (in) | Inertial force |
| F (rheo) | Rheological force |
| F (surf) | surface tension force |
| H | Distance between electrodes |
| HL 504 FB | Polypropylene of molecular weight 181000 g/mol purchased from Borealis. |
| HPN-68 L | Nucleating agent of norborane basis purchased from Milliken |
| h_t | Terminal diameter of the electrified polymer jet |
| IEM | Institut für elektrische Maschinen (Institute for electric machines) |
| i-PP | isotactic polypropylene |
| IR | Infrared spectrum |

| | |
|------------|-------------------------------------------------------------------------------------------------|
| ITA | Institut für Textiltechnik an der RWTH-Aachen (Institute for textile technology at RWTH-Aachen) |
| kV | Kilovolt |
| L | Length of the needle |
| L/D | Length to diameter ratio of a tube |
| LCPP | Long chain polypropylene |
| Mc, Me | Critical molecular weight between two entanglement points |
| MCHM 562 P | Polypropylene of unknown molecular weight purchased from Basell |
| MCHM 648 P | Polypropylene of molecular weight 186000 g/mol purchased from Basell |
| PAOS | Poly alkoxy silane |
| PDMS | Poly dimethylsiloxane |
| PP 12000 | Polypropylene of molecular weight 12000 g/mol |
| PP 190000 | Polypropylene of molecular weight 190000 g/mol |
| PP 250000 | Polypropylene of molecular weight 250000 g/mol |
| PP 340000 | Polypropylene of molecular weight 340000 g/mol |
| PP 580000 | Polypropylene of molecular weight 580000 g/mol |
| R | Radius of the needle |
| SCPP | Short chain polypropylene |
| SEM | Scanning electron microscopy |
| TEOS | Tetraethoxysilane |

| | |
|--------------------|--------------------------------------------------|
| UHTCs | Ultra high temperature ceramics |
| Viscosity breaking | Agents used to reduce the polymer melt viscosity |
| WAXS | Wide angle x-ray scattering |
| γ | Surface tension |
| ΔH | Melt enthalpy |
| ΔP | Pressure loss |
| ζ | Segmental friction force |
| τ | Relaxation time of a polymer |

List of Publications

Parts of this thesis have been published and presented at:

Posters

- Euronanoforum Conference, Duesseldorf, Germany (19-21 June 2007), title: Electrospinning of poly(propylene) nanofibers, authors: I. Hassounah, D. Grafahrend, K. Schaefer & M. Moeller.
- 1st Aachen-Dresden International Textile Conference, Aachen, Germany (29-30 November 2007), title: Melt electrospinning of poly(propylene) nanofibers, authors: I. Hassounah, K. Schaefer & M. Moeller.
- 2nd Aachen-Dresden International Textile Conference, Dresden, Germany (04-05 December 2008), title: Obtaining poly(propylene) nanofibers by melt electrospinning through additives, authors: I. Hassounah, H. Thomas & M. Moeller.
- 3rd Aachen-Dresden International Textile Conference, Aachen, Germany (26-27 November 2009), title: generation of PP nanofibers by melt electrospinning, authors: I. Hassounah, H. Thomas & M. Moeller.

Manuscripts

- 1st Aachen Dresden International Textile Conference, Aachen, Germany (29-30 November 2007), title: Melt electrospinning of poly(propylene) nanofibers, authors: I. Hassounah, K. Schaefer & M. Moeller.
- 2nd Aachen-Dresden International Textile Conference, Dresden, Germany (04-05 December 2008), title: Obtaining poly(propylene) nanofibers by melt electrospinning through additives, authors: I. Hassounah, H. Thomas & M. Moeller.

Other Publications

Posters

- 2nd Aachen-Dresden International Textile Conference, Dresden, Germany (04-05 December 2008), title: Melt electrospinning of polypropylene: Influence of applied voltage on structure formation, authors: Dirk Grafahrend, Ibrahim Hassounah, Martin Rosenthal, Julia Lleixa Calvet, Guilleme Colombe, Doris Klee, Paul D. Dalton, Dimitri A. Ivanov, Martin Moeller.

Manuscripts

- 2nd Aachen-Dresden International Textile Conference, Dresden, Germany (04-05 December 2008), title: Melt electrospinning of polypropylene: Influence of applied voltage on structure formation, authors: Dirk Grafahrend, Ibrahim Hassounah, Martin Rosenthal, Julia Lleixa Calvet, Guilleme Colombe, Doris Klee, Paul D. Dalton, Dimitri A. Ivanov, Martin Moeller.
- 80 Years Department of Textiles : Proceedings International Conference "Latest Advances in High Tech Textiles and Textile-Based Materials", Ghent, Belgium (23-25 September 2009), title: M. Electrospinning of polymer melt : steps towards an upscaled multi-jet process, authors: Hacker, C.; Jungbecker, P.; Seide, G.; Gries, T.; Hassounah, I.; Thomas, H.; Moeller, pages 71-76.

Lectures

- 49th Dornbirn Man-Made Fibers Congress, Wien, Austria (15-17 September 2010), title: Generation of Nanofibers from PP by Melt Electrospinning, authors: Helga Thomas, D. Grafahrend, I. Hassounah, M. Moeller, Ch. Hacker, Ph. Jungbecker, T. Gries.
- Techtexil Symposium, Frankfurt exhibition, Frankfurt, Germany (24 – 26 May 2011), title: Generation of polypropylene nanofibres by melt electrospinning, authors: Dr. Helga Thomas, Dirk Grafahrend, Ibrahim Hassounah, Prof. Dr. Martin Moeller, Christoph Hacker, Philip Jungbecker, Prof. Dr.-Ing. Thomas Gries.

Summary

This dissertation is concerned about developing of melt electrospinning strategies of thermoplastic polymers. The goal was to generate polypropylene nanofibers from the polymer melt instead from the polymer solution. Through this method, organic, toxic or environmentally non-friendly solvents can be avoided offering a clean process for nanofibers production. Melt electrospinning necessitates the use of polymer melts with lower melt viscosity since high melt viscosities inhibit the formation of ultrafine fibers.

The generation of ultra-fine polypropylene nanofibers to utilize these fibers in filter media was studied. The ultra-fine size fibers below 1 μm offer great surface area that assists us to be used as filter media. At the beginning, a simple melt electrospinning device was designed and the melt viscosity of polypropylene was influenced. The effect of the melt viscosity on the produced fiber diameter was studied. Furthermore, the effects of the ambient and the processing parameters on the electrospinning process and the resulting fiber diameter were studied.

In the next chapter, the melt viscosity of polypropylene was influenced by blending of different molecular weights polypropylenes, by addition of small molecules (sodium stearate) and by increasing of the melt temperature. The aim is to recognize the melt viscosity limits which enable us to obtain ultra-fine polypropylene fibers.

In the following chapter, process and ambient parameters and their effect on fiber diameter were studied. These parameters were investigated in order to optimize the conditions for generation of small fibers.

Furthermore and after investigation of the effect of melt viscosity and processing parameters, the chosen polypropylene mixtures were mixed with nucleating. Three different types of nucleating agents were used to enhance the nucleation process in polypropylene electrospun fibers. The amounts of nucleating agents were altered in order to obtain the highest possible melt enthalpy (ΔH) that indicates the highest degree of crystallization. The effects of nucleating agents' type and their amount on the fiber diameters and the degree of crystallization were studied.

Zusammenfassung

Diese Dissertation befasst sich mit der Entwicklung einer Schmelzelektrospinnenstrategie für thermoplastische Polymere. Ziel der Arbeit war, Nanofasern aus Polypropylen durch Schmelzelektrospinnen herzustellen, um die Emission organischer und giftiger Lösungsmittel zu vermeiden. Auch könnten andere thermoplastische Polymere, wie PP und PET, aus der Schmelze elektrogesponnen werden. Für das Elektrospinnen aus Schmelze sind niedrigere Schmelzviskositäten erforderlich, da hohe Schmelzviskositäten die Erzeugung feiner Fasern inhibieren.

In dieser Arbeit wurden die Möglichkeiten zur Herstellung von Polypropylen-Nanofasern mittels Schmelzelektrospinnen untersucht. Fasern unter 1 μm verfügen über eine große Oberfläche, die die Filtrationsleistungsfähigkeit erhöhen können. Zu Beginn der Arbeit wurden eine einfache Schmelzelektrospinnenanlage entwickelt und aufgebaut sowie die Möglichkeiten zur Beeinflussung der Schmelzviskosität von Polypropylen untersucht. Die Einflüsse von Schmelzviskosität und der Prozessparameter auf den Elektrospinnenprozess und die generierten Nanofaserdurchmesser wurden untersucht.

Im folgenden Kapitel dieser Arbeit wurde die Schmelzviskosität durch Mischen von Polypropylen mit unterschiedlichem Molekulargewicht, durch Zusatz von Gleitmitteln (z. B. Natriumstearat) und durch Erhöhung der Schmelztemperatur modifiziert. Das Ziel dieser Arbeiten war, den Bereich der Schmelzviskosität zu erfassen, in dem die Herstellung von PP-Nanofasern möglich ist.

In dem darauf aufbauenden Kapitel wurden die Einflüsse der Prozess- und Umgebungsparameter auf den Faserbildungsprozess untersucht.

Das abschließende Kapitel der Arbeit befasst sich mit der Untersuchung des Einflusses von Nukleierungsmitteln, die den (hinsichtlich der Schmelzviskosität) optimierten Polypropylenen zugemischt wurden. Dazu wurden drei verschiedene Nukleierungsmittel mit dem Ziel verwendet, den Kristallisationsgrad in den generierten Nanofasern zu erhöhen. Die Konzentration des jeweiligen Nukleierungsmittels wurden variiert, um die Schmelzenthalpie zu erhöhen und den Einfluss auf den Faserdurchmesser zu untersuchen.

Chapter 1: Introduction to electrospinning

1 Introduction

In the last decades, a great interest was attracted towards nanotechnology for various applications in industrial and scientific fields. Applications of nanomaterials are established in many scientific fields ranging from filtration systems for automotive industry to scaffolds as implants for life sciences and medicine. Nanotechnology is defined as science dealing with nanoscale objects [1]. It is based on different techniques, reactions and processes generating nanoscaled objects, structures, systems or devices [1]. Today, composites, electrical conductors, coatings, wound dressings [2], catalysts, sensor or information technology [3] can be constructed of nano-objects. Due to unique properties and very promising performance of nano-scaled objects used in these applications, nanotechnology in general achieved much attention among researchers and industry. Nano-objects of various shapes like particles, fibers, tubes, droplets or rods have been described [1]. In this research, generation of nanofibers especially for air filtration processes has been established.

The main principle of nanotechnology is that objects will possess extremely new characters when it is minimized in their dimensions. Different nanostructures can be made with a proper control of the architectural parameters [1]. This control has led to the understanding that in nanoscience, apart from size also shape, surface and composition are also critical factors. In fact, almost all physical and chemical properties of nanomaterials are observed to differ significantly from their bulk counterparts [4].

The term nanofiber is used for elongated cylindrical bodies with diameters less than 1 μm [5]. Such fibers exhibit unusual and some times superior properties [6, 7] as high length to diameter ratio [6-14], extremely large fiber surfaces, flexibility in surface and material functionality [7, 14, 15], high bending performance [14]. High aspect ratios (>1000) result in high surface areas, which are very attractive for applications in filtration and catalysis [2, 6, 7,

9-11, 13, 14]. For example, one gram of fibrous mat (density = 1 gm/cm³) with fiber diameters of 100 nm exhibits a surface area of about 100 m² [13].

Due to the broad spectrum of applications for nanofibers, there is an increasing demand to establish techniques or processes for cost effective nanofiber production. Nanofibers have been generated by such different processes as microwave arc heating, melt-blown spinning or electrospinning.

Firstly, microwave arc heating was used for generation of ultra high temperature ceramic (UHTCs) nanofibers and for sintering large amount of ceramics at high temperature in short period of time [16]. Baldrige et. al. developed a method for generation of zirconium diboride nanofibers with average fiber diameters of 10 nm. A powder of zirconium diboride was placed in an alumina arc and heated by microwaves for 10-45 seconds [16]. During heating of the microsize particles, sintering transformed these particles into nanofibers [16].

Secondly, nanofibers from thermoplastic polymers were generated by aerodynamic forces in melt-blown spinning. Therefore, polymer melt passed through a v-slot shape orifice while a hot air jet was supplied through the slot [13]. This allowed the polymer melt to be stretched to form fibers [13]. High deformation forces, due to air jet, reduce the fiber diameter to nanometer dimensions [13]. Hills Inc and Irema Filters developed an innovative melt-blown technique that can lead to the generation of nanofibers from polypropylene down to a fiber diameter of 250 nm [17, 18]. The generation of melt blown fibers is closely connected to the usage of a very fine orifice and suitable polypropylene types with high melt flow index. However, high investment costs for melt blown machinery and equipment require a high material throughput for beneficial and profitable industrial use.

Thirdly, for special applications demanding lower amounts of nanofibers exhibiting special functionality, e. g. in medicine, electrospinning offers an appropriate and cost effective technology. Apart from lower investment costs for establishing the technology, electrospinning is not only restricted to thermoplastic melts but can also be used for the generation of nanofibers from polymer solutions and dispersions. Therefore, in this research electrospinning was used for generating nanofibers.

Especially electrospun fibers add value to air filtration systems as filter efficiency can be drastically enhanced. Very small nanofiber amounts, due to the increased free surface, are

capable of increasing the filtration effect and lead better recovery characteristics. Such filters show enhanced dust particle deposition especially for small particles (sub-micron-to nanoscale objects). Besides the increased free surface, remnant charges on electrospun fibers attribute to the filter improvement. This is a simple example how small amounts of nano-objects generated by a handy nanotechnological process can improve performance. Therefore, nanotechnology seems capable to improve processes and contribute to protection of the environment. Additionally, melt electrospinning itself avoids the use of toxicological and environmental critical solvents and has to be considered as environmental friendly technique.

This thesis is divided into five chapters describing melt-electrospinning for generation of nanofibers. Main aim of this work was the generation of nanofibers from isotactic polypropylene by melt electrospinning. The effects of (i) temperature control of the spinning room and (ii) of chemical and processing parameters on the fiber diameter are specially addressed.

The **first chapter** gives a short introduction to nanofibers and nanotechnology.

The **second chapter** discusses the state of the art and explains the theoretical background of electrospinning. Main focus is the production of thin fibers.

The **third chapter** concentrates on controlling the melt viscosity by changing chemical and technical parameters during electrospinning. The influence of melt viscosity on the resulting fiber diameter is discussed.

The **fourth chapter** describes the effect of process and ambient parameters on the fiber diameters and their homogeneity.

Finally the **fifth chapter** discusses the stabilization of the polypropylene nanofibers by addition of nucleation agents.

2 References

1. Ramakrishna, S.; Fujihara, K.; Teo, W.-E.; Lim, T.-C.; Ma, Z. *An Introduction to Electrospinning and Nanofibers*; World Scientific Printers, Singapore, **2005**, 425.
2. Kowalewski, T. A.; Błóński, S.; Barral, S. Experiments and Modelling of Electrospinning Process. *Bull Pol Acad Sci - Te* **2005**, *53*, 385-394.
3. Lu, P.; Bing, D. Applications of Electrospun Fibers. *Recent Patents on Nanotechnology* **2008**, *2*, 169-182.
4. Ozin, G. A.; Arsenault, A. C. *Nanochemistry: A Chemical Approach to Nanomaterials*; RSC Pub., Cambridge, **2005**, 628.
5. Grafe, T.; Graham, K. In *Polymeric Nanofibers and Nanofiber Webs: A New Class of Nonwovens*, International Nonwovens Technical Conference, Atlanta, Georgia, U. S. A., 24-26.09.2002.
6. Acatay, K.; Simsek, E.; Akel, M.; Menciloglu, Y. Electrospinning of Low Surface Energy Quaternary Ammonium Salt Containing Polymers and Their Antibacterial Activity. *Nato Sci Ser Ii Math* **2004**, *169*, 97-106.
7. Huang, Z.-M.; Zhang, Y.-Z.; Kotaki, M.; Ramakrishna, S. A Review on Polymer Nanofibers by Electrospinning and Their Applications in Nanocomposites. *Compos Sci Technol* **2003**, *63*, 2223-2253.
8. Frenot, A.; Chronakis, I. S. Polymer Nanofibers Assembled by Electrospinning. *Curr Opin Colloid In* **2003**, *8*, 64-75.
9. He, J.-H.; Wan, Y.-Q.; Yu, J.-Y. Application of Vibration Technology to Polymer Electrospinning. *Int J Nonlinear Sci* **2004**, *5*, 253-262.
10. Subbiah, T.; Bhat, G.; Tock, R.; Parameswaran, S.; Ramkumar, S. Electrospinning of Nanofibers. *J Appl Polym Sci* **2005**, *96*, 557-569.

-
11. Wang, A.; Hsieh, A.; Rutledge, G. Electrospinning of Poly(MMA-Co-MAA) Copolymers and Their Layered Silicate Nanocomposites for Improved Thermal Properties. *Polymer* **2005**, *46*, 3407-3418.
 12. McKee, M.; Hunley, M.; Layman, J.; Long, T. Solution Rheological Behavior and Electrospinning of Cationic Polyelectrolytes. *Macromolecules* **2006**, *39*, 575-583.
 13. Ellison, C.; Phatak, A.; Giles, D.; Macosko, C.; Bates, F. Melt Blown Nanofibers: Fiber Diameter Distributions and Onset of Fiber Breakup. *Polymer* **2007**, *48*, 3306-3316.
 14. Schaefer, K.; Thomas, H.; Dalton, P.; Moeller, M. *Multifunctional Barrier for Flexible Structure: Textile, Leather and Paper*; Springer Series in Materials Science, Heidelberg, **2007**, 125-138.
 15. Carroll, C.; Joo, Y. Electrospinning of Viscoelastic Boger Fluids: Modeling and Experiments. *Phys Fluids* **2006**, *18*, 1-14.
 16. Baldridge, T.; Gupta, M. Zirconium Diboride Nanofiber Generation Via Microwave Arc Heating. *Nanotechnology* **2008**, *19*, 1-7.
 17. New Technology Supports Nanoscale Filtration of Ultra-Fine Dust. http://www.irema.de/docs/artikel_technologynews_eng.pdf (accessed 16.02.2012).
 18. Wilkie, A. Announces Nanofiber Meltblown Fabric. <http://www.hillsinc.net/nanomeltblownfabric.shtml> (accessed 22.02.2007).

Chapter 2: State of the art

1 Electrospinning

Electrospinning is an electrostatic spinning process [1-18]. In this process, electric field strength is used as a driving force to draw nanofibers from polymer solutions and melts [2, 4, 7, 8, 10, 13, 19-21]. For the formation of fibers, a sufficient amount of chain entanglements is a requirement on the liquid state. Generally, high molecular weight and sufficient polymer concentrations favor fiber generation, while in electrospraying, small molecules are used, which are converted into tiny droplets or particles [22]. Diameters of electrospun fibers can range from 3 nm to 1.5 mm [2-4, 8, 9, 14, 23-26].

1.1 History

Although electrospinning technique attracted special interest in the last decades, its fundamental ideas turn back more than 400 years. In the late 1500, William Gilbert was the first who observed the reaction of a fluid under high electric charge. [27] He observed the formation of a cone, when a piece of charged amber was placed near to the droplet of water [27].

In 1914, John Zeleny published a work on the behavior of fluids at the tip of metallic capillaries [28]. He tried to simulate the behavior of fluid droplets under the influence of the electric field [19]. The first US patent appeared was written by Formhals in 1934 [2, 4, 5, 29, 30]. In the period in between 1934 to 1944, Formhals published series of patents describing experimental pathways and setups to generate polymer filaments by electrical forces [30]. In 1969, Taylor developed an understanding for the critical conditions required to convert the fluid droplet into a cone, which is generally termed as Taylor cone [28, 31]. In 1938, I. V. Petryanov-Sokolov and N. D. Rozenblum could create electrospun cellulose acetate using a mixture of dichloroethane and ethanol as solvent [27]. Their work led to the formation of a factory for gas masks in 1939 in Tver [27].

Though electrospinning was investigated a long time ago, it started to gain continuous interest in the last 20 years. This can be concluded from an increasing number of publications published in last years. Figure 2-1 shows the number of publications on electrospinning published each year [32].

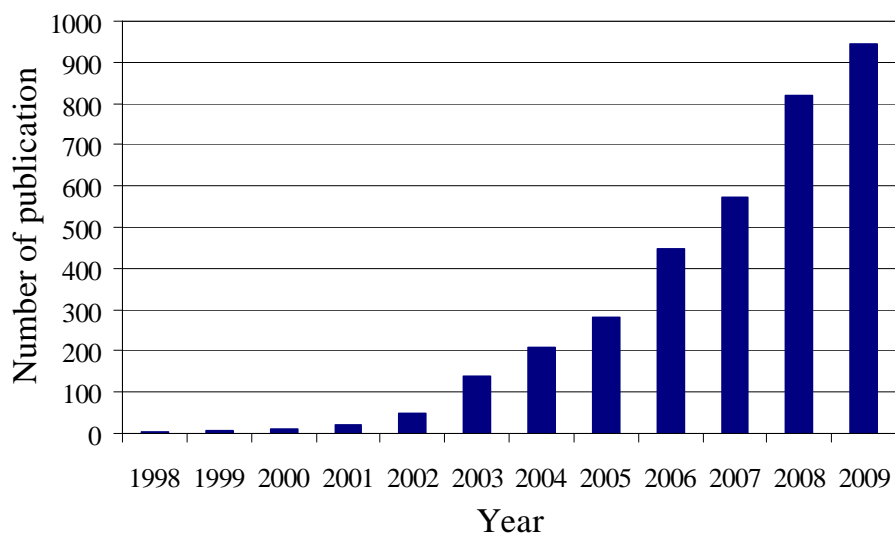


Figure 2-1: Publication number on electrospinning in the last decade [32]

However, most of the newer publications on electrospinning deal with spinning from polymer solutions. Almost 99% of papers published on electrospinning of polymer solutions, while less than 1 % of publications are based on melt electrospinning [32]. 1981 Larrondo et. al. were the first authors who published the setup for producing fibers from the melt by using a heat reservoir [1, 33, 34]. In their work, they showed the possibility to obtaining fibers from melts of linear polyolefins as polypropylene and polyethylene [1, 33, 34]. Their studies focus on understanding the principle that defines melt electrospinning. One major drawback of this study can be attributed to the fact that efforts only led to production of thick fibers in range of 50 – 400 μm . However, they identified melt viscosity of the medium used to be an influential parameter which affects the fiber diameter significantly.

Also the attempts of other researchers like Reneker et. al. [35], Khurana et. al. [36] and Lyons et. al. [31, 37] did not lead to the generation of polypropylene nanofibers by electrospinning of melts.

In 2007, Dalton et. al was first to obtain polypropylene nanofibers by addition of viscosity breaking agents forming nitroxide radicals [38]. However, by addition of viscosity breaking agents the degradation process cannot be controlled precisely, especially when the polymer is exposed to longer heating periods [38].

Since 1995, strong theoretical developments were created in the field of driving mechanism of electrospinning process [39]. More than that, extensive work has been done on the development of a Taylor cone as well on jet instabilities produced during electrospinning by Reznik et. al. [39]. Nowadays almost 100 polymers were successfully electrospun from the solution and/or melt [40]. However, in case of melt electrospinning a small distance between the spinning electrodes (4 cm) was necessary to spin the molten polymer, thus restricting the action of electrical forces to stretch the fiber material to form ultrafine fibers.

1.2 Electrospinning process

An electrospinning apparatus consists of three basic elements a high voltage supplier, a spinneret fitted with a pump and a collector [8, 19, 29, 30]. The spinneret is usually connected to the power supply whereas the collector is grounded. The process is started by pushing the polymer solution or melt through a metallic capillary tube to form a droplet at the spinneret tip and ends with formation of fibers by electrical forces which are collected on the target [2, 5, 15, 22, 25, 26, 29, 30, 41-43].

Electrospinning is described by electrohydrodynamic theory [29]. Three stages happen in electrospinning to create fibers: Cone formation, thinning and elongation of the jet and finally solidification of the jet forming fibers [29]. In the first step, where the conical shape is formed, a balance occurs between different forces acting on the cone as shown in Figure 2-2 [29].

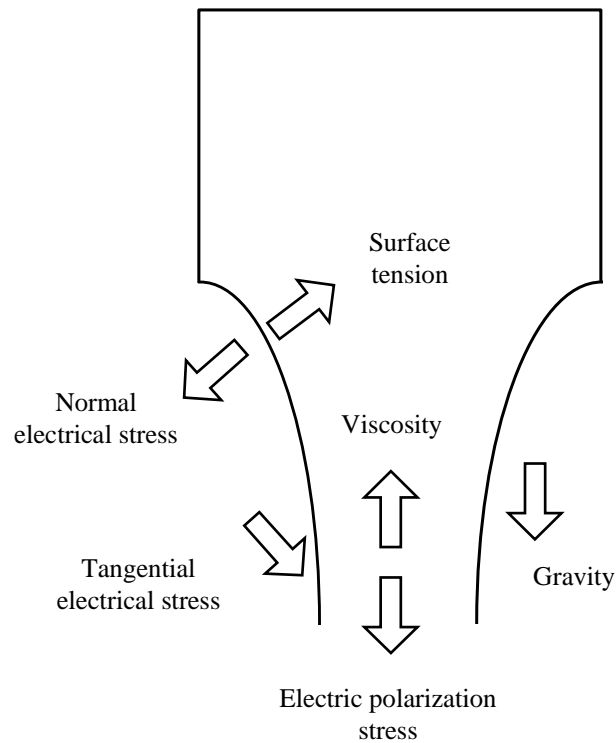


Figure 2-2: Schematic illustrations show the forces acting on the polymer jet at the conical region [29]

These forces are gravity, normal and tangential electric stresses, viscosity and surface tension [29]. Increasing viscosity slows down the formation of the cone, while the increase surface tension retards the formation of new surfaces [29]. Viscosity and surface tension are working against electrical stress, which tends to reduce the surface charge density by creating new surfaces to increase the distance between them [29].

At the last stage of electrospinning before solidification, the terminal diameter of the electrified jet, h_t , is reached due to the balance of repulsion of surface charges by surface tension [29]. Longer spinning distances lead to finer fibers by the action of the electrical field [29].

1.3 Developing of instabilities in electrospun polymer jets

To start the electrospinning process, the electrostatic repulsion of the charges on the droplet surface has to exceed the surface tension of polymer melt/solution. After crossing the critical value of electric field strength, a polymer jet is formed and stretched onto its way to the target. During flying, the polymer jet undergoes stretching and thinning through different instability processes. Five types of instabilities are recognized: Rayleigh instability, electric field induced instability, Varicose instability, whipping or bending instability and kink instability

[2, 5, 7, 13, 20, 29, 30, 37, 43-45]. These instabilities are caused by the repulsion of charges on the jet surface [2, 5, 15, 25, 29, 30, 37, 43]. Rayleigh, electric field induced and varicose instabilities are known as axis symmetric instabilities, while the bending or whipping instability is known as axis asymmetric instability [2, 8, 9, 12, 13, 37, 40, 44-46].

Rayleigh instability is driven by surface tension of the fluid [9]. This instability tends to break the polymer jet into small droplets and it becomes more important when the polymer jet becomes thinner [2, 9, 37, 40]. It predominantly happens with electrified jets of small molecules or with short polymer chain lengths [2, 9, 37, 40]. Rayleigh instability can be suppressed when the applied electric field and surface charge exceed a threshold given by the coefficients of the surface tension and the fiber diameter, i. e. Laplace pressure [44, 45]. Thus, the dominant instability in this stage depends strongly on the viscosity and the conductivity of the polymer jet [29]. By increasing the amount of conductive species in the jet, the axis symmetric instability will be suppressed [29].

A similar effect results from an electric field instability as the charge distribution along the fiber becomes inhomogeneous resulting in an unevenness of the lateral repulsion forces along the fibers [2, 37, 40]. Both instabilities result in the formation of a bead in string structure, also called varicose instability, and ultimately it breaks up into single droplets. Varicose can be suppressed if the viscoelastic relaxation of the elongated polymer solution is slower than vitrification of the polymer fibers, while the Rayleigh instability and the electric field instability occur directly at the beginning of the fibers [45].

Further enhanced non axis symmetric varicose effect is caused by small lateral fluctuation in the centerline of the jet, this results in an instability that bends the jet further and a whipping typical for electrospinning [13, 40]. The straight jet centerline is started to vibrate in zigzag shape [31]. It is corresponding to the visible region of the jet before the bending instability occurs [31]. The whipping instability corresponds to long wavelength oscillation of the jet centerline and it occurs at some distance from the droplet tip [12, 37]. Ramakrishna et. al. explained the existence of bending instability on the basis of perturbed jet [47]. Once bending instability forms, the columbic forces cause repulsion of charges in random manner (Figure 2-3) [47].

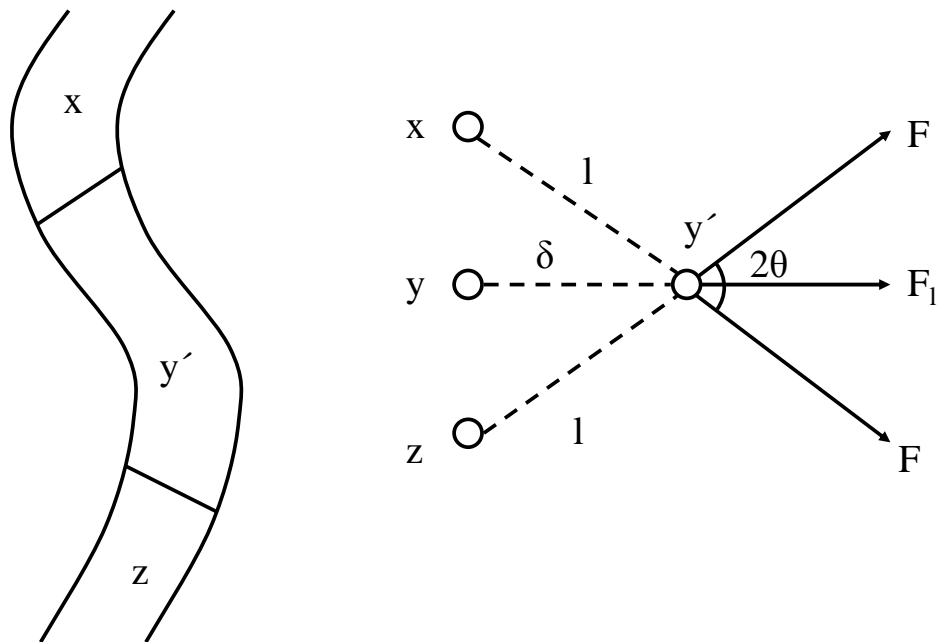


Figure 2-3: Repulsion of charges on the polymer jet causes bending of the jet in random manner in the bending instability region [47].

Once the node y is moving to y' , the coulombic forces x and z pushes the node y' further far away [47].

Bending instability disappears at high electric field strength and high flow rates resulting in formation of straight jets along the distance between electrodes [31]. If the jet is broken into droplets within the bending instability region, the instability is called Kink instability [31].

1.4 Solution electrospinning and melt electrospinning

The main difference between solution and melt electrospinning is that in case of solution electrospinning solid fibers are formed by evaporation of the solvent, while in case of melt electrospinning fibers are formed by cooling down [25, 40, 47-49]. Due to the differences in viscosity, large differences in fiber diameters obtained from the polymer solution and melt can be observed. In solution electrospinning thin fibers, in the case of melt electrospinning usually coarse fibers are generated. By evaporation of the solvent, strong reduction in the polymer jet will happen resulting in formation of thin polymer strands on the target [47]. On the other hand, the high melt viscosity in the case of melt electrospinning impeded forming of fibers during electrospinning, especially when the temperature in the spinning area slows down. Therefore, fast solidification of the jet interferes with the electrical forces that stretch the fibers [47].

To overcome this problem is a big challenge in electrospinning, especially for polymers which have no proper solvents at room temperature as polypropylene and polyethylene terephthalate [16].

In order to control the high melt viscosities and to prevent the polymer jet from fast solidification, the chemical and processing parameters have to be optimized e. g. by increasing the temperature of melt and spinning room as well as by adjustment of melt viscosity through addition of lower molecular weight polymer chains or slipping agents.

2 References

1. Larrondo, L.; Manley, R. Electrostatic Fiber Spinning from Polymer Melts. I. Experimental-Observations on Fiber Formation and Properties. *J Polym Sci Pol Phys* **1981**, *19*, 909-920.
2. Shin, Y. M.; Hohman, M. M.; Brenner, M. P.; Rutledge, G. C. Electrospinning: A Whipping Fluid Jet Generates Submicron Polymer Fibers. *Appl Phys Lett* **2001**, *78*, 1149-1151.
3. Liu, W.; Graham, M.; Evans, E.; Reneker, D. Poly(Meta-Phenylene Isophthalamide) Nanofibers Coating and Post Processing. *J Mater Res* **2002**, *17*, 3206-3212.
4. Frenot, A.; Chronakis, I. S. Polymer Nanofibers Assembled by Electrospinning. *Curr Opin Colloid In* **2003**, *8*, 64-75.
5. Acatay, K.; Simsek, E.; Akel, M.; Menciloglu, Y. Electrospinning of Low Surface Energy Quaternary Ammonium Salt Containing Polymers and Their Antibacterial Activity. *Nato Sci Ser Ii Math* **2004**, *169*, 97-106.
6. He, J.-H.; Wan, Y.-Q.; Yu, J.-Y. Allometric Scaling and Instability in Electrospinning. *Int J Nonlinear Sci* **2004**, *5*, 243-252.
7. He, J.-H.; Wu, Y.; Zuo, W.-W. Critical Length of Straight Jet in Electrospinning. *Polymer* **2005**, *46*, 12637-12640.
8. Subbiah, T.; Bhat, G.; Tock, R.; Parameswaran, S.; Ramkumar, S. Electrospinning of Nanofibers. *J Appl Polym Sci* **2005**, *96*, 557-569.
9. Wang, A.; Hsieh, A.; Rutledge, G. Electrospinning of Poly(MMA-co-MAA) Copolymers and Their Layered Silicate Nanocomposites for Improved Thermal Properties. *Polymer* **2005**, *46*, 3407-3418.
10. Carroll, C.; Joo, Y. Electrospinning of Viscoelastic Boger Fluids: Modelling and Experiments. *Phys Fluids* **2006**, *18*, 1-14.
11. Dalton, P. D.; Joergensen, N. T.; Groll, J.; Moeller, M. Patterned Melt Electrospun Substrates for Tissue Engineering. *Biomedical Materials* **2008**, *3*, 1-11.
12. Mohmeyer, N.; Mueller, B.; Behrendt, N.; Hillenbrand, J.; Klaiber, M.; Zhang, X.; Smith, P.; Altstaedt, V.; Sessler, G.; Schmidt, H.-W. Nucleation of Isotactic Polypropylene by Triphenylamine-Based Trisamide Derivatives and Their Influence on Charge-Storage Properties. *Polymer* **2004**, *45*, 6655-6663.
13. Chronakis, I. Novel Nanocomposites and Nanoceramics Based on Polymer Nanofibers Using Electrospinning Process - a Review. *J Mater Process Tech* **2005**, *167*, 283-293.
14. Gupta, P.; Elkins, C.; Long, T.; Wilkes, G. Electrospinning of Linear Homopolymers of Poly(Methyl Methacrylate): Exploring Relationships between Fiber Formation,

- Viscosity, Molecular Weight and Concentration in a Good Solvent. *Polymer* **2005**, *46*, 4799-4810.
15. Li, D.; Ouyang, G.; McCann, J.; Xia, Y. Collecting Electrospun Nanofibers with Patterned Electrodes. *Nanoletters* **2005**, *5*, 913-916.
 16. Lee, S.; Obendorf, S. Developing Protective Textile Materials as Barriers to Liquid Penetration Using Melt-Electrospinning. *J Appl Polym Sci* **2006**, *102*, 3430-3437.
 17. Lu, C.; Chen, P.; Li, J.; Zhang, Y. Computer Simulation of Electrospinning. Part I. Effect of Solvent in Electrospinning. *Polymer* **2006**, *47*, 915-921.
 18. Sigmund, W.; Yuh, J.; Park, H.; Maneeratana, V.; Pyrgiotakis, G.; Daga, A.; Taylor, J.; Nino, J. Processing and Structure Relationships in Electrospinning of Ceramic Fiber Systems. *J Am Ceram Soc* **2006**, *89*, 395-407.
 19. Błasińska, A.; Krucińska, I.; Chrzanowski, M. Dibutyrylchitin Nonwoven Biomaterials Manufactured Using Electrospinning Method. *Fibres Text East Eur* **2004**, *12*, 51-55.
 20. Theron, S.; Yarin, A.; Zussman, E.; Kroll, E. Multiple Jets in Electrospinning: Experiment and Modeling. *Polymer* **2005**, *46*, 2889-2899.
 21. Naebe, M.; Lin, T.; Tian, W.; Dai, L.; Wang, X. Effects of MWNT Nanofillers on Structures and Properties of PVA Electrospun Nanofibres. *Nanotechnology* **2007**, *18*, 1-8.
 22. Shenoy, S.; Bates, W.; Frisch, H.; Wnek, G. Role of Chain Entanglements on Fiber Formation During Electrospinning of Polymer Solutions: Good Solvent, Non-Specific Polymer-Polymer Interaction Limit. *Polymer* **2005**, *46*, 3372-3384.
 23. Dalton, P.; Klee, D.; Möller, M. Electrospinning with Dual Collection Rings. *Polymer* **2005**, *46*, 611-614.
 24. McKee, M.; Hunley, M.; Layman, J.; Long, T. Solution Rheological Behavior and Electrospinning of Cationic Polyelectrolytes. *Macromolecules* **2006**, *39*, 575-583.
 25. Schaefer, K.; Thomas, H.; Dalton, P.; Moeller, M. *Multifunctional Barrier for Flexible Structure: Textile, Leather and Paper*; Springer Series in Materials Science, Heidelberg, **2007**, 125-138.
 26. Lee, H.; Yoon, H.; Kim, G. H. Highly Oriented Electrospun Polycaprolactone Micro/Nanofibers Prepared by a Field-Controllable Electrode and Rotating Collector. *Appl Phys a-Mater* **2009**, *97*, 559-565.
 27. Filatov, Y.; Budyka, A.; Kirichenko, V. *Electrospinning of Micro- and Nanofibers: Fundamentals and Applications in Separation and Filtration Processes*; Begell House Inc., New York, **2007**, 488.

-
28. Buchko, C.; Chen, L.; Shen, Y.; Martin, D. Processing and Microstructural Characterization of Porous Biocompatible Protein Polymer Thin Films. *Polymer* **1999**, *40*, 7397-7407.
 29. Hohman, M.; Shin, M.; Rutledge, G.; Brenner, M. Experimental Characterization of Electrospinning: The Electrically Forced Jet and Instabilities. *Polymer* **2001**, *42*, 9955-9967.
 30. Huang, Z.-M.; Zhang, Y.-Z.; Kotaki, M.; Ramakrishna, S. A Review on Polymer Nanofibers by Electrospinning and Their Applications in Nanocomposites. *Compos Sci Technol* **2003**, *63*, 2223-2253.
 31. Lyons, J. Melt Electrospinning of Polymers: A Review. *Polymer News* **2005**, *30*, 170-178.
 32. References About Electrospinning. <http://isiknowledge.com> (accessed 16.02.2012).
 33. Larrondo, L.; Manley, R. Electrostatic Fiber Spinning from Polymer Melts. II. Examination of the Flow Field in an Electrically Driven Jet. *J Polym Sci Pol Phys* **1981**, *19*, 921-932.
 34. Larrondo, L.; Manley, R. Electrostatic Fiber Spinning from Polymer Melts. III. Electrostatic Deformation of a Pendant Drop of Polymer Melt. *J Polym Sci Pol Phys* **1981**, *19*, 933-940.
 35. Reneker, D.; Haul, H.; Rangkupan, R.; Lennhoff, J. Electrospinning Polymer Nanofibers in a Vacuum. *Polymer Preprints* **2003**, *44*, 68-69.
 36. Khurana, H. S.; Patra, P. K.; Warner, S. B. Nano Fibers from Melt Electrospinning. *Abstr Pap Am Chem S* **2003**, *226*, 67.
 37. Lyons, J. Melt-Electrospinning of Thermoplastic Polymers : An Experimental and Theoretical Analysis. PhD. Thesis, Drexel University, Philadelphia, **2004**.
 38. Dalton, P.; Grafahrend, D.; Klinkhammer, K.; Klee, D.; Möller, M. Electrospinning of Polymer Melts: Phenomenological Observations. *Polymer* **2007**, *48*, 6823-6833.
 39. Reznik, S.; Yarin, A.; Theron, A.; Zussman, E. Transient and Steady Shapes of Droplets Attached to a Surface in a Strong Electric Field. *J Fluid Mech* **2004**, *516*, 349-377.
 40. Klinkhammer, K. Melt Electrospinning of Scaffolds for Tissue Engineering. Diploma Thesis, RWTH Aachen, Aachen, **2005**.
 41. He, J.-H.; Wan, Y.-Q.; Yu, J.-Y. Application of Vibration Technology to Polymer Electrospinning. *Int J Nonlinear Sci* **2004**, *5*, 253-262.
 42. Teo, W. E.; Ramakrishna, S. Electrospun Fibre Bundle Made of Aligned Nanofibres over Two Fixed Points. *Nanotechnology* **2005**, *16*, 1878-1884.

-
43. Teo, W. E.; Ramakrishna, S. A Review on Electrospinning Design and Nanofibre Assemblies. *Nanotechnology* **2006**, *17*, 89-106.
 44. Hohman, M.; Shin, M.; Rutledge, G.; Brenner, M. Electrospinning and Electrically Forced Jets. I. Stability Theory. *Phys Fluids* **2001**, *13*, 2201-2220.
 45. Hohman, M.; Shin, M.; Rutledge, G.; Brenner, M. Electrospinning and Electrically Forced Jets. II. Applications. *Phys Fluids* **2001**, *13*, 2221-2236.
 46. Yu, J.; Fridrikh, S.; Rutledge, G. The Role of Elasticity in the Formation of Electrospun Fibers. *Polymer* **2006**, *47*, 4789-4797.
 47. Ramakrishna, S.; Fujihara, K.; Teo, W.-E.; Lim, T.-C.; Ma, Z. *An Introduction to Electrospinning and Nanofibers*; World Scientific Printers, Singapore, **2005**, 425.
 48. Ellison, C.; Phatak, A.; Giles, D.; Macosko, C.; Bates, F. Melt Blown Nanofibers: Fiber Diameter Distributions and Onset of Fiber Breakup. *Polymer* **2007**, *48*, 3306-3316.
 49. Ogata, N.; Lu, G.; Iwata, T.; Yamaguchi, S.; Nakane, K.; Ogihara, T. Effects of Ethylene Content of Poly(Ethylene-Co-Vinyl Alcohol) on Diameter of Fibers Produced by Melt-Electrospinning. *J Appl Polym Sci* **2007**, *104*, 1368-1375.

Chapter 3: Influence of melt viscosity on melt electrospinning process

1 Abstract

Melt electrospinning is a useful technique for generating nanofibers by electrically driven forces. Advantage of this technique is the possibility of generating fine fibers without need of any solvent. It is a suitable solution for thermoplastic polymers that have no convenient solvents at room temperature as polypropylene or polyethylene. However, the generation of fine fibers with diameters below 1 μm still remains a big challenge. The generation of ultrafine fibers is restricted by fast fiber solidification in the spinning room as well as by high melt viscosities which constrain the stretching of the polymer jet forming a thin thread of the polymer. Apart from temperature adjustment of the spinning area, the melt viscosity of polypropylene was significantly reduced by reduction of the friction between melt and surrounding wall, e. g. the orifice as well as by disturbing the chain-chain interactions. The latter influences the degree of crystallization which was found to be essential for generation of fine fibers. In this chapter melt viscosity and crystallization behavior of high molecular weight polypropylene was influenced by compounding with internal and external slipping agents as well as by adjustment of melt temperature and application of a heat gradient to the spinning room. The electrospun fibers were characterized by scanning electron microscopy (SEM), in order to investigate their diameters and homogeneities, and by dynamic scanning calorimeter (DSC) to study the effect of small molecules used as viscosity reducing agents on the crystallization behavior in the polypropylene fibers.

2 Introduction

During electrospinning, the polymer melt is charged by application of high voltages leading to the formation of a polymer jet that arises from the spinneret towards the target. A main problem of melt electrospinning is the generation of coarse fibers due to high melt viscosities of the polymer which influence and constrain the elongation of the polymer jet driven by electrical forces. One possibility to influence the spinning process and facilitate generation of fine fibers is to reduce melt viscosity. Therefore, viscosity and viscosity influencing factors are important parameters for adjusting the fiber characteristics.

Viscosity is defined as an internal fluid property, which refers to the resistance of a fluid to flow under the effect of shear or extensional stresses [1]. According to their flow behavior, fluids are classified into Newtonian fluids as water and glycerin and non-Newtonian fluids as polymers. Newtonian fluids show constant viscosity at different shear rates, while for non-Newtonian, the viscosity of the fluid is changing at different shear rates [2]. Polymers show viscoelastic behavior [2]. At lower and fast shear deformations, polymers react as elastic materials; the shape of the material will return to its initial position after removing of the applied force [2]. On the other hand, at higher shear stresses, non linear viscous behavior is appearing and viscosity depends on the shear rate [2].

Aim of the work was to study the influence of melt viscosity on the behavior of polypropylene during electrostatic spinning. Apart from detection of viscosity ranges that enable electrospinning in general, this included the investigation of viscosity affecting factors as temperature, molecular weight, molecular weight distribution and structure of polypropylene in the presence and absence of the slipping agents on the resulting fiber shape.

2.1 Parameters affecting melt viscosity

Viscosity is generally caused by forces acting on macromolecules as Van der Waals or London forces which are week dielectric force [3]. These week forces acting on the polymer chains are partially caused by their molecular structure (linear or branched molecules) and correlate to the viscoelastic behavior. Other parameters and small substances significantly alter (e.g. increase or reduce) melt viscosity.

2.1.1 Effect of molecular parameters

Generally, increasing the molecular weight of polymer chains increases the value of viscosity, due to segmental friction forces (ζ) and the formation of the entanglements [4, 5]. A critical number is M_e or M_c which correspond to crossing points between chains [2, 6] in melts. By increasing the chain length, above the critical molecular weight (M_c : molecular weight between two entanglement points) the entanglements lead to an increase of melt viscosity, and consequently in an increase of the proportion of deformation due to chain uncoiling [2, 6, 7]. Shear viscosity has different proportionalities before and after the critical molecular weight [7]. Before the viscosity is proportional to the molecular weight, while after M_c viscosity is proportional to $(M)^{3.5}$ as shown in equations 1 and 2 [2, 5, 7, 8].

$$M < M_c \rightarrow \eta \sim M \quad (1)$$

$$M > M_c \rightarrow \eta \sim M^{3.5} \quad (2)$$

Above M_c , shear deformation requires rearrangement of the entanglements and significant coil deformation. Theoretically, this has been described by the reptation theory, where the terminal relaxation time τ is given by the time a polymer chain needs to reptate out of the original entanglement confinement [2, 5, 7]. By increasing the molecular weight, the terminal relaxation time is increased [7].

The relation between molecular weight polydispersity, branching and viscosity is a crucial factor for electrospinning. The polymer chain length has to be sufficient to guarantee enough entanglements and formation of a continuous jet [4, 6, 9-11]. On the other hand, too high viscosities cause some difficulties when stretching the polymer droplet and jet [6]

2.1.2 Effect of external parameters

The main external parameters affecting melt viscosity are shear rate and temperature. Normally with shearing, the chain configurations are changed from coiled to extended state. The viscosity reduction is caused by slipping and orientation of chains under the influence of shearing. Figure 3-1 shows the relation between shear rate and viscosity.

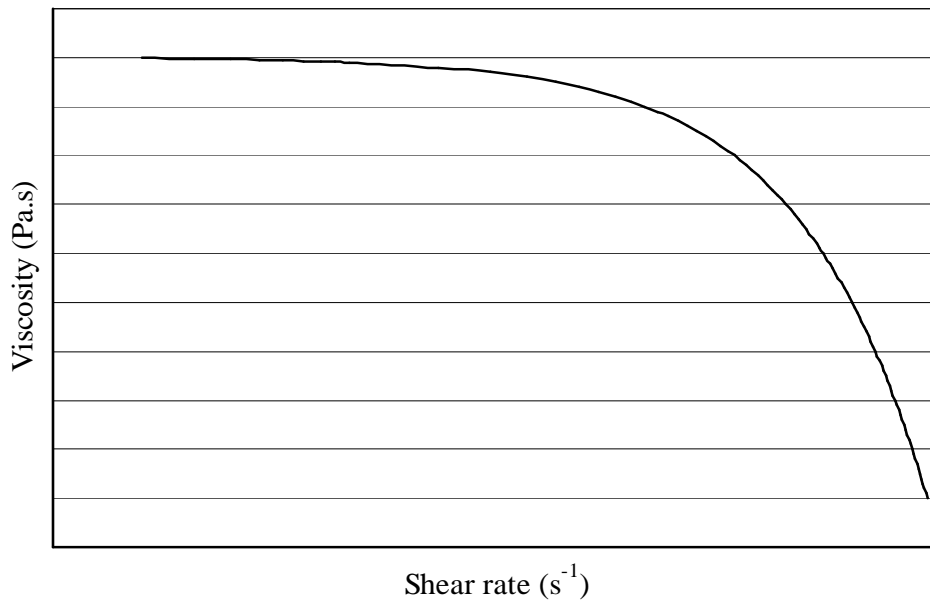


Figure 3-1: Shear-rate dependent viscosity of a polymer melt.

Additionally, shear rate alters the friction of the polymer melt with the wall of the spinneret.

In addition to the shear viscosity, elongational or extensional viscosity has to be taken into consideration. Elongation viscosity becomes significant in the electrospinning area, where the fiber cross section is reduced by applying an extensional stress as electrical field [12]. The elongational viscosity at the linear range of deformation can be up to 3 times the value of zero shear viscosity [13]. Although shear and elongational viscosities are time dependant behaviors, the reaction at high shear or elongation rate in non-linear range is completely different [13]. With shear rate, the melt viscosity is reducing with increasing the shear rate while in case of elongational viscosity the viscosity value is increasing by increase of the elongation stress [13].

2.2 Viscosity measurement

In this chapter, a cone-plate rheometer was used to measures the viscosity in a wide range of applied shear rates. The zero shear rate values were determined to compare the viscosity of polymer melts at low shear rate applications as in electrospinning.

2.3 Control of melt viscosity

Controlling of melt viscosity can be achieved by reduction of the molecular weight, verification of the molecular weight distribution, introducing long chain branching or by addition of slipping agents [4]. However, increase of temperature leads to polymer degradation as well as to undesirable side reaction products [14].

Reduction of the molecular weight is one possibility to reduce the viscosity. This can be achieved either by addition of radical generating substances or by blending of polymers with different molecular weights [15]. Viscosity breaking agents perform controlled radical degradation of the polymer. The regularity in chain scission is a result of forming stable radicals due to formation of a hindered structure. In case of polypropylene, peroxide or nitroxide radical forming auxiliaries are used preferably attacking the tertiary carbon atom [16]. The degradation reaction starts with initiation step, where the radicals are formed at high temperatures [16].

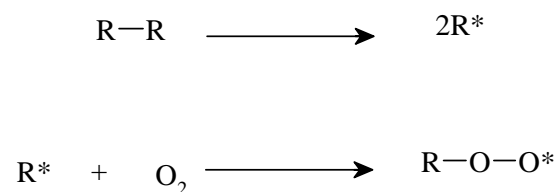


Figure 3-2: Initiation step in polypropylene radical degradation with peroxide radicals

In the second step, the peroxide radical attacks the tertiary carbon atom or abstract the H^* from tertiary carbon atom leading to subsequent cleavage of the chains starting from this point via β -cleavage causing reduction of molecular weight [16], Figure 3-3. The chain cleavage process is terminated by radicals recombination or by disproportionation [16].

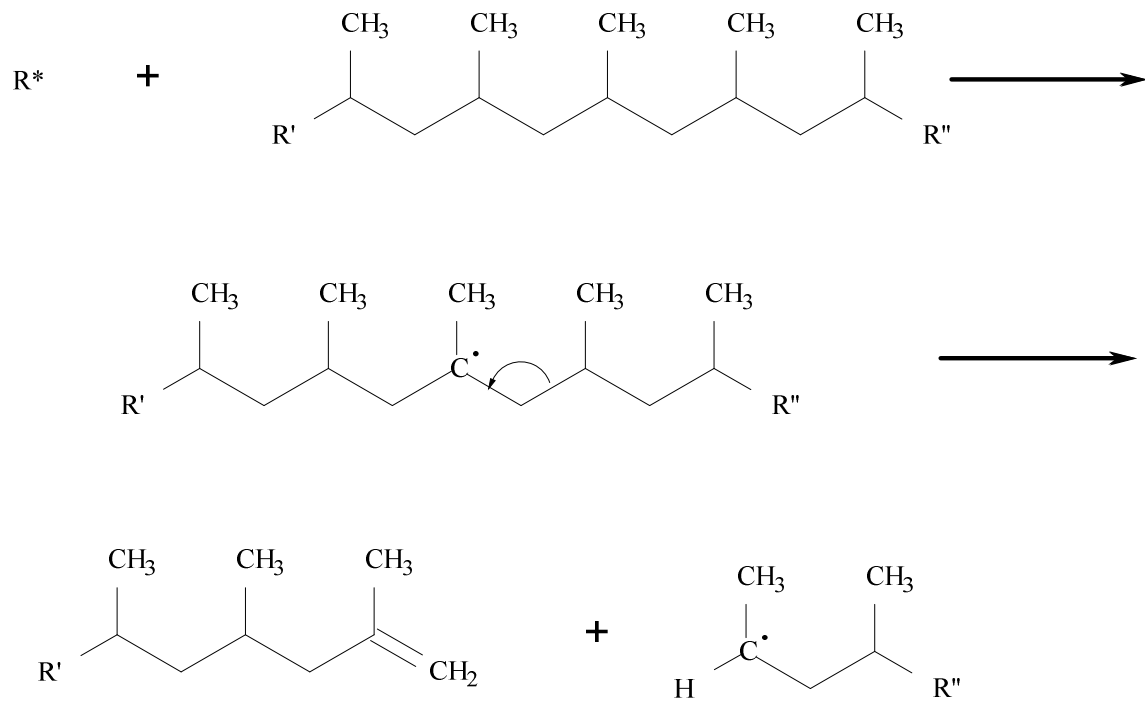


Figure 3-3: β -cleavage causes reduction of polypropylene chain length

Apart from controlled polymer degradation in the presence viscosity breaking additives also uncontrolled polymer scission can occur. Since this interferes with the fiber formation by changing from jetting to dripping mode, longer term exposure of the polymer melt to higher temperatures should be avoided [6, 10].

A reduction of the process viscosity at low temperature without affecting the polymer chain length can be affected by internal slipping agents, which are compatible to the molten polymer at the processing temperature range [7, 8, 15, 17]. Slipping agents can be small molecules or nanoparticles which interfere with the polymer chains [7, 15]. This leads to a reduced melt viscosity without reducing the number of entanglements [15]. Stearates are usually used to reduce the frictional forces between an outer wall (e.g. spinneret) and polypropylene melts.

With nanoparticles, Mackay et al. could reduce the melt viscosity of polystyrene to 80 % [3, 8, 17]. Incorporation of the small particles into the polymer melts obviously can reduce the entanglements with minimal changes in radius of gyration [8].

3 Experimental

3.1 Electrospinning

The electrospinning device consists of a high voltage supply (Eltex KNH34 purchased from Eltex Elektrostatic GmbH, Weil am Rhein, Germany), a cylindrical (used to collect parallelly oriented fibers) or a flat target (for non-woven), a syringe pump (type HA 11 plus Harvard Apparatus purchased from Hugo-Sachs Elektronik GmbH, March-Hugstetten, Germany), a heating chamber (manufactured by DWI workshop) and a heat gun (Leister, purchased from Klappenbach GmbH, Hagen, Germany). The collection distance was varied between 40-80 mm. The flow rate was fixed at 0.2 mL/h and the electric field strength was altered from 2-7.5 kV/cm. The first electrospinning device shown in Figure 3-4 was used to test the productivity of the polymer to be electrospun. The electrospinning system was subsequently modified into the electrospinning device shown in Figure 3-5, where a heat gradient was introduced between the electrodes to enable the introduction of whipping instability for further stretching of the polypropylene fibers. The heat gradient was created by blowing a portion of a hot air blown by the heat gun through the lower orifice of the heating chamber as shown in Figure 3-5.

Polymer sticks were filled into 2 mL glass syringes and molten at varying temperatures in the heating chamber by a heat gun. The temperatures investigated for melt electrospinning ranged from 220°C to 275°C. The warm air-current provided a technical feasible heat source and allowed working with high melting polymers. The heating chamber enabled homogeneous distribution of the temperature around the syringe. A high positive voltage was applied to the spinneret and the fibers were collected either onto a grounded rotating aluminum cylinder (diameter 80 mm, length 100 mm) or a grounded aluminum plate. The grounded cylinder was rotated at a speed of 2000 rpm. Both collectors were covered with aluminum foil.

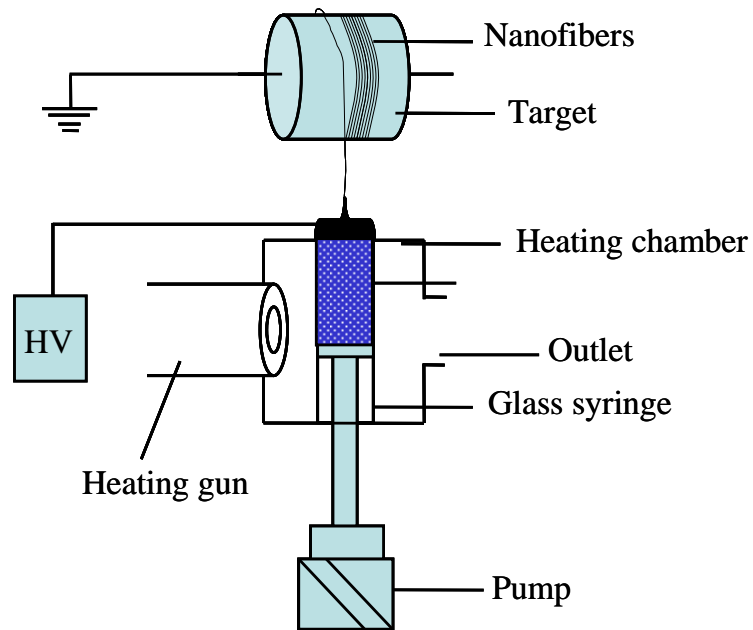


Figure 3-4: Schematic illustration of the setup of the electrospinning device using a rotating cylinder as target for collection of aligned fibers.

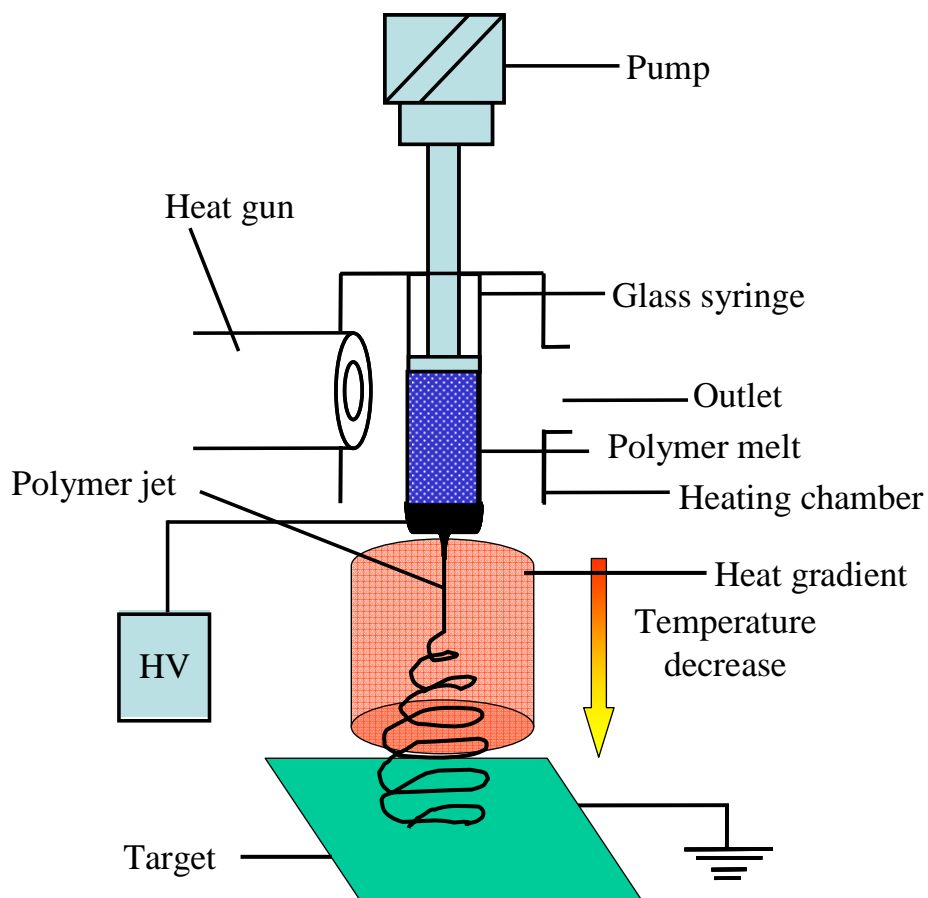


Figure 3-5: Schematic illustration of the setup of the electrospinning device using a flat aluminum plate as target for collection of non-wovens.

3.2 Materials

3.2.1 Isotactic polypropylene

Isotactic polypropylenes (i-PP) with molecular weights 12000, 190000, 250000, 340000 and 580000 g/mol were purchased from Aldrich-Sigma (Taufkirchen, Germany). Further on these polymers are referred to as PP 12000, PP 190000, PP 250000, PP 340000 and PP 580000. In addition i-PP HL 504 FB with Mw 181000 g/mol was purchased from Borealis (Gent, Belgium) and Profax PF 814 as long chain branched polypropylene (Mw 1157 000 g/mol) was purchased from Basell Polyolefine GmbH (Mainz, Germany).

3.2.2 Preparation of polypropylene blends

Blends of short chain i-PP (SCPP = PP 12000) and long chain i-PP (LCPP = PP 190000, PP 250000, PP 340000 and PP 580000) were prepared by mixing them in a Plastograph[®] kneader type 30 EHT with rheometer (Brabender[®] GmbH and Co. KG, Duisburg, Germany) and kneading at 200°C with mass ratio (SCPP : LCPP): (99:1, 95:5, 90:10, 80:20, 60:40, 40:60 and 20:80)

3.2.3 Additives

As slipping agents, PDMS (poly dimethylsiloxane), purchased from DOW Cогins, and sodium stearate were used in this chapter. PAOS (polyalkoxysilane) was synthesized by one pot synthesis via catalytic condensation of TEOS (tetraethoxysilane) with acetic anhydride according to the following mechanism [18-20]:

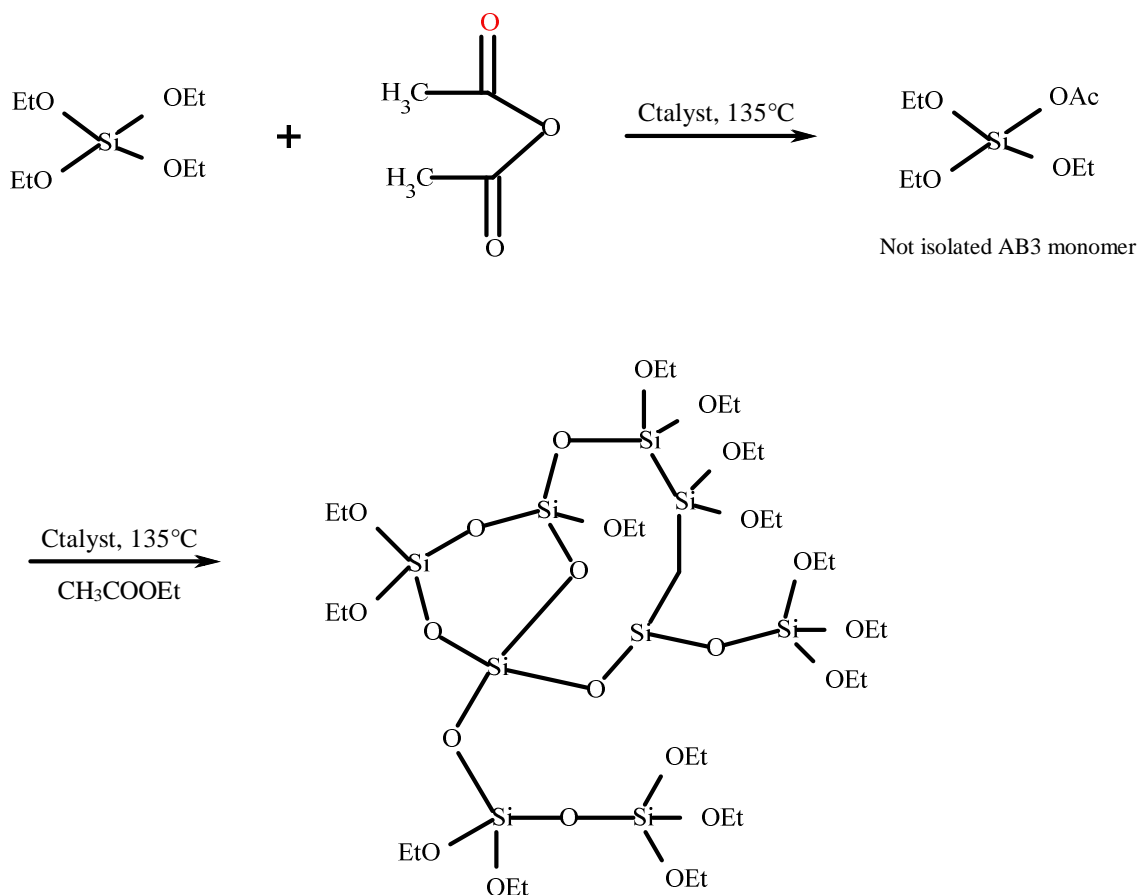


Figure 3-6: One pot catalytic condensation synthesis of PAOS

Sodium stearate was synthesized by esterification reaction using ethanol as a solvent. Stearic acid and sodium hydroxide were purchased from Sigma Aldrich (Taufkirchen, Germany), dissolved in ethanol and mixed. Sodium stearate was isolated by evaporation of ethanol using a rotary evaporator.

Alkoxyamine Irgatec CR 76 was purchased from Ciba Spezialitätenchemie Lampertheim GmbH (Lampertheim, Germany) and Di-tertbutylperoxide was obtained from Sigma-Aldrich (Taufkirchen, Germany). Both auxiliaries were used as viscosity breaking additives as received.

Addition of auxiliaries was performed using a twin screw extruder. The mixtures were prepared in the form of sticks by injection of the mixtures into a stick form mold.

3.3 Characterization methods

The viscosities of polypropylene blends and mixtures were measured by a stress controlled cone-plate rheometer of type DSR SR-200 (Rheo service, Reichelsheim, Germany) applying shear rates between 0.5-1000 s⁻¹. The melt viscosity was measured at 220°C, as most of the blended materials were electrospun at this temperature.

Fibers were characterized by scanning electron microscopy (Hitachi S-3000 N, Hitachi High-Technologies Europe GmbH, Krefeld, Germany). For analysis, the aluminum foil with the electrospun fibers was fixed onto an aluminum SEM stub and subsequently gold-coated and analyzed. An electron beam of 15 kV and working distance of 7-15 mm were used to image the electrospun material. The presented fiber diameters were measured using representative images of the electrospun fibers (average numbers of 200 independent measurements).

For thermal analysis, dynamic scanning calorimeter (DSC) measurements of the spun fibers were performed on a Perkin Elmer DSC. A sample of 7-10 mg was closed in an aluminum pan and measured at heating rate of 10°C/min from 50 to 200°C.

3.4 Results and discussion

3.4.1 Influence of melt temperature

Due to the temperature influence on melt viscosity, the initial investigations on the spinning performance were carried out at temperature range between 190°C and 240°C for polypropylene (Mw: 190000 g/mol) blended with 4 wt.-% sodium stearate. Figure 3-7 shows the relation between temperature of the melt and zero shear viscosity which is reduced with increasing temperature. Arising the melt temperature from 185°C to 205°C results in significant fiber diameter reduction from 22 ± 9.7 μm to 1.8 ± 1.3 μm. Above 205°C no further reduction in fiber diameter was detected. This already demonstrates that the melt temperature influences the resulting diameters of electrospun fibers to a special extent.

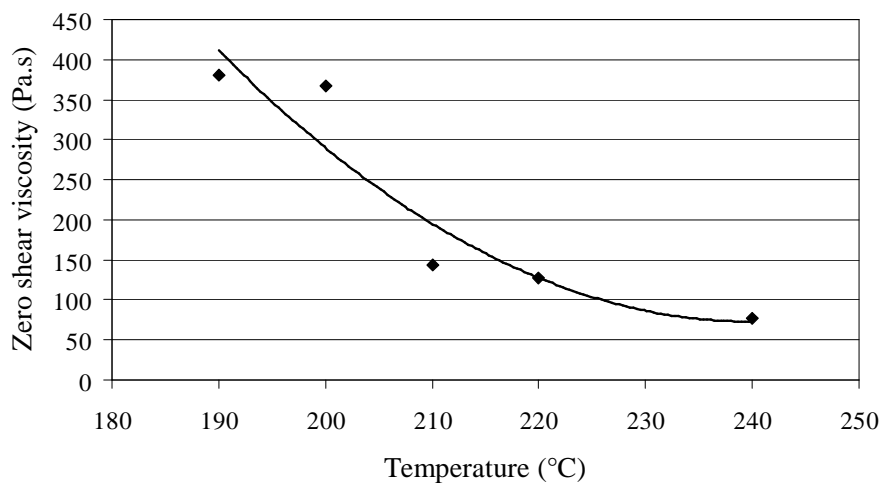


Figure 3-7: Relation between temperature and zero shear viscosity for PP 190000 containing 4 wt.-% sodium stearate.

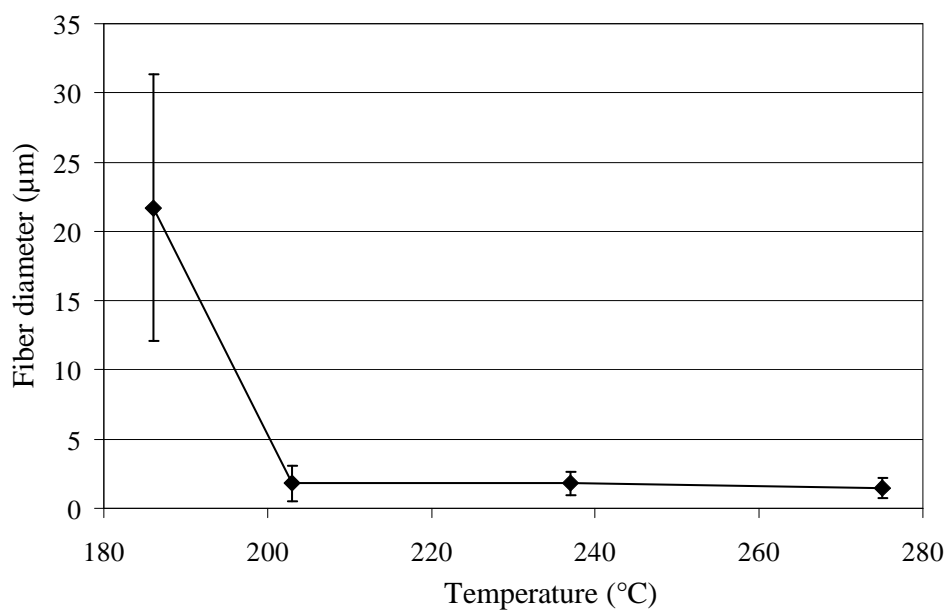


Figure 3-8: Relation between temperature and fiber diameter for PP 190000 containing 4 wt.-% sodium stearate electrospun at applied voltage 25 kV and the distance between electrodes of 8 cm.

3.4.2 Influence of molecular weight

The zero shear viscosity increases with the length of polypropylene chain by increased chain entanglements. This is shown in Table 3-1 for different polypropylene types with a molecular weights of 12 000 g/mol and 580 000 g/mol.

Table 3-1: Ranges of zero shear viscosities of different molecular weights polypropylenes measured at 220°C.

| Polypropylene | Zero shear viscosity (Pa.s) |
|---------------|-----------------------------|
| PP 12000 | 0.51 |
| PP 190000 | 860 |
| PP 250000 | 3006 |
| PP 340000 | 5686 |
| PP 580000 | 14992 |

With special regard to the spinning performance of these materials only with lower molecular weight polypropylene (12 000 g/mol) fibers were obtained, Figure 3-9. This is due to the low melt viscosity (zero shear viscosity = 0.51 Pa.s).

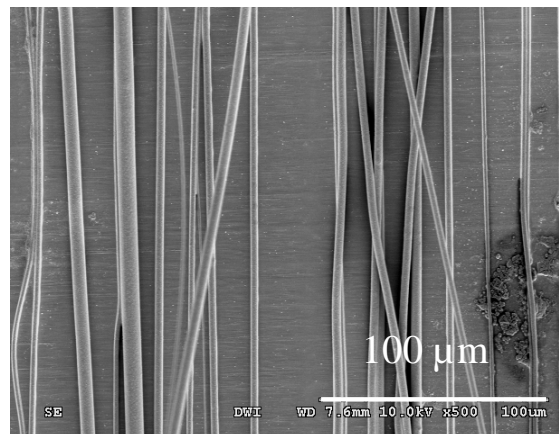


Figure 3-9: SEM graph of melt electrospun polypropylene fibers of molecular weight 12000 g/mol produced at flow rate 0.2 ml/h, applied voltage 26.5 kV/cm, distance between electrodes of 4 cm and rotation speed 2000 RPM.

The alignment of the fibers in Figure 3-9 results from using a rotating collector at a rotation speed of 2000 RPM. Therefore, it cannot be excluded that the fibers were additionally stretched by mentioned forces resulting from the movement of the collector.

3.4.3 Polypropylene with bimodal molecular weight distribution

The melt viscosity can be influenced by addition of short polymer chains to longer ones to enhance the electrospinnability of higher molecular weight polypropylenes. The zero shear viscosity is also increasing with the portion of higher molecular weight polypropylene in blended polypropylenes due to increase of entanglements between polymer chains. This can be seen in Table 3-2 for different polypropylene blends of PP 12000 containing different concentrations of PP 190000.

Table 3-2 : Zero shear viscosity ranges of blends mass ratios for the blend PP 190000 and PP 12000 measured at 220°C.

| PP blends | Zero shear viscosity (Pa.s) |
|----------------------------------------|------------------------------------|
| 60 wt.-% PP 190000 + 40 wt.-% PP 12000 | 75 |
| 80 wt.-% PP 190000 + 20 wt.-% PP 12000 | 112 |
| 90 wt.-% PP 190000 + 10 wt.-% PP 12000 | 156 |
| 99 wt.-% PP 190000 + 1 wt.-% PP 12000 | 240 |
| PP 190000 | 860 |

The increase in zero shear viscosity influences the fiber diameter independently on the electric field strength as shown in Figure 3-10. By increasing the mass fraction of long polymer chain, the fiber diameter is consequently increased.

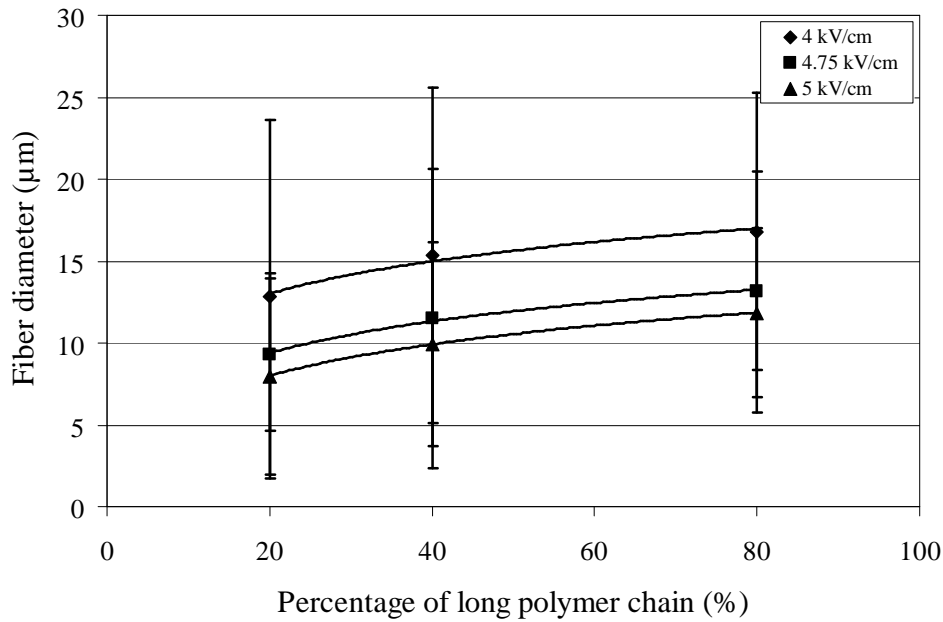


Figure 3-10: Relation between the concentration of PP 190000 in PP 12000 and fiber diameter for fibers electrospun at 4, 4.75 and 5 kV and at distance between electrodes 4 cm.

This is consistent with the zero shear viscosity, Table 3-2 caused by increasing the possibility of long chains to entangle with each other.

Table 3-3: Molecular weight of LCPP and zero shear viscosity measured at 220°C.

| PP blends | Zero shear viscosity (Pa.s) |
|----------------------------------------|-----------------------------|
| 40 wt.-% PP 190000 + 60 wt.-% PP 12000 | 51 |
| 40 wt.-% PP 250000 + 60 wt.-% PP 12000 | 92 |
| 40 wt.-% PP 580000 + 60 wt.-% PP 12000 | 1688 |

As hypothesis it was supposed that the produced fiber diameter of electrospun fibers increases together with the increasing chain length of LCPP. In contrast Figure 3-11 shows that the electrospun fiber diameters (at different electric field strengths) are reduced with increasing chain length of LCPP.

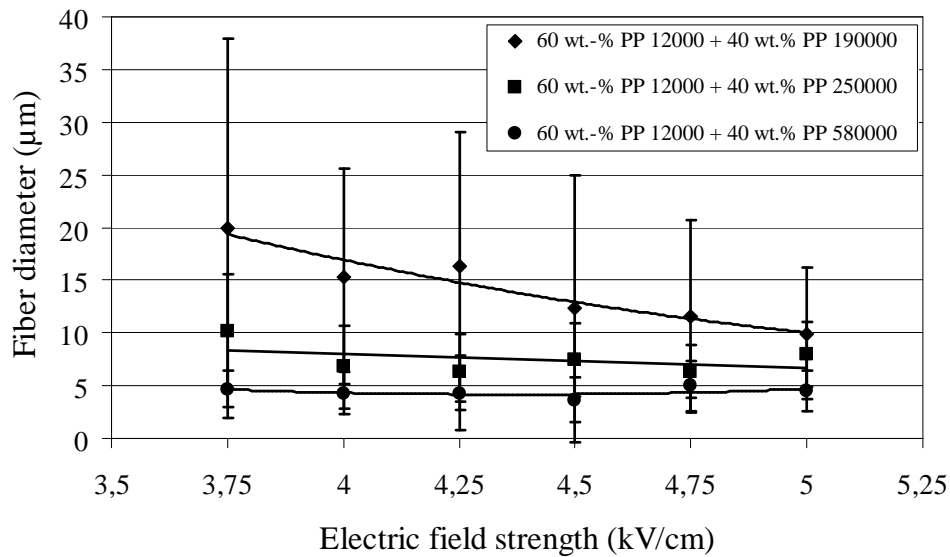


Figure 3-11: Relation between electric field strength and fiber diameter of different polypropylene blends electrospun at different electric field strength, applied voltage ranged from 15-20 kV and at distance between electrodes 4 cm.

This might be due to existence of an equilibrium between relaxation time and deformation of the polypropylene fibers before solidification, i. e. the deformation of fibers will be reduced by increasing of the relaxation time resulting in formation of thin fibers.

3.4.4 Influence of molecular structure

Long chain branched polypropylene molecules are used to reduce the melt viscosity of the lower polypropylene types. Figure 3-12 shows that the melt viscosity is reduced around 33% by addition of Profax PF 814.

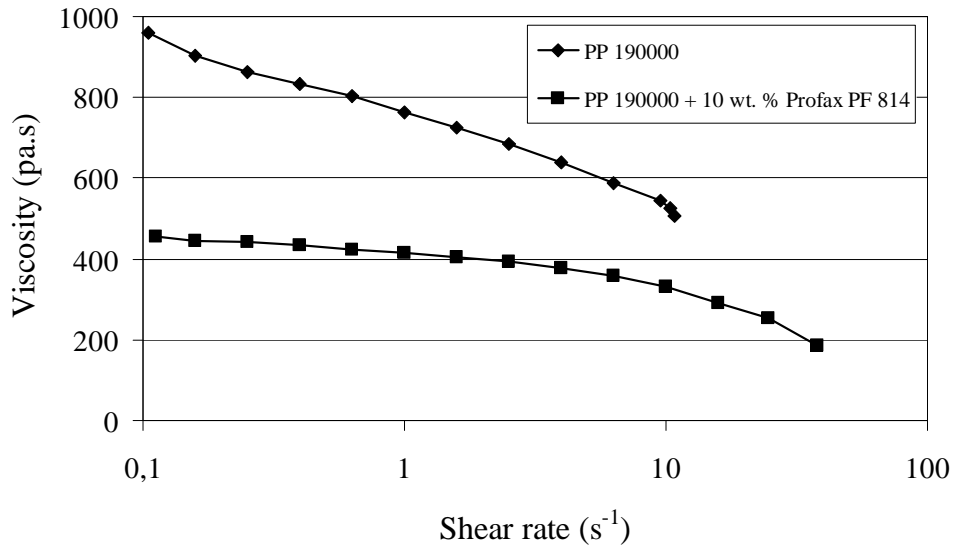


Figure 3-12: Relation between molecular structure and melt viscosity of the produced polypropylene mixture containing 10 wt.-% Profax PF 814 and PP 12000.

By electrospinning of the polypropylene blend containing Profax PF 814, the resulted electrospun fiber diameters are larger than of electrospun PP 190000, Figure 3-13. This might be due to the high expansion rate of Profax PF 814 in molten phase as a consequence of its nature and exhibits a pronounced strain hardening resulting in limiting of the polymer stretching by electrical forces [21].

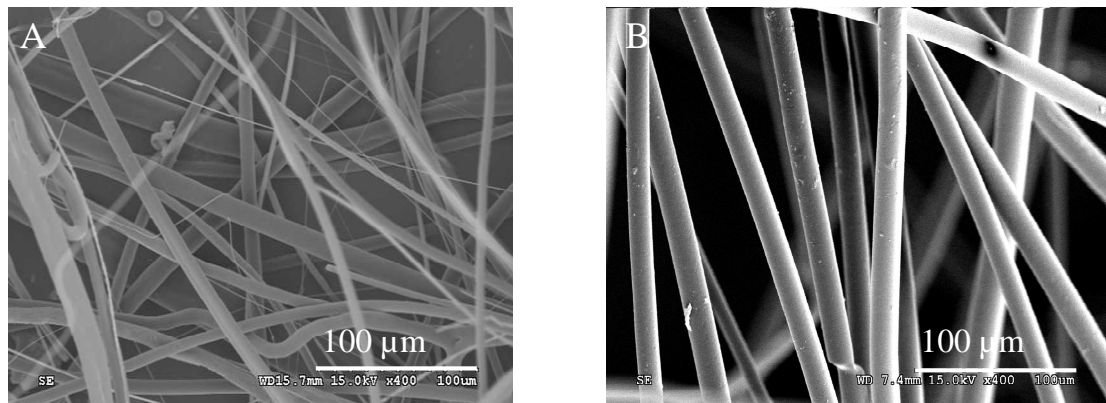


Figure 3-13: SEM graphs show electrospun polypropylene fibers of PP 190000 (A) and PP 190000 containing Profax PF 814 (B) electrospun at electric field strength 3.13, Applied voltage 25 kV and the distance between electrodes of 8 cm.

3.4.5 Effect of slipping agents

3.4.5.1 Influence of type of slipping agent

By addition of small molecules or nanoparticles which are compatible to the polypropylene matrix melt viscosity of high molecular weight polypropylene can be altered. To check the performance of the slipping agents on reduction of melt viscosity different slipping agents were mixed with PP 190000. Table 3-4 shows that sodium stearate reduced the zero shear viscosity significantly rather than the used nanoparticles PAOS and PDMS. This could be due to the limited miscibility of PAOS and PDMS in PP matrix comparable to the miscibility of sodium stearate [22].

Table 3-4: Zero shear viscosity ranges of polypropylene mixtures containing different types of slipping agents measured at 220°C.

| Polypropylene mixture | Zero shear viscosity (Pa.s) |
|------------------------------------------|------------------------------------|
| PP 190000 | 860 |
| 99 wt.-% PP 190000 + 1 wt.-% PDMS | 426 |
| 99 wt.-% PP 190000 + 1 wt.-% PAOS | 352 |
| 95 wt.-% PP 190000 + 5 wt.-% Na-stearate | 262 |

As a result of melt viscosity reduction by slipping agents, electrospun fibers were found to be smaller in size with narrower fiber diameter distribution compared to electrospun PP 190000 (shown in Figure 3-14).

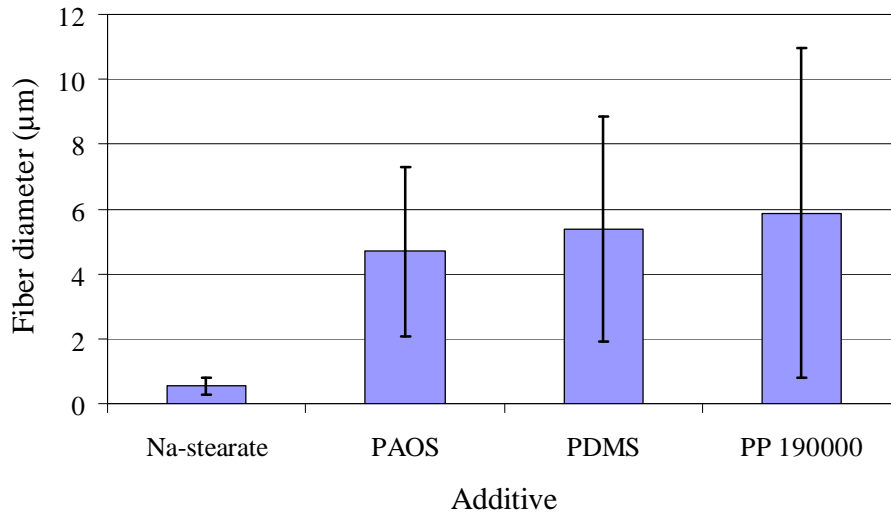


Figure 3-14: Fiber diameter ranges of polypropylene fibers containing different types of slipping agents electrospun at electric field strength 3.13 kV/cm, applied voltage 25 kV and at distance between electrodes 8 cm.

Figure 3-14 shows that by addition of sodium stearate fine fibers in the range of 0.54 ± 0.26 μm were generated. This can be attributed to the small size of the stearate molecules which assists it to interfere with the polymer chains resulting in reduction of the melt viscosity. Therefore, sodium stearate has been chosen as slipping agent for further experiments due its potential of generating of ultra-fine fibers.

3.4.5.2 Effect of slipping agent concentration

With the feasibility of producing ultrafine fibers by compounding polypropylene with sodium stearate, the influence of concentrations of sodium stearate was tested with specific regard to melt viscosity, resulting fiber diameter and fiber properties. Figure 3-15 shows that by addition of only 1 wt.-% sodium stearate melt viscosity was reduced significantly. Further observable reduction occurs at concentrations higher than 2 wt.-%.

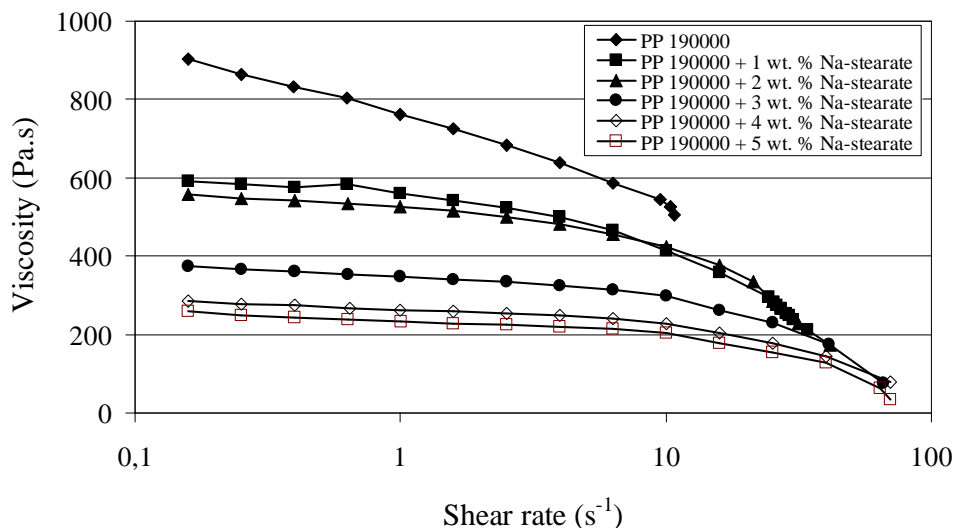


Figure 3-15: Melt viscosity ranges of different polypropylene mixtures containing different concentrations of sodium stearate.

Figure 3-16 shows that by increasing the amounts of sodium stearate, fiber diameters were reduced from $1.77 \pm 0.90 \mu\text{m}$ to $0.55 \pm 0.26 \mu\text{m}$ and their homogeneity were increased.

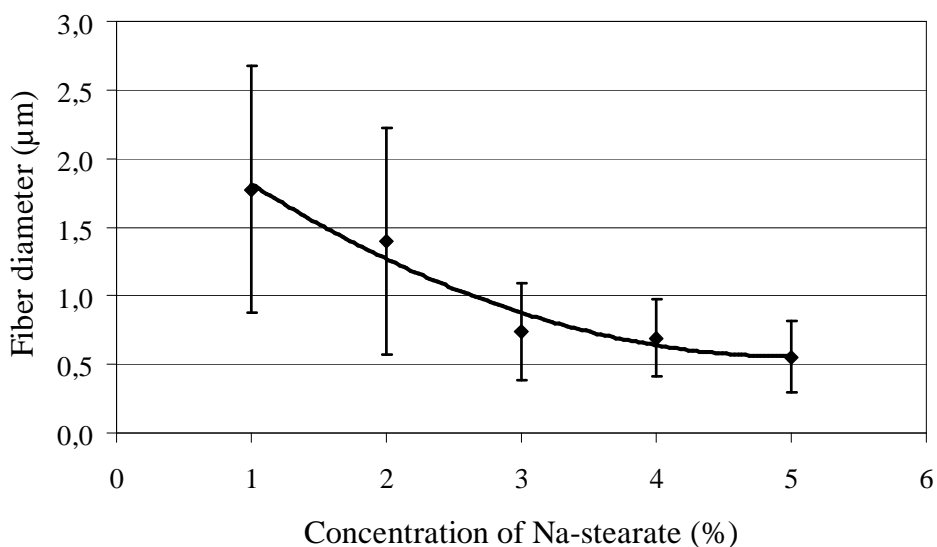


Figure 3-16: Relation between concentration of sodium stearate and fiber diameter of fibers electrospun at electric field strength 2.75 kV/cm, applied voltage 22 kV and at distance between electrodes 8 cm.

This leads to the assumption that the existence of sodium stearate in concentrations above 2 wt.-% possibly not only acts as an outer slipping agent but also reduces crystallinity. Figure 3-

17 shows that by addition of sodium stearate, the melt enthalpy is significantly reduced from 115 J/g down to 82.5 J/g.

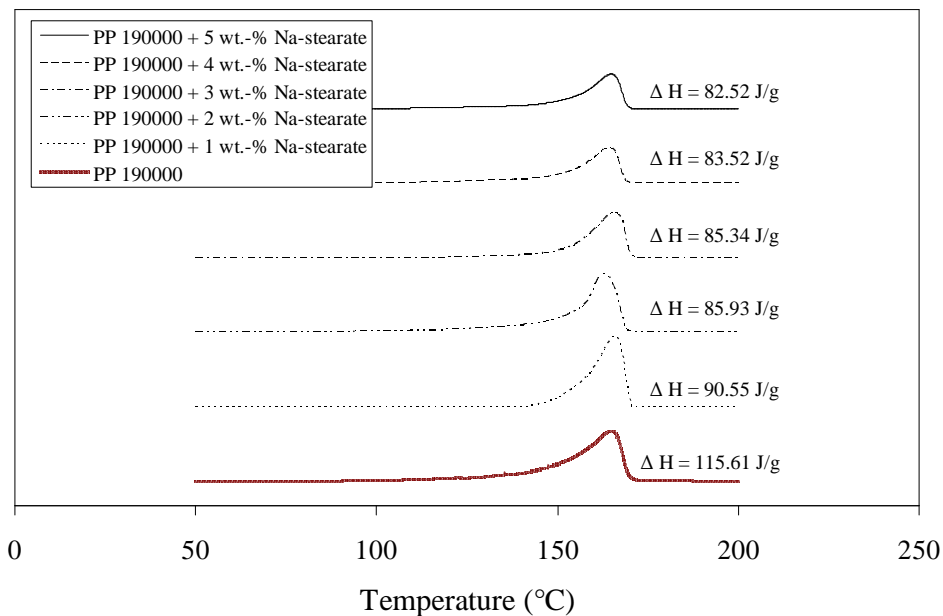


Figure 3-17: DSC measurements show the reduction of degree of crystallization by addition of sodium stearate.

This indicates that sodium stearate at high concentrations reduces the crystal formation. This obviously has consequences for the accessible fiber fineness. SEM graphs in Figure 3-18 shows that by reduction of melt viscosity and degree of crystallization; polypropylene fibers down to 500 nm were resulted indicating that the reduction of crystallinity of PP is an essential factor for generating of nanoscaled fibers via electrospinning.

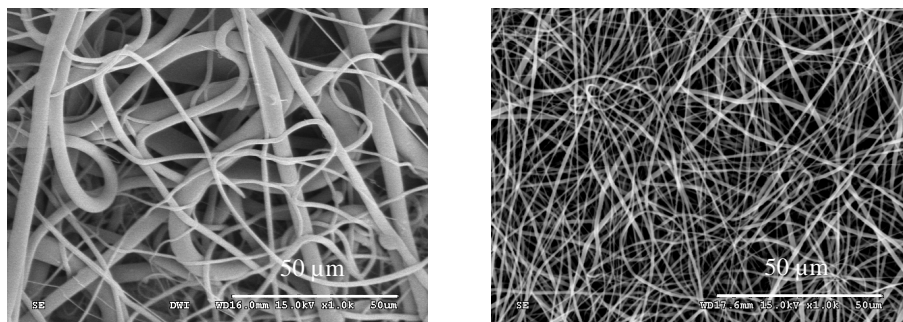


Figure 3-18: SEM graphs shows electrospun polypropylene fibers containing sodium stearate electrospun at electric field strength 2.75 kV/cm, applied voltage 22 kV and at distance between electrodes of 8 cm. Left: Polypropylene fibers containing 1 wt.-% sodium stearate (fiber diameter: $1.79 \pm 1.23 \mu\text{m}$). Right: Polypropylene fibers containing 5 wt.-% sodium stearate (fiber diameter: $0.552 \pm 0.26 \mu\text{m}$).

3.4.6 Influence of viscosity breaking agents

3.4.6.1 Type of viscosity breaking agent

In order to test the efficiency of viscosity breaking agents on the melt viscosity of polypropylene, Irgatec CR 76 (Nitroxide radicals) and Di-tertbutylperoxide were mixed with HL 504 FB by twin mini-lab extruder at 200°C and electrospun at electric field strength 3.13 kV/cm. It was detected that the mixture containing peroxides has lower viscosity than that containing nitroxide auxiliaries as shown in Table 3-5.

Table 3-5 Zero shear viscosity of polypropylene mixtures containing radical auxiliaries

| Polypropylene mixture | Zero shear viscosity (Pa.s) |
|------------------------------------------|-----------------------------|
| HL 504 FB | 56 |
| HL 504 FB + 1 wt.-% Irgatec CR 76 | 49 |
| HL 504 FB + 1 wt.-% Di-tertbutylperoxide | 15 |

This result has an influence on the electrospun fiber diameter and fiber homogeneity. Figure 3-19 shows that the fiber diameter containing peroxides are thicker than fibers containing nitroxides auxiliaries. This could be due to the sudden viscosity reduction because of the high chain scission rate caused by peroxides. This results in increasing of the flow rate to the limit which is not more controllable.

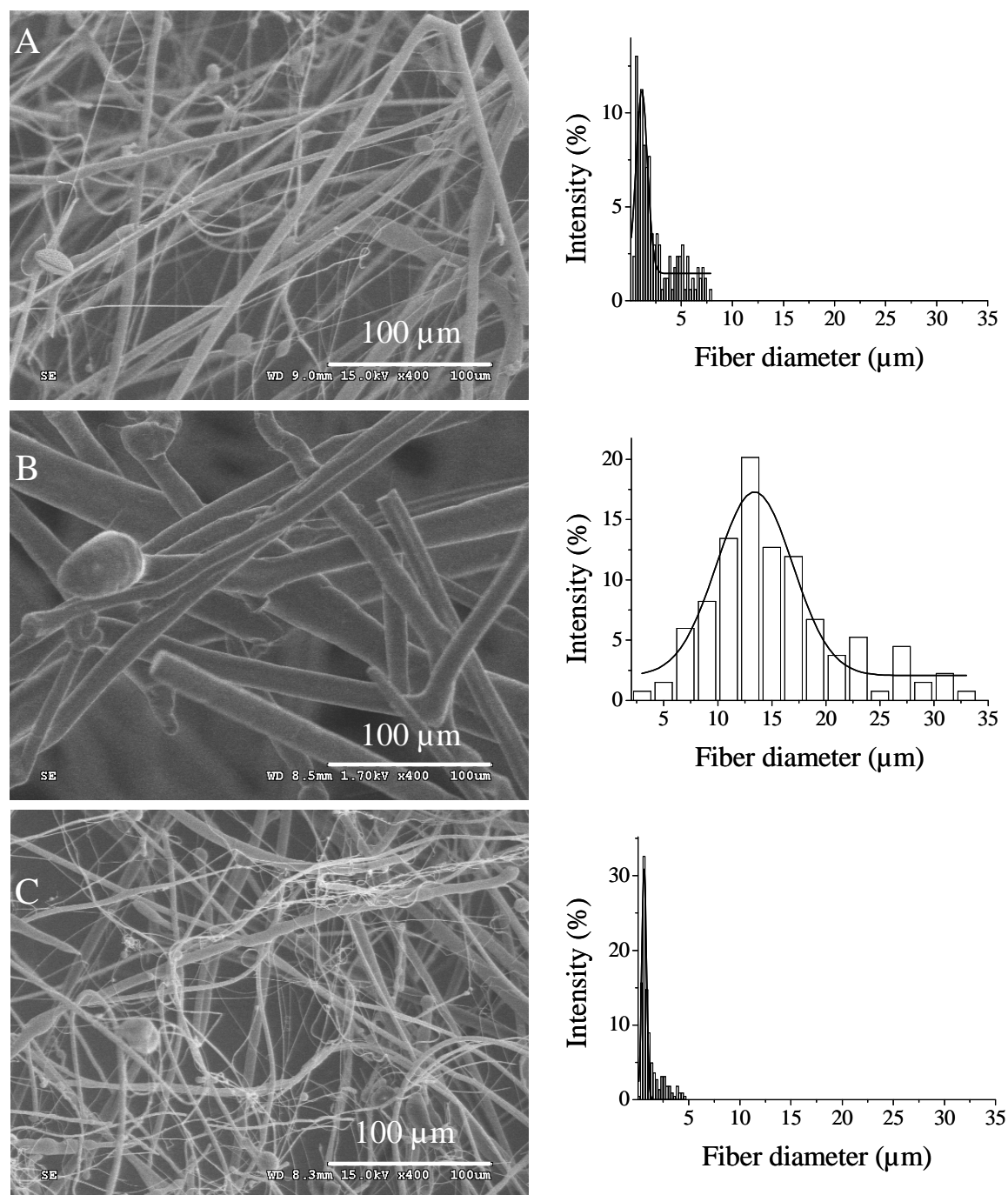


Figure 3-19: SEM graphs shows polypropylene fibers electrospun at electric field strength 3.13 kV/cm, applied voltage 18 kV and at the distance between electrodes 8 cm. A: HL 504 FB (fiber diameter: $2.80 \pm 2.61 \mu\text{m}$), B: HL 504 FB containing di tert. butyl peroxide (fiber diameter: $1.21 \pm 1.07 \mu\text{m}$) and C: HL 504 FB containing Irgatec CR 76 (fiber diameter: $15.26 \pm 6.08 \mu\text{m}$). The fiber diameter distributions show that fibers contain nitroxide radicals is smaller in size with narrower fiber diameter distribution than those fibers contain peroxide radicals.

3.4.6.2 Effect of degradation time and amount of viscosity breaking agent

The chain scission process can be continued during melt electrospinning by already formed radicals resulting in changed fiber properties with time. For this, it is necessary to regulate the chain scission process during electrospinning to keep the fiber properties as long as melt electrospinning occurs. Therefore, sodium stearate was added to polypropylene containing different concentrations of Irgatec CR 76 to reduce the chain scission through chelating of stearate molecules with acid scavengers resulted from catalytic synthesis of polypropylene and to test the effect of vis-breaking agent concentration on the electrospun fiber diameter. Figure 3-20 shows that the electrospun fiber diameter is reduced with increasing the amount of Irgatec CR 76 and most of the obtained fibers have diameters below 1 μm . This indicates that by increasing the radical concentration, more active species exist in the polypropylene matrix and the scission rate is increased.

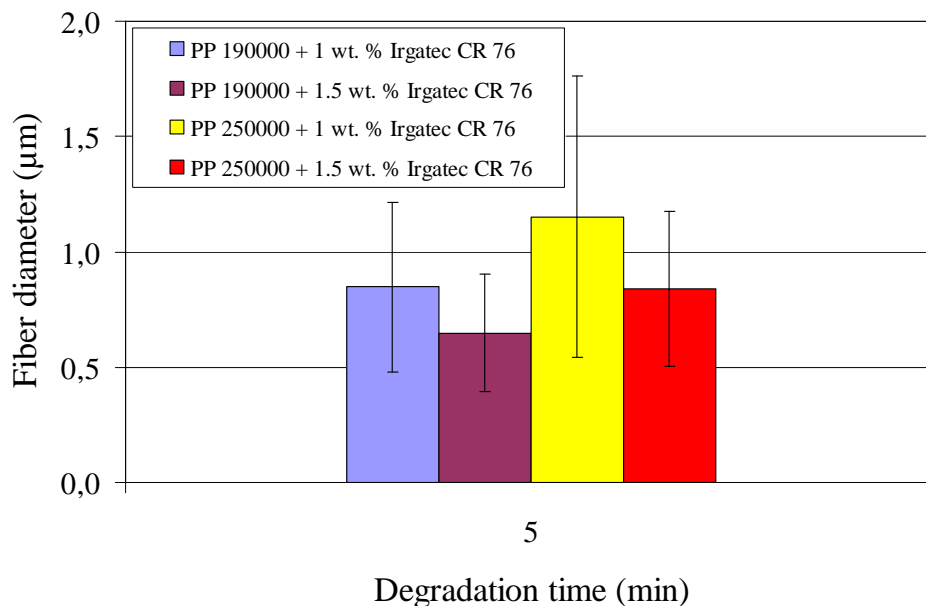


Figure 3-20: Relation between the amount of radicals and fiber diameter of polypropylene fibers containing 5 wt.-% sodium stearate electrospun at electric field strength 3.13, applied voltage 25 kV and at the distance between electrodes of 8 cm.

In absence of sodium stearate, the scission process takes place in vigorous way as the acid scavengers facilitate the chain scission rate. This can be shown in Figure 3-21 when polypropylene HL 504 FB containing 1 wt.-% Irgatec CR 76 was electrospun at different time intervals. Figure 3-21 shows that by increase the duration of electrospinning, beads start to

Chapter 3: Influence of melt viscosity on melt electrospinning process: Effect of 61 degradation time and amount of viscosity breaking agent

appear. After 10 minutes of starting electrospinning the bead-free fibers are not produced due to uncontrolled chain degradation as a result of long heating periods. As a consequence of that, the jetting mode of the polymer jet was replaced by dripping mode.

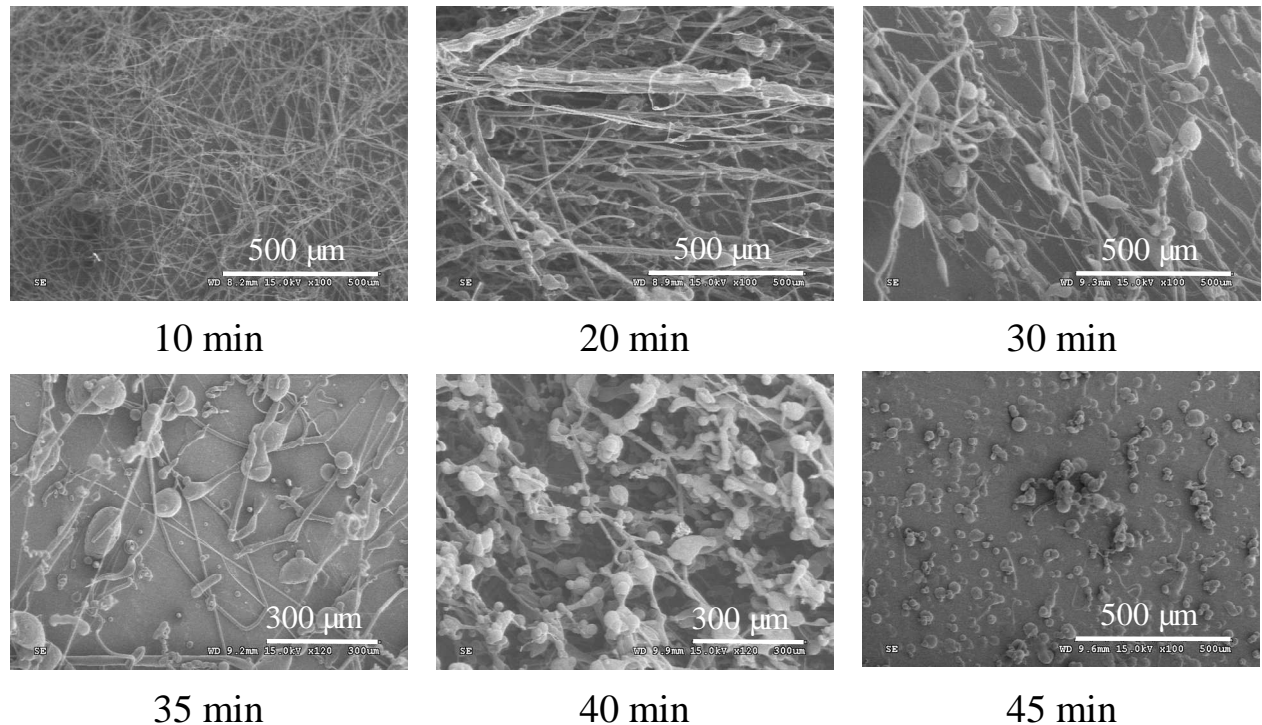


Figure 3-21: SEM graphs shows the developing of morphology of the electrospun polypropylene fibers (PP HL 504 FB containing 1.5 wt.-% Irgatec CR 76) at different electrospinning durations at electric field strength 3.13 kV/cm, applied voltage 25 kV and at the distance between electrodes of 8 cm.

4 Summary

Melt viscosity is a crucial factor in melt electrospinning; it enhances or retards the stretching of the polymer jet by electrical forces. The melt viscosity of polypropylene can be modified by increasing the temperature, mixing different chain lengths of the polymer, adding slipping agent, or of viscosity breaking agents.

Increase the melt temperature can reduce the fiber diameter significantly; however, overheating of the polymer has to be avoided to prevent degradation of the polymer.

Polypropylene blends modified with only short chain length polymer and containing no other additive can be electrospun. However, the smallest fiber diameter can be obtained was larger than 1 μm .

Further reduction of fiber diameter was obtained by reduction of melt viscosity and degree of crystallization by addition of sodium stearate. Sodium stearate at low concentration is acting as an outer slipping agent; however, by increasing its concentration, it significantly reduces the diameter of the generated fibers into the range of 500 nm. This is due to its propensity in districting of crystallization of polypropylene when added in high concentrations.

Using nitroxide and peroxide radicals in electrospinning has to be controlled, as the degradation process can continue during the electrospinning process. Degradation process can be slowed down by addition of stearates as chelating agents for acid scavengers. Results show the possibility to produce fibers with diameters smaller than 1 μm . In absence of stearate, the fiber morphology is changed with electrospinning time resulting in formation of beaded fibers and finally beads at longer electrospinning duration more than 10 minutes.

5 References

1. Webster, J. G. *The Measurement, Instrumentation and Sensors Handbook*; CRC Press LLC, Boca Raton, **1999**, 1500.
2. Hiemenz, P. C. *Polymer Chemistry the Basic Concepts*; Marcel Dekker Inc., New York, **1996**, 736.
3. He, J.-H.; Wan, Y.-Q.; Yu, J.-Y. Allometric Scaling and Instability in Electrospinning. *Int J Nonlinear Sci* **2004**, *5*, 243-252.
4. Struglinski, M.; Graessley, W.; Fetters, L. Effects of Polydispersity on the Linear Viscoelastic Properties of Entangled Polymers. 3. Experimental Observations on Binary Mixtures of Linear and Star Polybutadienes. *Macromolecules* **1998**, *21*, 783-789.
5. Fetters, L.; Lohse, D.; Milner, S.; Graessley, W. Packing Length Influence in Linear Polymer Melts on the Entanglement, Critical, and Reptation Molecular Weights. *Macromolecules* **1999**, *32*, 6847-6851.
6. Ramakrishna, S.; Fujihara, K.; Teo, W.-E.; Lim, T.-C.; Ma, Z. *An Introduction to Electrospinning and Nanofibers*; World Scientific Printers, Singapore, **2005**, 425.
7. Jahani, Y.; Barikani, M. Effect of Side Chain Branched Pp, Epdm and Hdpe as a Third Component on Melt Extensional Behaviour of Ternary Blends. *Iran Polym J* **2005**, *14*, 693-704.
8. Tuteja, A.; Mackay, M.; Hawker, C.; Horn, B. V. Effect of Ideal, Organic Nanoparticles on the Flow Properties of Linear Polymers: Non-Einstein-Like Behavior. *Macromolecules* **2005**, *38*, 8000-8011.
9. Graessley, W. W. Entangled Linear, Branched and Network Polymer Systems - Molecular Theories *Adv Polym Sci* **1982**, *47*, 67-117.
10. Warner, S.; Buer, A.; Grimler, M.; Ugbohue, S.; Rutledge, G.; Shin, M. A Fundamental Investigation of the Formation and Properties of Electrospun Fibers; M98-D01, **1999**, 1-10.
11. Ellison, C.; Phatak, A.; Giles, D.; Macosko, C.; Bates, F. Melt Blown Nanofibers: Fiber Diameter Distributions and Onset of Fiber Breakup. *Polymer* **2007**, *48*, 3306-3316.
12. Barnes, H. A. *A Handbook of Elementary Rheology*; University of Wales Institute of Non-Newtonian Fluid Mechanics, Wales, **2000**, 210.
13. Münstedt, H.; Laun, H. Elongational Behaviour of Low Density Polyethylene Melt II. Transient Behaviour of Constant Stretching Rate and Tensile Creep Experiments. Comparison with Shear Data. Temperature Dependence of the Elongational Properties. *Rheol Acta* **1979**, *18*, 492-504.
14. Lyons, J. Melt-Electrospinning of Thermoplastic Polymers : An Experimental and Theoretical Analysis. PhD. Thesis, Drexel University, Philadelphia, **2004**.

15. Hassounah, I.; Thomas, H.; Moeller, M. Obtaining Poly(Propylene) Nanofibers by Melt Electrospinning through Additives, Second Aachen-Dresden International Textile Conference, Dresden, Germany, 26-27.11.2008.
16. Moore, E. P. *Polypropylene Handbook*; Hanser/Gardner Publications, Inc. / Hanser Publishers, Munich, New York, Cincinnati, **1996**, 420.
17. Mackay, M. E.; Dao, T.; Tuteja, A.; Ho, D.; Horn, B. V.; Kim, H.-C.; Hawker, C. Nanoscale Effects Leading to Non-Einstein-Like Decrease in Viscosity. *Nat Mater* **2003**, *2*, 762-766.
18. Jaumann, M.; Rebrov, E.; Kazakova, V.; Muzafarov, A.; Goedel, W.; Möller, M. Hyperbranched Polyalkoxysiloxanes Via AB(3)-Type Monomers. *Macromol Chem Phys* **2003**, *204*, 1014-1026.
19. Zhu, X.; Peter, K.; Moeller, M.; Melian, C.; Adams-Buda, A.; Demco, D. Hyperbranched Poly Alkoxysiloxane - a Unique Silica Precursor for the Preparation of Nanocomposites. *Polym Prepr* **2006**, *47*, 1133-1134.
20. Zhu, X.; Jaumann, M.; Peter, K.; Möller, M.; Melian, C.; Adams-Buda, A.; Demco, D.; Blümich, B. One-Pot Synthesis of Hyperbranched Polyethoxysiloxanes. *Macromolecules* **2006**, *39*, 1701-1708.
21. Stang, J.; Münstedt, H. Effect of Long-Chain Branching on the Foaming of Polypropylene with Azodicarbonamide. *J Cell Plast* **2006**, *42*, 445-467.
22. Spiegelberg, S.; Alteheld, A.; Zhu, X.; Peter, K.; Möller, M. Method for Producing Composite Materials US 2009/0155562 A1, 18.06.2009.

Chapter 4: The Influence of ambient and processing parameters on melt electrospinning of polypropylene

1 Abstract

With melt electrospinning of polypropylene, polymer nanofibers can be produced via stretching the polymer jet by an external electrical field. Beside the chemical and physical properties of the polypropylene melt which affect the electrospinning process; other parameters play an important role in determining the produced fiber diameter and fiber diameter distribution. The processing and ambient parameters affect the stretching forces which have a direct influence on fiber diameter, fiber morphology and degree of crystallization. In this research polypropylene nanofiber manufacturing processes were optimized. The morphology of the generated nanofibers was characterized by scanning electron microscopy (SEM).

2 Introduction

The generation of nanofibers is of interest for many industrial applications such as filtration and tissue engineering due to their extremely high aspect ratio (high length to diameter ratio). Comparing to the conventional spinning techniques such as melt blown spinning, electrospun nanofibers are created by electrical forces. Nanofibers have been electrospun from the polymer melts and solutions in a cost effective manner suitable for specific applications which do not require large amounts of non wovens.

Besides the generation of nanofibers by solution electrospinning, polymer nanofibers can be generated by melt electrospinning as well. However, few works were done describing the generation of fibers by melt electrospinning [1-5]. The reason behind the existence of few published works in this topic was due to high melt viscosity of the polymer melts which retards the stretching of polymer jet into nanofibers.

In this research, polypropylene was electrospun into nanofibers to generate non-woven for filtration process. Polypropylene has been chosen because of: 1) Its competitive prices comparable to other polymers 2) Commercial availability with wide spectrum of molecular weight and distributions, 3) low glass transition temperature (0°C) and 4) High melting point (160°C). These properties enable us to use polypropylene nanofibers at high service temperatures.

Besides those parameters directly influencing the polymer melts as melt viscosity, processing and ambient parameters including electric field strength, the distance between electrodes or humidity are known to affect the electrospinning process and the resulting fibers. Lyons et al. studied the influence of processing parameters on the generated polypropylene fiber diameter in an attempt to generate ultra-fine fibers. However, he could obtain only fibers above 1 μm [3].

The aim of this research is to generate polypropylene nanofibers via melt electrospinning and to optimize the processing and ambient parameters including electric field strength, flow rate, distance between electrodes, needle diameter ...etc. to generate ultra-fine polypropylene fibers. The high melt viscosity of polypropylene was altered by addition of sodium stearate as slipping agent.

2.1 Influence of the heat gradient

Generally in electrospinning processes, a gap between electrodes exists which facilitates the elongation of the electrospun fibers before solidification on its way to the target. The solidification process occurs in this gap via evaporation of the solvent in case of solution electrospinning or by cooling down of the melt in case of melt electrospinning. In melt electrospinning, heating the region between electrodes enables the polymer jet to remain in the molten phase and additional elongation of the jet/fiber can take place before deposition [6-8]. Too fast or too slow cooling of the polymer jet leads to poor quality fibers [8]. Fast cooling of the polymer jet leads to generation of thick fibers, while slow cooling results in fused fibers on the target due to incomplete solidification of the polymer jet [8].

The heating gradient between the electrodes controls the solidification process and final fiber diameter. A heat gradient with a large hot area facilitates the formation of thin fibers due to an increase of whipping, elongation and thinning before the fiber is collected.

2.2 Influence of the electric field strength

Electric field strength is the force that stretches the polymer solution or melt into fine strands by applying a high voltage [9]. During electrospinning, the shape of the pendant droplet at the tip of the capillary is varied as a result of charge repulsions on the droplet surface which occurs before the critical voltage required ejecting the polymer jet [10-12]. Once the barrier of the critical electric field strength is surpassed, and the balance between electric field strength, viscosity, gravity, aerodynamic, surface tension and inertia forces is established, the pendant droplet is deformed into Taylor cone with a half cone angle around 49.3° [2, 3, 13-15]. In order to obtain a successful constructing of the polymer thread (jet) the electric field strength has to overcome the other forces affecting the formation of the parent polymer jet, see Figure 4-1 [16].

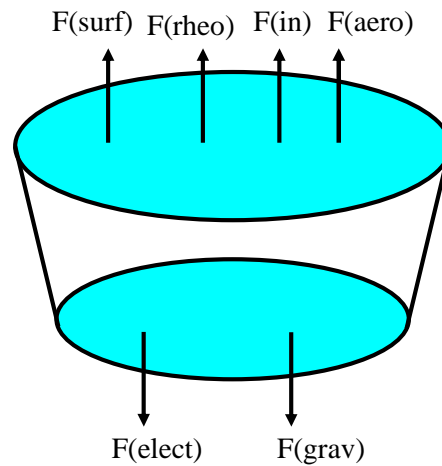


Figure 4-1: Jet analysis shows a balance between different forces affecting on the polymer melt jet during electrospinning. F (surf): Surface tension forces, F (in): Force of inertia, F (aero): aerodynamic force, F (elect): electrical force, F (grav): force of the gravity and F (rheo): Viscosity) (source: DTU, Danish Polymer center, Prof. Jørgen Lyngaae-Jørgensen).

Taylor et al. concluded that the critical voltage for ejection of the polymer jet was found to be a function of distance between electrodes (H), length of the needle (L), radius of the tube (R) and surface tension (γ) [3, 13, 17-20]. Altering the electric field strength significantly affects the velocity and amount of material drawn from pendant droplet which consequentially influences the Taylor cone and fiber diameter [2]. The Taylor cone becomes shorter and more concave in shape in the case of increasing of the electric field strength, while the fiber diameter is reduced by increasing the electric field strength [13, 20, 21].

Baumgarten et al. observed that within wide range of applied voltages, the fiber diameter is reduced and then increased again [22]. This fluctuation in the fiber diameter was interpreted as following: At low applied voltage, the spinning velocity is low resulting in generation of large fibers due to drawing of polymer chains with coiled configuration. Increasing the applied voltage results in charging of the polymer jet and increase the drawing force ending with the formation of thin fibers [18]. By further voltage increase, more material will be pulled out from the nozzle with high velocity, resulting in formation of thick fibers due to resizing of the Taylor cone, Figure 4-2 [22].

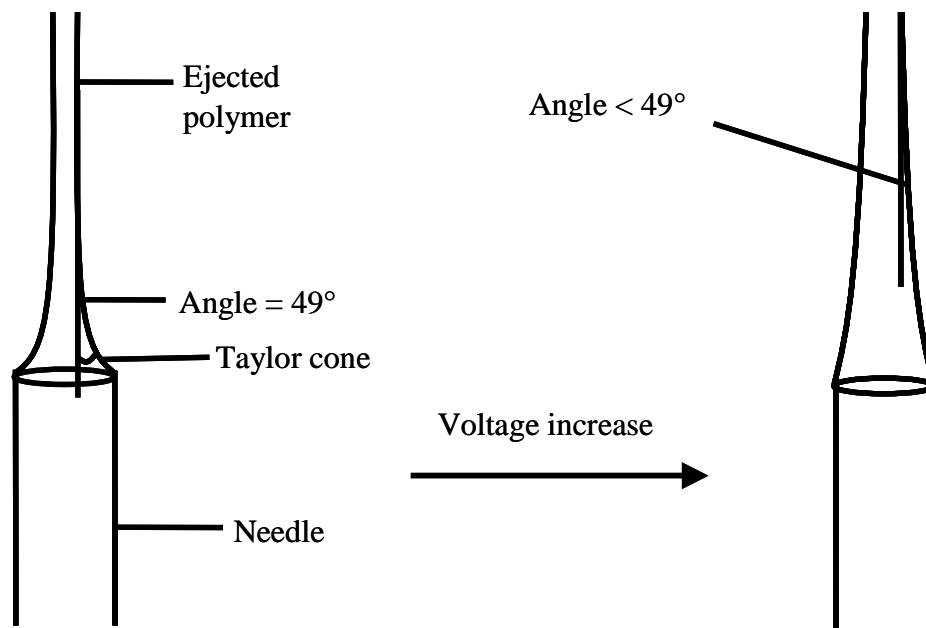


Figure 4-2: The half cone angle of the polymer electrospun jet at very high applied voltage is reduced resulting in formation of thick fibers.

2.3 Influence of the flow rate

The flow rate of the polymer melt or solution determines the amount of the material available for electrospinning [16]. It has an affect on the polymer jet velocity and consequently the fiber diameter [15]. The fiber diameter is increasing with the supply rate due to higher volume of the material drawn from the nozzle [16, 23, 24]. Low flow rates are necessary to have a stable cone-jet mode with obvious bending instability resulting in reduction of fiber diameter [23].

Ramakrishna et. al. observed that the fiber diameter is reduced with increasing the flow rate [16]. They explained that by increasing of the corresponding charges on the jet consequently with the flow rate which results in stretching of polymer jet strongly by charge repulsions to form thin fibers [16].

2.4 Effect of the distance between electrodes

The distance between electrodes affects the morphology and fiber diameter and diameter distribution of the electrospun fibers [15]. The whipping instability would be induced by increasing the distance and facilitates elongation of the jet [15]. Both the distance between the electrodes and the electric field strength are closely related and can not be regarded independently.

In melt electrospinning, it is difficult to generate thin fibers by increasing the distance between electrodes due to a high threshold value of electric field strength as a result of high melt viscosity in comparison to solution electrospinning. Therefore, the areas of electrospinning with melt electrospinning are smaller than in case of solution electrospinning, Figure 4-3.

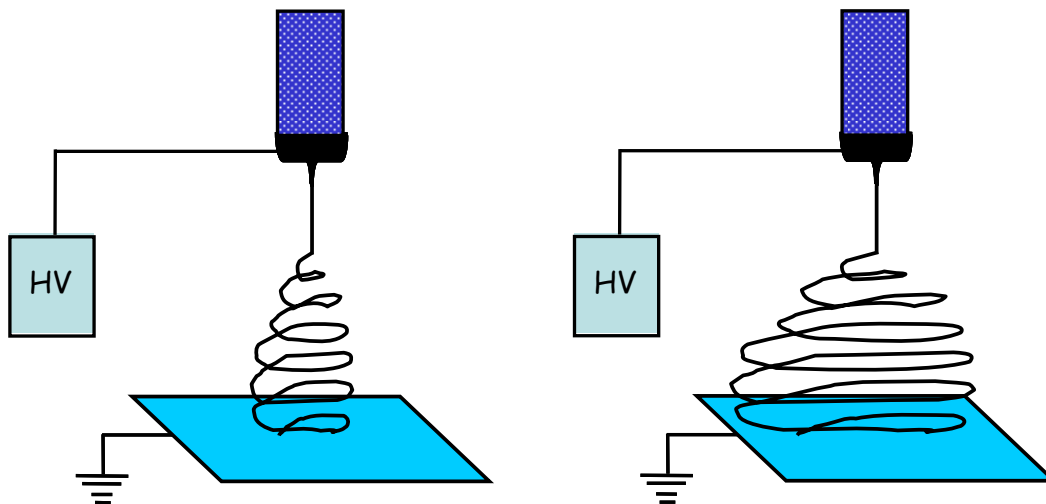


Figure 4-3: Difference in electrospinning area between melt electrospinning (left) and solution electrospinning (right)

In literature on melt electrospinning, mostly small distances were used for fiber generation. However, mostly large fiber diameters have been observed due to absence of whipping instability [2-5]. Introducing a heat gradient between electrodes facilitates the electrospinning of high viscous polymer melts at large distances. The heat gradient enables whipping instability by preventing the fast solidification of the polymer jet and results in finer fibers [7].

2.5 Influence of the needle diameter

The nozzle diameter has been found to have a minor effect on the electrospinning process [16]. However, for much smaller diameter spinnerets, which are enough to compress polymer melts, the fiber diameters are increasing with reduction of needle diameter, due to die swell phenomena [16, 25].

In laminar flow of polymer melts, the die swell can be separated into three components [25]: A small Newtonian swell, a sudden elastic recovery at the exit and an additional swelling due to slow stress relaxation [25]. The sudden elastic recovery happens due to recoiling of polymer chains once the wall shear stress is disappeared at the die exit [25]. The additional

swelling can be reduced in long capillaries with high values of L/D by fading the memory effect of the first normal stresses gained during passing of polymer melts through the die [25].

Industrially, the term of pressure loss (ΔP) is concerned. Pressure loss is the amount of pressure required to compress the polymer chains close to each other upon their passing through a narrow canal, and it will be lost at the capillary tip through chain expansion by recoiling and sudden elastic recovery [25].

2.6 Influence of the spinning environment

Ambient conditions including the surrounding atmosphere, relative humidity, air pressure, etc. have a significant effect on the fiber diameter and their homogeneity [15].

Depending on the type of electrospun polymer and its interaction toward humidity, the fiber diameter can alter with humidity. With hydrophilic polymers, small fiber diameters can be generated at high humidity due to reduced surface tension with the humid air. On the other side, for hydrophobic polymers, the surface tension is increased with humidity resulting in formation of thick fibers in an attempt to reduce the contact surface with the humid air.

2.7 Effect of the rotation speed

The speed of a rotating mandrel has an essential effect on the alignment and mechanical properties of the electrospun fibers. When the value of the rotation speed overcomes the value of the fiber ejection, the jet and solidifying fibers become stretched. In that case, a combination of a fiber drawing process and melt electrospinning process is achieved. The linear velocity is increasing with the rotation speed leading to arranging of polymer chains longitudinally forming crystals [9]. The increase of rotation speed stretches the polymer jet strongly resulting in more oriented chains [16]. WAXS results demonstrated by Ramakrishna et. al. shows that the degree of crystallization is increased and high molecular orientation is induced by increasing the speed of rotation disc [16].

3 Experimental

3.1 Electrospinning

The electrospinning device consists of a high voltage supply (Eltex KNH34 purchased from Eltex Elektrostatic GmbH, Weil am Rhein, Germany), a cylindrical (used to collect parallelly oriented fibers) or a flat target (for non-woven), a syringe pump (type HA 11 plus Harvard Apparatus, purchased from Hugo-Sachs Elektronik GmbH, March-Hugstetten, Germany), a heating chamber (manufactured by DWI workshop) and a heat gun (Leister, purchased from Klappenbach GmbH, Hagen, Germany). The collection distance was varied between 40-260 mm. The flow rate was varied between 0.2-1 mL/h and the electric field strength was altered from 2-7.5 kV/cm. The first electrospinning device shown in Figure 4-4 was used to test the influence of flow rate in absence of air flow between electrodes, which can accelerate the polymer jet, as well as, the influence of the gravity can be neglected. The electrospinning system was subsequently modified into the electrospinning system shown in Figure 4-5, where a heat gradient was introduced between the electrodes to enable a whipping instability for further stretching of the polypropylene fibers. The heat gradient was created by blowing a portion of a hot air blown by the heat gun through the lower orifice of the heating chamber as shown in Figure 4-5.

Polymer sticks were filled into 2 mL glass syringes, and melted at 220°C by a heat gun for electrospinning. The warm air-current provided a simple heat source and allowed working with high melting polymers. The heating chamber allowed homogeneous distribution of the temperature around the syringe. Unless otherwise indicated, a high positive voltage was applied to the spinneret and the fibers were collected either onto a grounded rotating aluminum cylinder (diameter 80 mm, length 100 mm) or a grounded aluminum plate. The grounded cylinder was rotated at a speed of 2000 rpm. Both collectors were covered with aluminum foil.

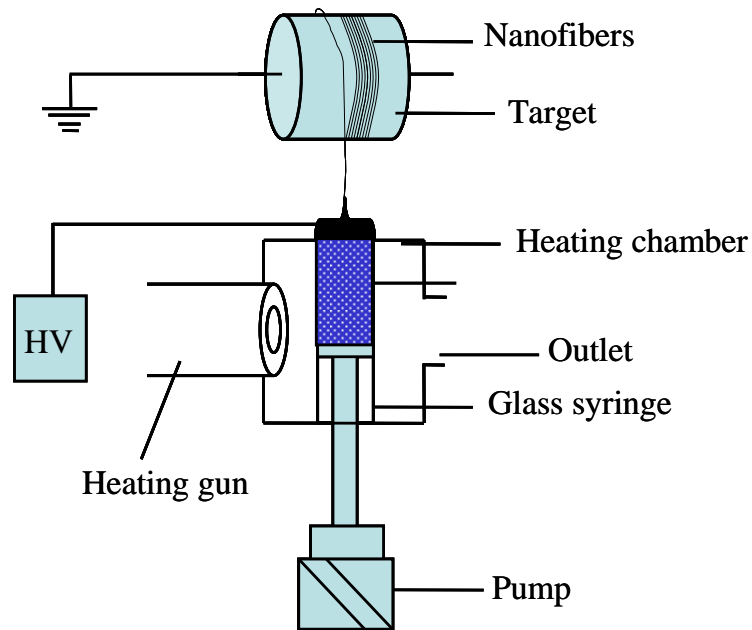


Figure 4-4: Schematic illustration of the setup of the electrospinning device using a rotating cylinder as target for collection of aligned fibers

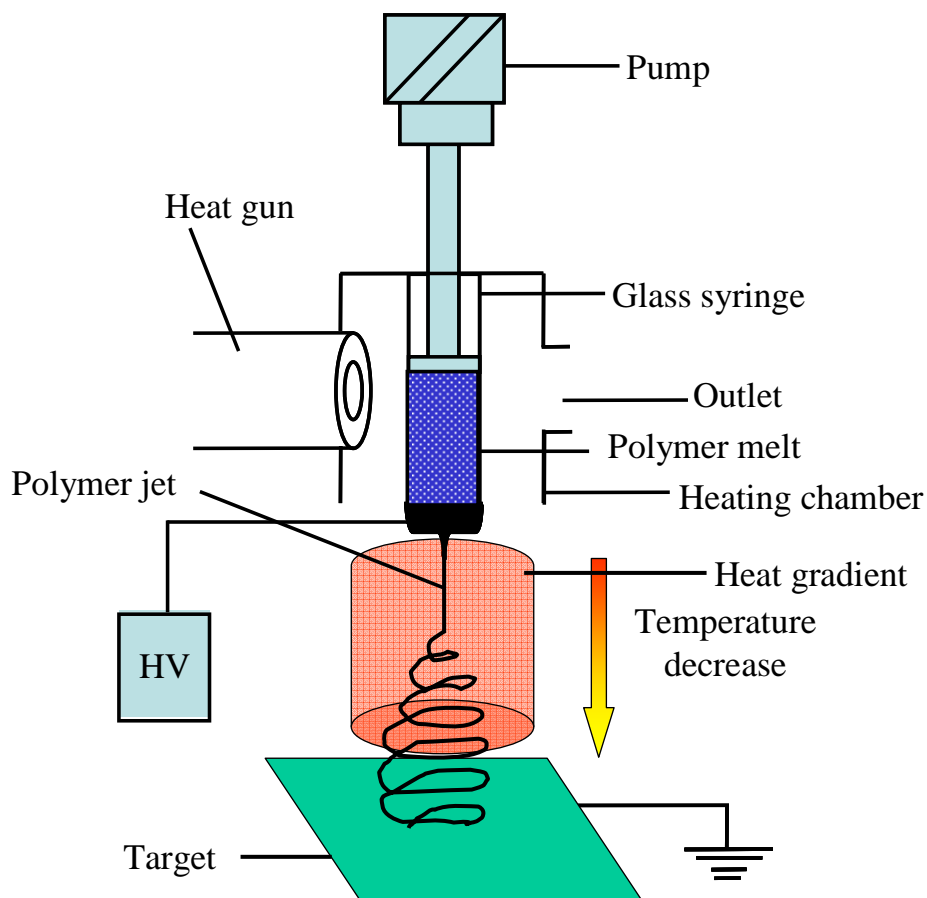


Figure 4-5: Schematic illustration of the setup of the electrospinning device using a flat aluminum plate as target for collection of non-wovens.

3.2 Materials

3.2.1 Polypropylene

Polypropylenes of molecular weights 12000, 190000 and 250000 g/mol were purchased from Aldrich-Sigma (Taufkirchen, Germany), they are further on referred to as PP 12000, PP 190000 and PP 250000. MCHM 648 P (isotactic polypropylene with molecular weight of 181000g/mol and with melt flow index of 18 g/ 10 min) and MCHM 562 P (isotactic polypropylene with melt flow index of 15 g/ 10 min) were purchased from Basell polyolefin GmbH (Mainz, Germany).

3.2.2 Synthesis of sodium stearate and preparation of viscosity breaking agent

Sodium stearate was synthesized by esterification reaction using ethanol as a solvent. Stearic acid and sodium hydroxide were purchased from Sigma Aldrich (Taufkirchen, Germany), dissolved in ethanol and mixed. The sodium stearate was isolated by evaporation of ethanol using a rotary evaporator.

3.2.3 Preparation of the samples

The polypropylenes were used as delivered or blended with sodium stearate as slipping agent by twin screw extruder. The mixtures are prepared in the form of sticks by injection into a stick form mold.

3.3 Characterization methods

Fibers were characterized by scanning electron microscopy with a (SEM) Hitachi S-3000 N, Hitachi High-Technologies Europe GmbH, (Krefeld, Germany). Therefore, the aluminum foil with the electrospun fibers was fixed onto an aluminum SEM stub; afterwards gold-coated and analyzed. An electron beam of 15 kV and working distance of 7-15 mm were used to image the electrospun material. Fiber diameters were measured using SEM (average numbers of 200 independent measurements) and representative images of the electrospun fibers are presented.

The temperature as a function of distance between electrodes was measured by GTH 1150 digital thermometer purchased from Greisinger electronic (Regenstauf, Germany).

3.4 Results and discussion

3.4.1 Influence of spinneret design

PP 190000 was compounded with 5 wt.-% sodium stearate and electrospun at the electric field strength 2.75 kV/cm (voltage 22 kV and the distance between electrodes was 8 cm). Four setups of the heat chamber were used in order to test the effect of chamber setup on the produced fiber diameter and its distribution as shown in Figure 4-6. SEM graphs in Figure 4-7 show that heating of the spinning area leads to a significant reduction of the fiber diameter to around 85-96 % (from $13.4 \pm 12 \mu\text{m}$ to $0.55 \pm 0.26 \mu\text{m}$).

By heating the air gap between the electrodes, small differences in fiber diameter were observed (setup B, C and D). For setup B, a copper wire of length 3 mm was introduced in the middle of the needle without blocking the nozzle to concentrate the electric field strength at the tip of the wire as well as to guide the polymer melt to the tip of the wire. During electrospinning, it was observed that part of the polymer jet was ejected in the direction perpendicular to the wire direction. This process results in production of meshes with less homogeneous fibers (wide fiber diameter distribution) as shown in Figure 4-7 B.

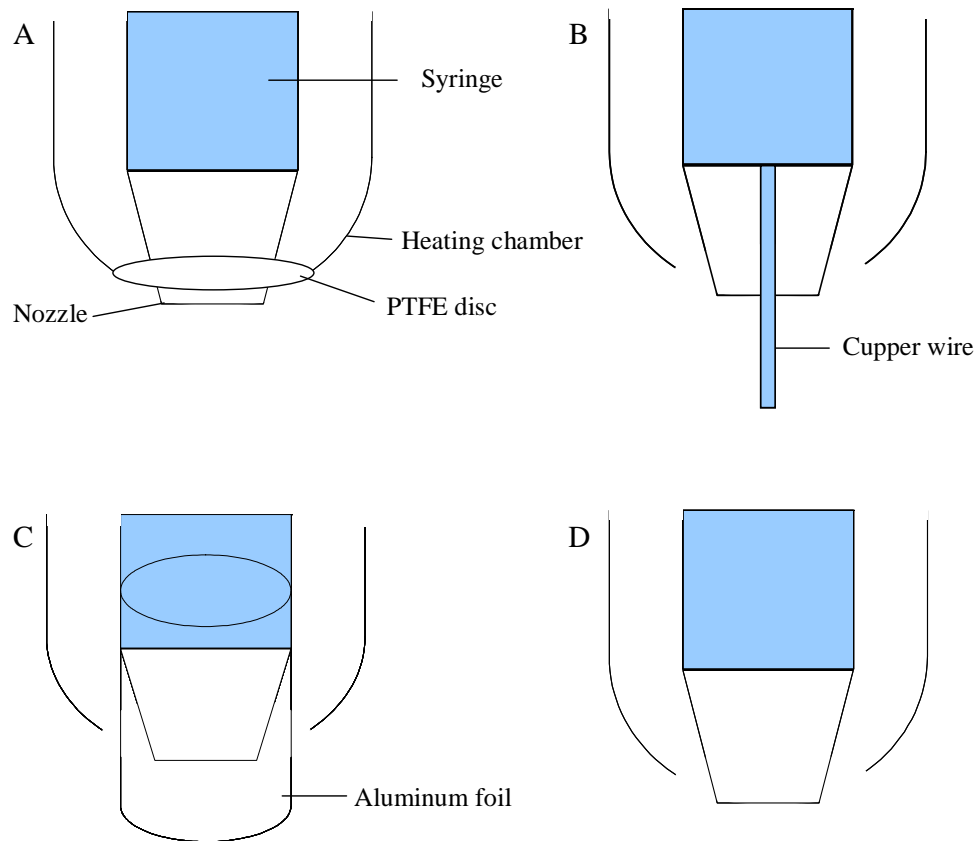


Figure 4-6: Schematic illustration shows four different setups of heat chamber. A: glass chamber with closed outlet, B: copper wire is arisen from the middle of the nozzle with length of 3 mm, C: An aluminum foil is surrounded the needle to heat the region between electrodes without disturbance of the polymer jet and D: simple setup with open outlet.

With setup C, the needle was surrounded by an aluminum foil without blocking the path of air flow to the heating chamber. The aim behind this setup is to keep the polymer melt in molten phase and to concentrate the jet in the middle of the path between electrodes without affecting the jet by air flow. The jet in this setup became more concentrated due to repulsion between charges on the aluminum foil surface and those on the polymer jet. Therefore, the only axial repulsions occur and the polymer was stretched strongly on its way to the collector. The produced fiber diameters as represented in Figure 4-7 C were found to be larger than these produced by the setup B due to limiting of whipping instability to a small area of the spinning process.

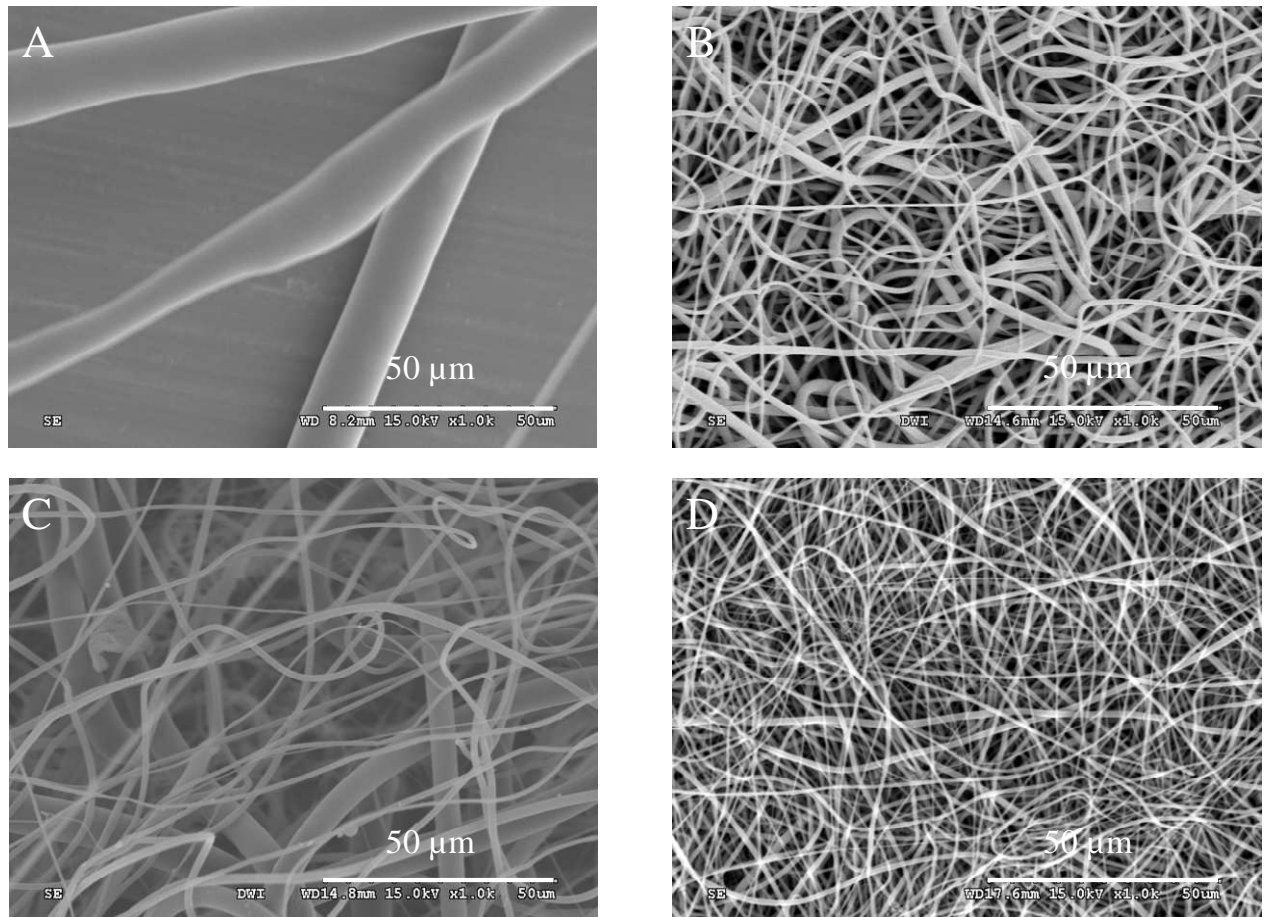


Figure 4-7: SEM graphs for polypropylene fibers produced by melt electrospinning at the electric field strength of 2.75 kV/cm, applied voltage of 22 kV and the distance between electrodes of 8 cm by different setups of the heating chamber. A: polypropylene fibers produced in the absence of heating area between electrodes ($13.38 \pm 11.94 \mu\text{m}$), B: polypropylene fibers produced in the presence of thin copper wire of length 3 mm (0.98 ± 0.38), C: polypropylene fibers produced in the presence of aluminum foil ($1.46 \pm 0.61 \mu\text{m}$) and D: polypropylene nanofibers produced by simple setup ($0.55 \pm 0.26 \mu\text{m}$).

With setup D, the cone jet configuration has been established with a clear whipping instability zone. As presented in Figure 4-7 D, the produced fiber diameter is small with narrow size distribution ($0.55 \pm 0.26 \mu\text{m}$).

3.4.2 Effect of heat gradient

The heat gradient area between needle and target was created by the fraction of hot air passing through the lower orifice of the heating chamber. The large area of heat gradient was created by closing the lateral orifice of the heat chamber as it is illustrated in Figure 4-8. Figure 4-9 shows the temperature of the heating zone is reduced with the distance between electrodes indicating the presence of the heat gradient. By increasing the air flow through the lower

Chapter 4: The Influence of ambient and processing parameters on melt electrospinning of 78 polypropylene: Effect of heat gradient

orifice, the temperature of the heat gradient was increased around 30 %. As a result, the polymer jet stayed in the molten phase for a longer period. Therefore, the elongation of polymer jet increased compared to the low heat gradient setup. The reduced stretching of the polymer jet with distance was caused by a combined effect of increasing melt viscosity with distance from the needle and reduction of charge density on the polymer jet. As polypropylene melts start to solidify at temperatures around 150°C, the solidification occurs at distances between 3 cm and 5 cm respectively as declared in Figure 4-9.

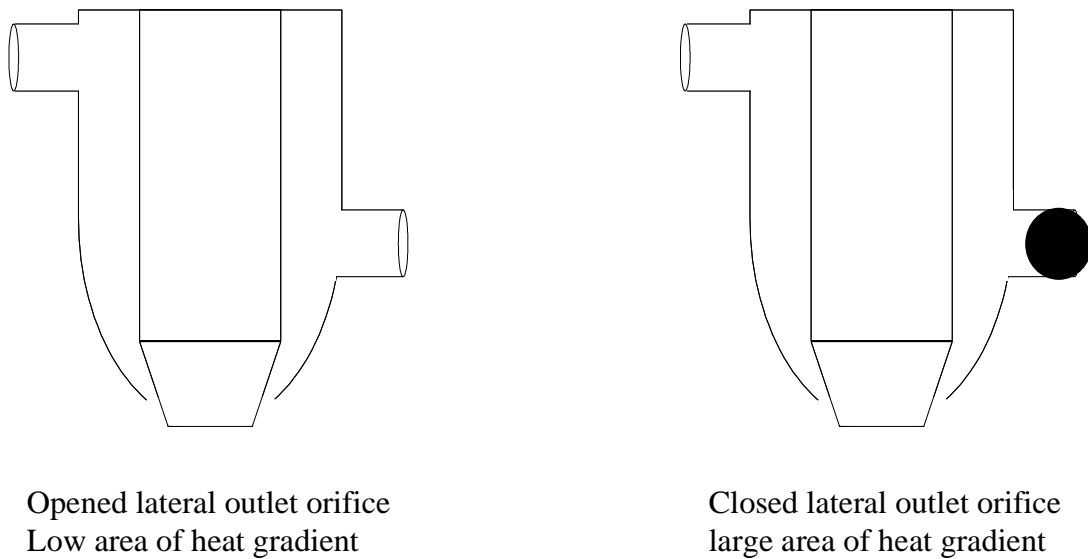


Figure 4-8: Schematic illustration shows the process of changing the air flow rate in order to increase the volume of heat gradient.

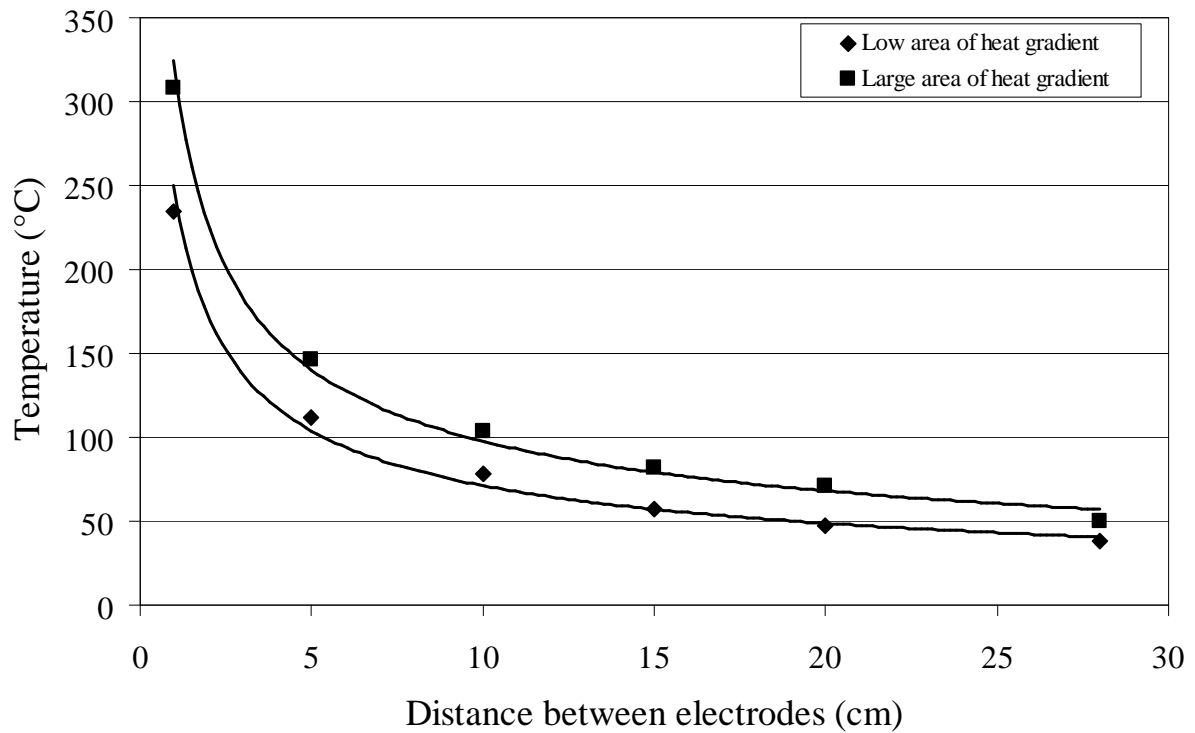
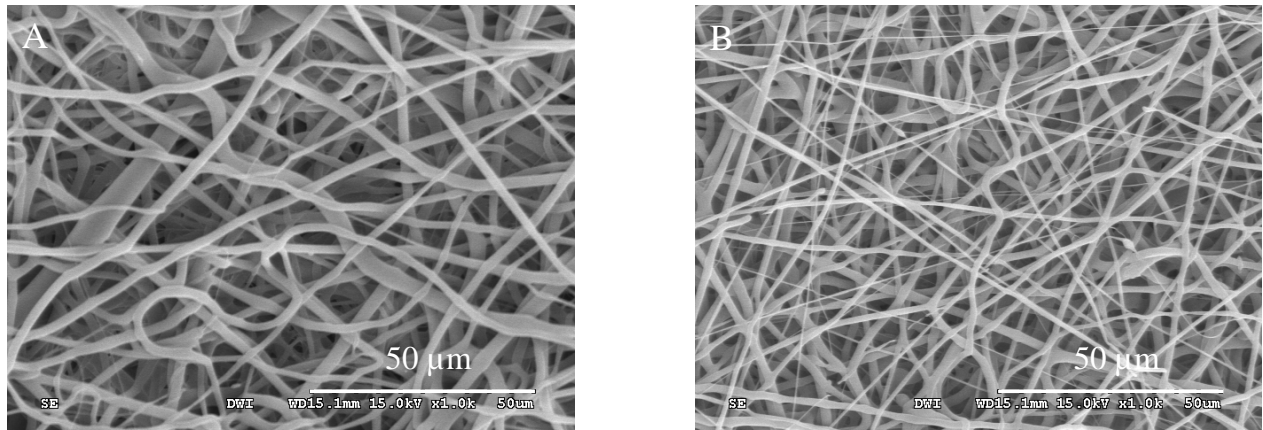


Figure 4-9: curves show the temperature of the air at different distances between electrodes for large and low heat gradient areas. The temperature was increased around 30% and the melting point was displaced 2 cm (from 3 cm to 5 cm) by increasing the air flow through the lower orifice of the heat chamber.

In addition to these results, the polypropylene fibers electrospun with a small area heat gradient are larger than those produced in the presence of a large area of heat gradient. Increasing the area of the heating zone leads to a reduction of the fiber diameter to around 38 % (from $1.50 \pm 0.72 \mu\text{m}$ to $0.92 \pm 0.43 \mu\text{m}$).



Opened lateral outlet orifice
FD: $1.50 \pm 0.72 \mu\text{m}$

Closed lateral outlet orifice
FD: $0.92 \pm 0.43 \mu\text{m}$

Figure 4-10: SEM graphs for PP 190000 containing 5 wt.-% sodium stearate electrospun at electric field strength of 3.13 kV/cm, at applied voltage of 25 kV and at the distance between electrodes of 8 cm produced in the presence of low (A) and large (B) areas of heat gradient.

3.4.3 Influence of electric field strength

PP 190000 was mixed with 5 wt.-% Na-stearate and was electrospun at 220°C at various electric field strengths. The electric field strength was changed either by alteration of the distances between electrodes at constant applied voltage (22 kV) or by changing the applied voltage at constant distance between electrodes (23 cm). Figure 4-11 demonstrates that changing the distance between electrodes and keeping the applied voltage constant led to formation of smaller fibers. This result indicates the importance of enlarging the distance between electrodes in order to induce whipping instability. At electric field strength 2.75 kV/cm and at the distance between electrodes 8 cm polypropylene nanofibers in the range of $552 \pm 260 \text{ nm}$ were generated. Figure 4-12 displays the SEM graph of the produced polypropylene nanofibers. The corresponding fiber size distribution shows that almost 93% of total mesh were nanofibers.

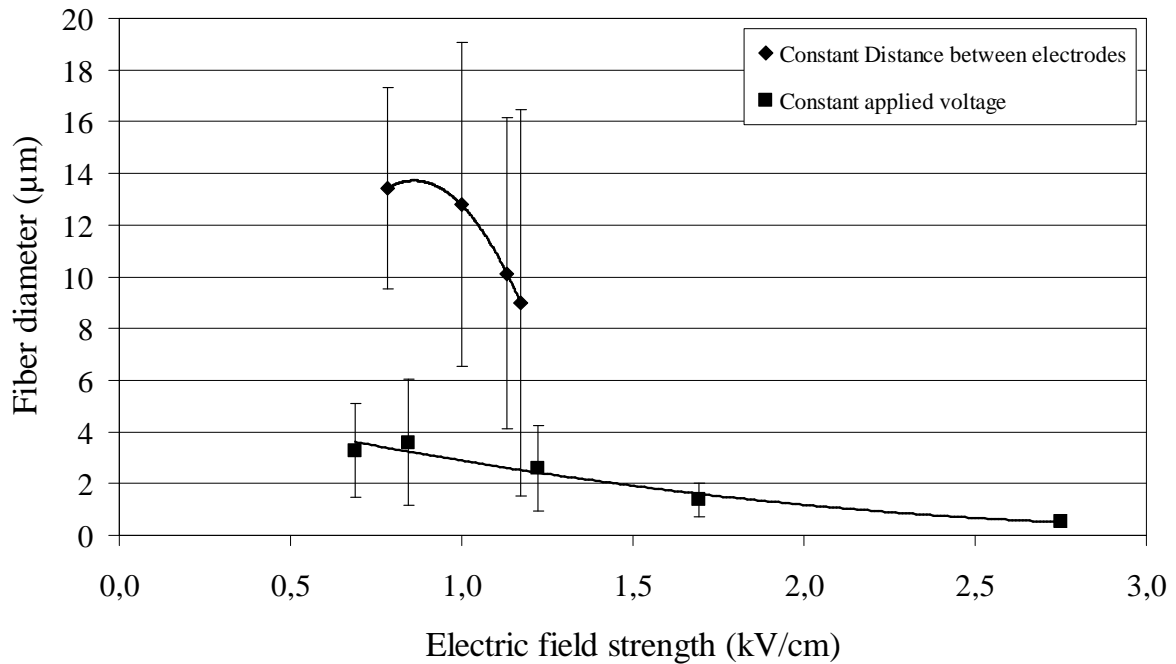


Figure 4-11: Graph shows the relation between electric field strength and fiber diameter for PP 190000 mixed with 5 wt.-% sodium stearate. The electric field strength was changed by two ways: changing the distance between electrodes at constant applied voltage (22 kV) and by changing the applied voltage at constant distance between electrodes (23 cm). The curve shows the importance of changing the distance between electrodes in order to create whipping instability to form thin fibers.

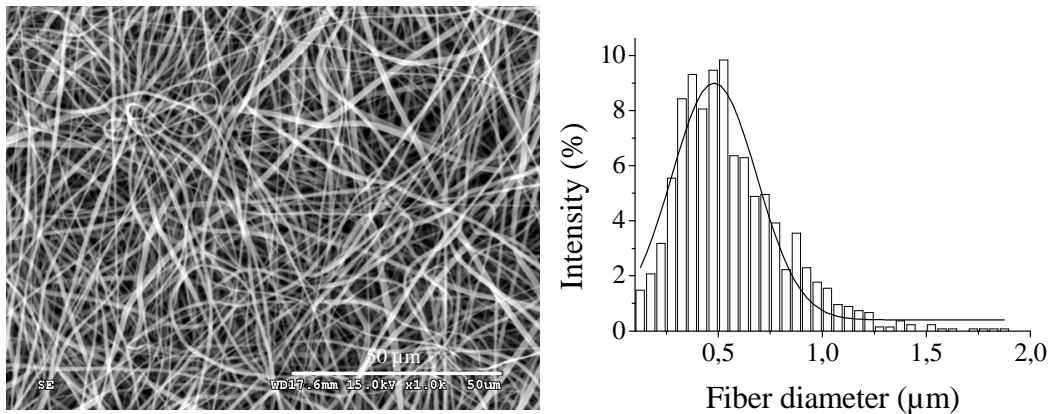


Figure 4-12: SEM graph shows polypropylene nanofibers produced by melt electrospinning containing 5 wt.-% sodium stearate electrospun at electric field strength of 2.75 kV/cm, applied voltage of 22 kV and the distance between electrodes of 8 cm (left). The fiber diameter distribution shows the fiber diameter of the produced mesh is around 552 ± 260 nm and the amount of nanofibers content reached 93.6% of the total mesh (right).

Pure PP 12000 was electrospun at 220°C with a cylindrical mandrel as target and at electric field strength ranging from 4 to 7 kV/cm. The distance between electrodes was fixed at 4 cm. It was found that the fiber diameter increased with electric field strength around 58.7% (from 3.36 ± 2.75 to 8.14 ± 5.40), Figure 4-13. The increase in fiber diameter is due to fast drawing of the polymer jet from the needle tip.

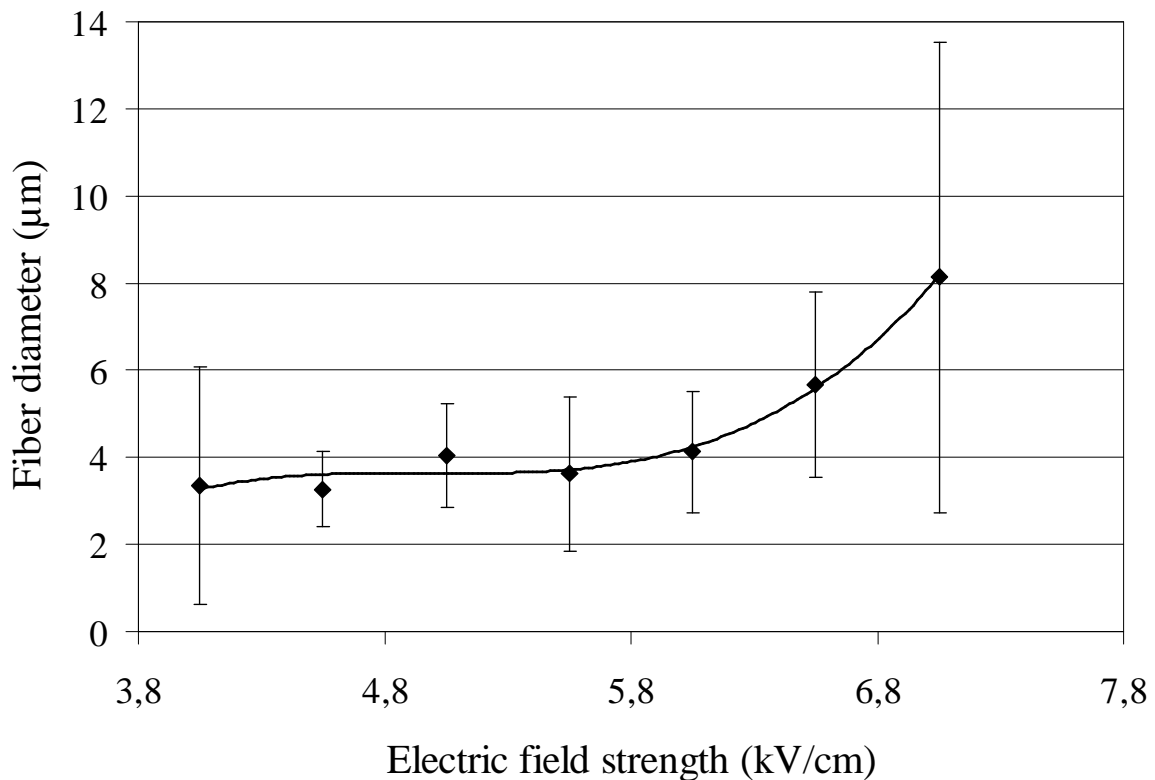


Figure 4-13: Relation between the applied voltage and the fiber diameter at flow rates 0.2 mL/h for poly(propylene) of molecular mass 12000 g/mol (PP 12000). The fibers were collected by rotator mandrel and the distance between electrodes was 4 cm, rotation speed 2000 RPM.

3.4.4 Influence of flow rate

PP 12000 was melted at 220°C and electrospun at electric field strengths 4, 5.5 and 6.25 kV/cm. Three flow rates were applied, 0.2, 0.5 and 1 mL/h. Figure 4-14 shows flow rate versus fiber diameter relation. By increasing the flow rate, more polymer material is ejected and the fiber diameter is increased. Figure 4-15 exhibits SEM graphs of PP fibers which were electrospun at electric field strength 4 kV/cm at three different flow rates (0.2, 0.5 and 1 ml/h). The homogeneity of the produced fibers was initially increased with increasing flow rate and then reduced again at higher flow rates.

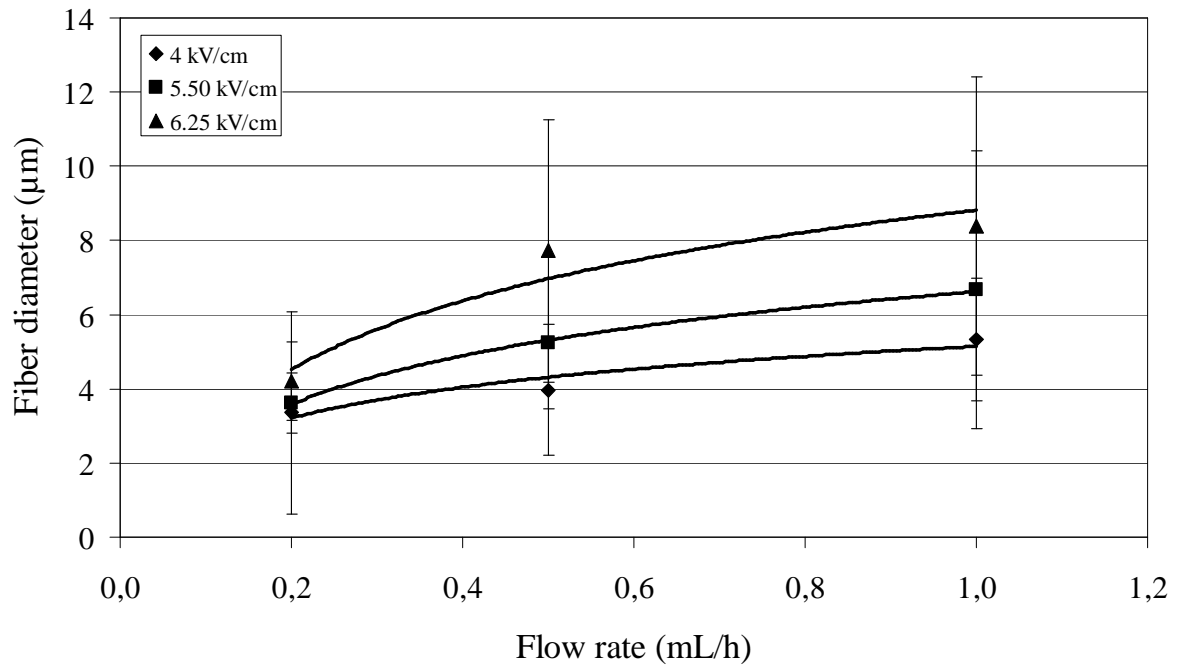


Figure 4-14: Graph shows the increase in fiber diameter with flow rate at three difference electric field strengths. The fibers were collected by cylindrical target at a rotation speed of 2000 RPM.

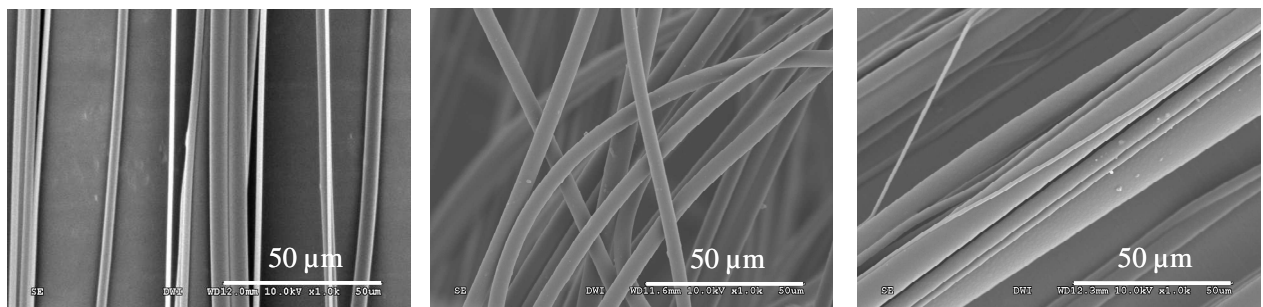


Figure 4-15: SEM micrographs showing the differences in the fiber diameter of PP fibers (PP 12000) produced at 16 kV and flow rates of 0.2 mL/h (A), 0.5 mL/h (B) and 1 mL/h (C), respectively.

3.4.5 Influence of the distance between electrodes

Polypropylene of molecular weight 190000 g/mol was electrospun at 220°C and different distances between electrodes. Figure 4-16 shows that the fiber diameter reduced by increasing the distance between electrodes, indicating the existence of whipping instability.

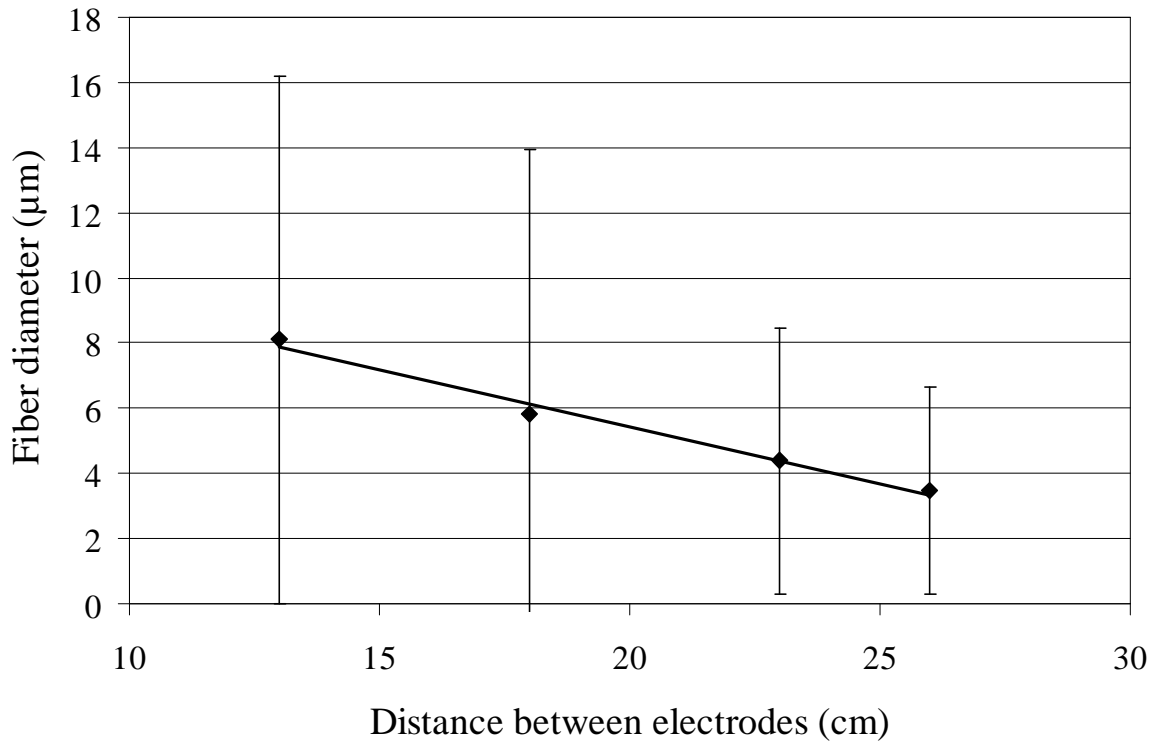


Figure 4-16: Relation between the distance between electrodes and the produced fiber diameter of PP 190000 electrospun by heat chamber with heat zone, the fibers were collected on the flat target and the applied voltage was 25 kV.

3.4.6 Influence of needle diameter

PP 190000 was melt electrospun at the electric field strength 0.96 kV/cm with spinneret diameters of 0.45 and 0.9 mm. As proved in Figure 4-17, the fiber diameter is decreased from $12.16 \pm 14.15 \mu\text{m}$ to $4.38 \pm 4.08 \mu\text{m}$ with increasing of needle diameter. During passing the polymer chains through a narrow needle, they were compressed. Once these chains leave the orifice, and due to the elasticity of the polymer chains, the load on them will be removed causing the expansion of the polymer droplet at the needle tip.

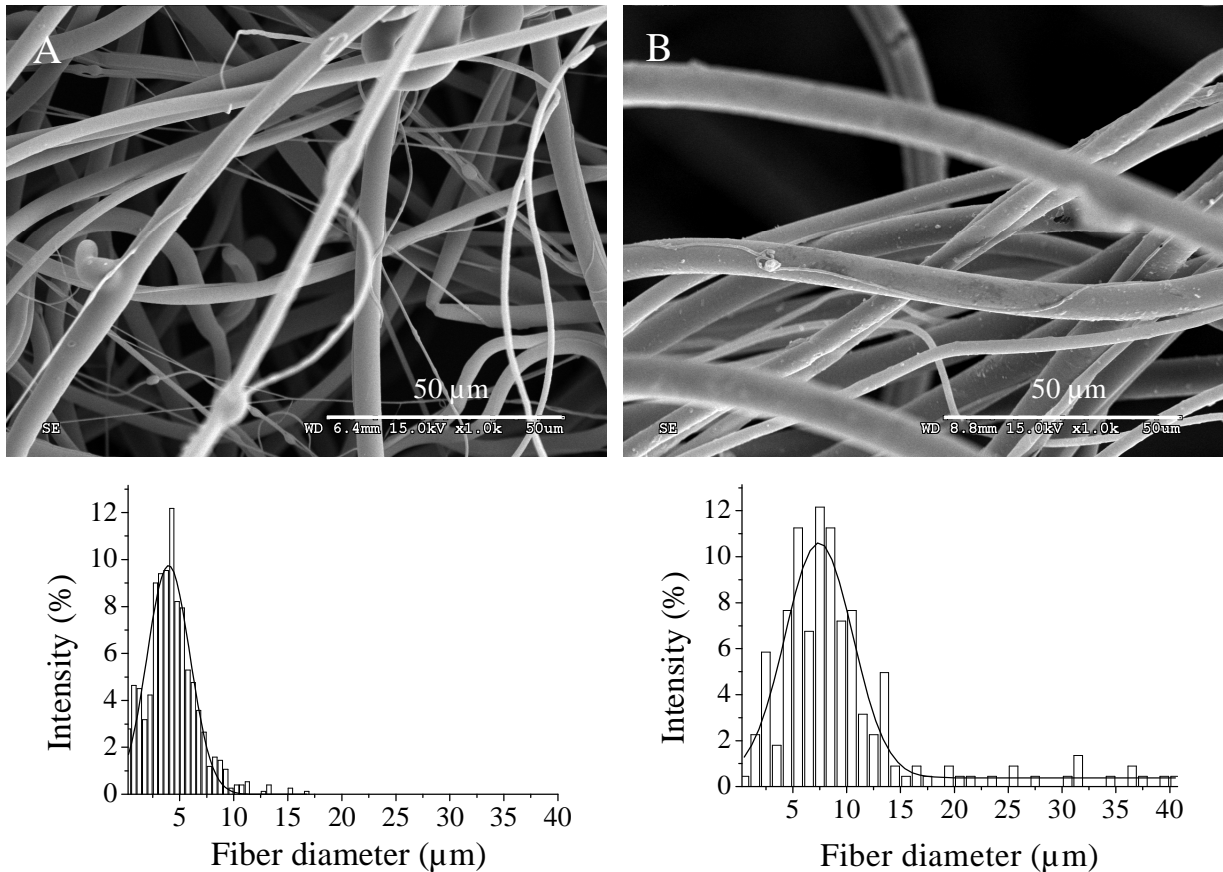


Figure 4-17: SEM graphs show the effect of needle diameter on the produced fiber diameter for PP 190000 electrospun at electric field strength of 0.96 kV/cm. Left: PP 190000 fibers electrospun using needle diameter of 0.9 mm (fiber diameter: $4.38 \pm 4.08 \mu\text{m}$). Right: PP 190000 fibers electrospun using needle diameter of 0.45 mm (fiber diameter: $12.16 \pm 14.51 \mu\text{m}$).

3.4.7 Influence of polarity

The polarity of electrodes was changed, the target was charged with positive charge; while the needle is grounded. The positive charge generator has been chosen as the system did not work with a negative charge generator. Electrospinning took place at electric field strength of 3.13 kV/cm, the applied voltage was 25 kV and the distance between electrodes was 8 cm. During electrospinning the non wovens were concentrated in a small area onto the target, while in the previously described system (charged needle and grounded collector) the fleeces were deposited on large area of the target (see Figure 4-18). This can be attributed to the pulling effect of the jet from the needle in contrast to repulsion forces induced when the needle is charged.

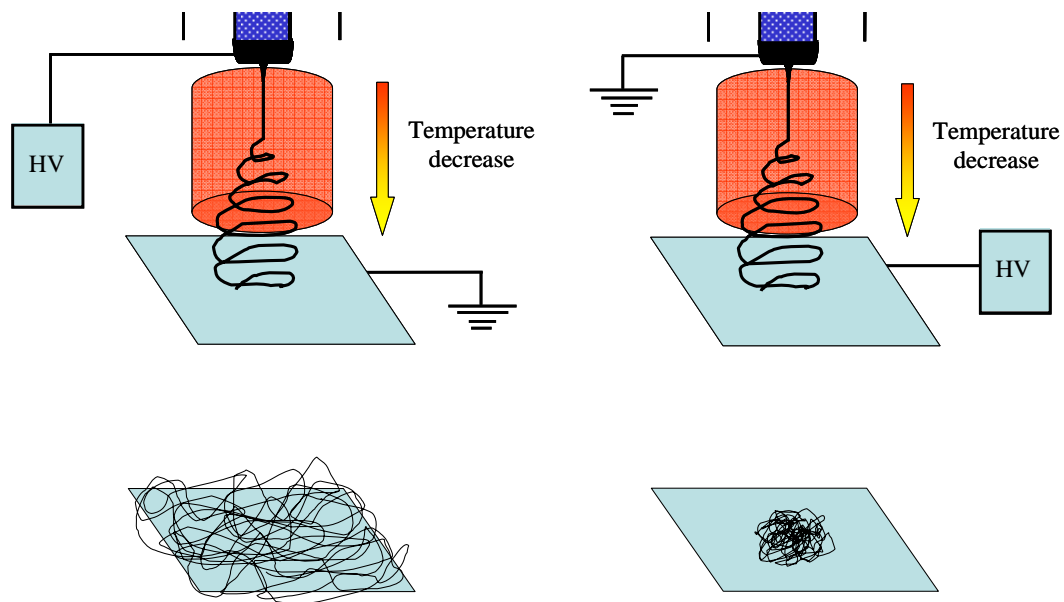


Figure 4-18: Schematic illustrations show the formation of non-concentrated and concentrated nonwovens depends on the polarity of the system.

The nonwoven area is reduced with increasing of the electric field strength. The distance between the electrodes was kept constant at 8 cm. Figure 4-19 shows the reduction of the nonwoven diameter with increasing electric field strength. This is a result of fast drawing of the polymer jet by the electric field strength. The jet has no chance to make a large area of whipping instability region. Furthermore, the fiber diameter is reduced by increase the electric field strength around 38 % from 1.85 ± 0.89 to 0.71 ± 0.34 μm . Figure 4-20 shows the relation between electric field strength and fiber diameter for of PP 190000 mixed with 5 wt.-% sodium stearate.

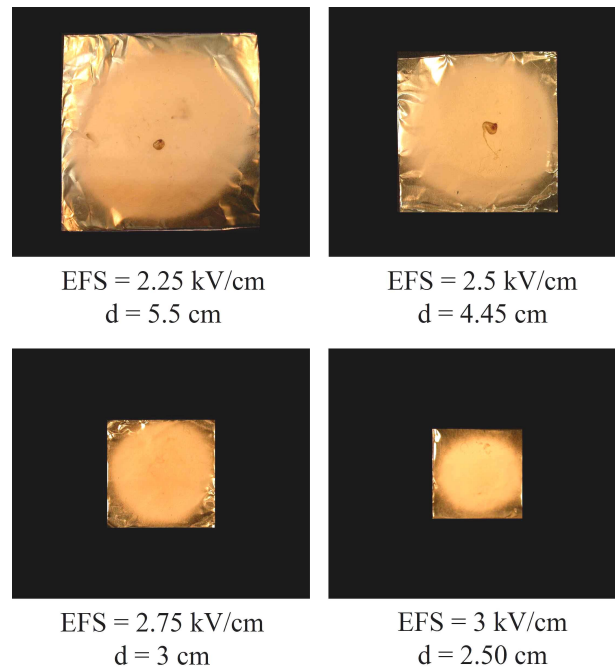


Figure 4-19: Graphs show the changing of fleece diameter by increasing of electric field strength. Fleeces are produced at distance between electrodes 8 cm and the electric field strength was varied by varying the applied voltage.

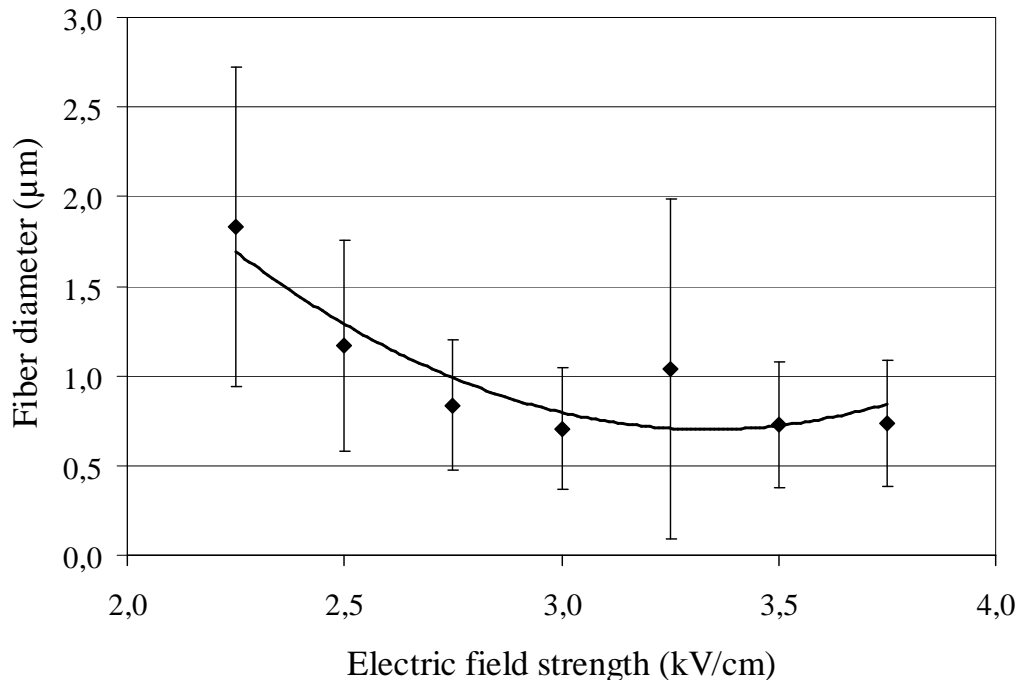


Figure 4-20: Graph shows the relation between electric field strength and the resulting fiber diameters electrospun by charged target and at the distance between electrodes 8 cm for the mixture of PP 190000 containing 5 wt.-% sodium stearate.

Changing the electric field strength at constant voltage does not result in a significant difference of the nonwoven diameter. Fiber diameters at constant electric field strength and varied distances ranged from $0.8 \pm 0.31 - 1.63 \pm 0.65 \mu\text{m}$.

3.4.8 Influence of humidity

A mixture of PP 190000 g/mol containing 5 wt.-% sodium stearate was electrospun at electric field strength 3.13 kV/cm on days with significantly different humidity. Figure 4-21 displays SEM graphs for electrospun polypropylene fibers produced at humidity 28 % and 9 % respectively. Fiber diameter distributions show that at low humid condition, fibers tend to have small diameters with narrow fiber diameter distribution. This is due to the hydrophobic nature of polypropylene surface, which tends to form small contact surfaces with humid air. The fiber diameter was reduced around 50 % from $4.67 \pm 4.44 \mu\text{m}$ to $2.33 \pm 0.91 \mu\text{m}$.

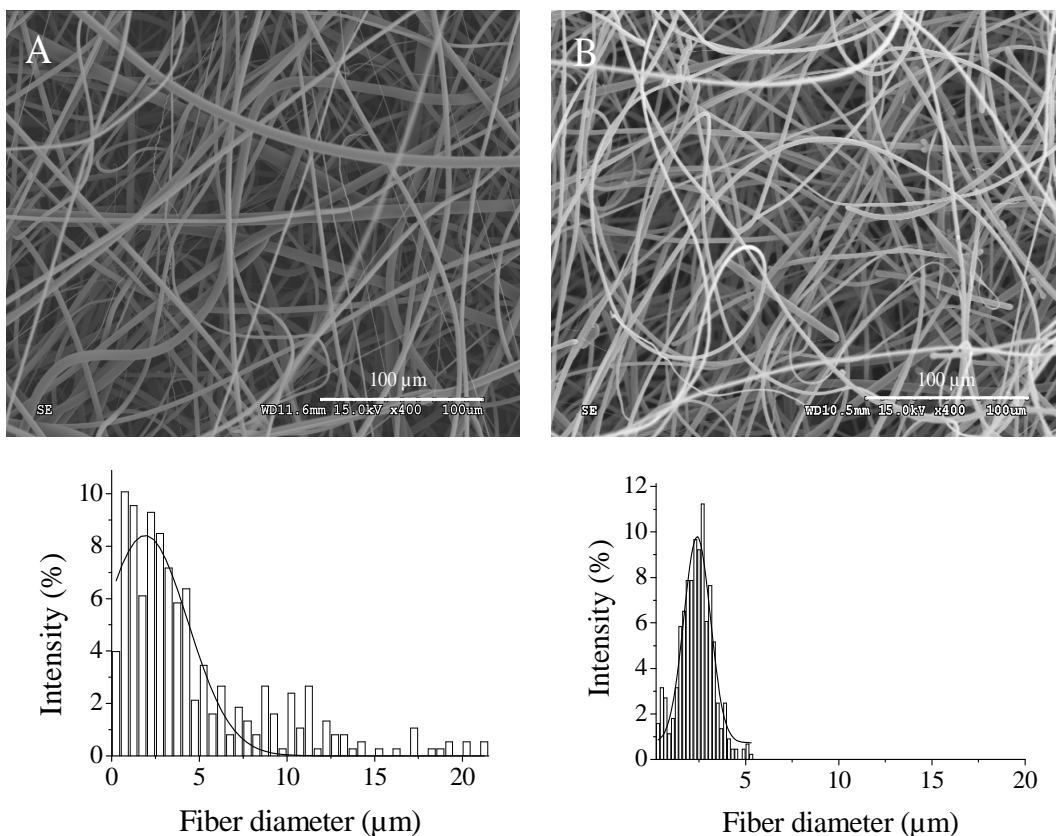


Figure 4-21: SEM graphs show the difference in the fiber diameter for mixture of poly(propylene) containing 5 wt.-% sodium stearate electrospun at electric field strength 0.96 kV/cm, at applied voltage 25 kV and the distance between electrodes was 26 cm. A) Humidity 28 %, fiber diameter: $4.67 \pm 4.44 \mu\text{m}$, B: humidity 9%, fiber diameter: $2.33 \pm 0.91 \mu\text{m}$. The fiber diameter distribution shows that at low humidity, more homogeneous fibers can be obtained.

3.4.9 Influence of rotation speed

Polypropylene MCHM 562 P was mixed with 1.1 wt.-% Irgatec CR 76 and electrospun at the electric field strength of 4.25 kV/cm and an applied voltage of 17 kV. The electrospun fibers were collected on the rotating mandrel collector with rotation speeds ranging from 268-1500 rpm. After collection of the samples, they were undergone SEM measurements. Figure 4-22 shows that the fiber diameter is reduced by increase of the rotation speed due to an increase of the stretching force at high rotation speeds.

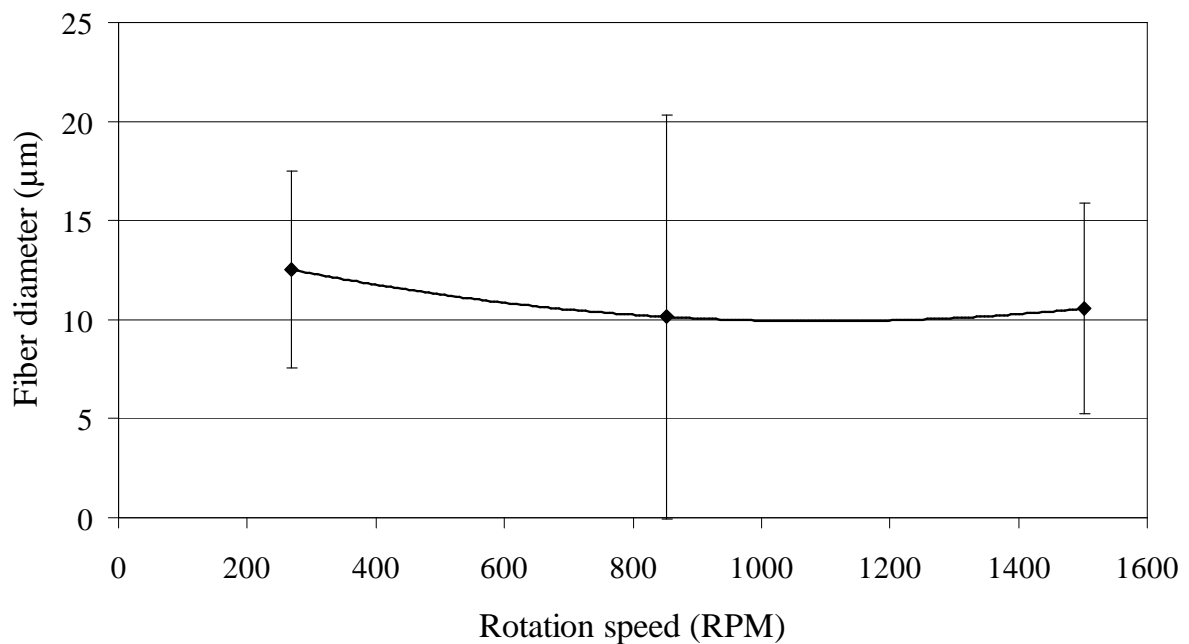


Figure 4-22: Graph shows the relation between rotation speed of the mandrel and fiber diameter for fibers electrospun at the electric field strength of 4.25 kV/cm at the applied voltage of 17 kV. The distance between electrodes was 4 cm.

SEM graph of the collected fibers exhibits the formation of relaxation zones which result from fast cooling of the polymer jet, Figure 4-23. During collection of the electrospun fibers on the cylinder, the polymer chains are stretched leading to formation of stress. After removal of the load on fibers, polymer chains start to relax resulting in creation of relaxed surface morphology.

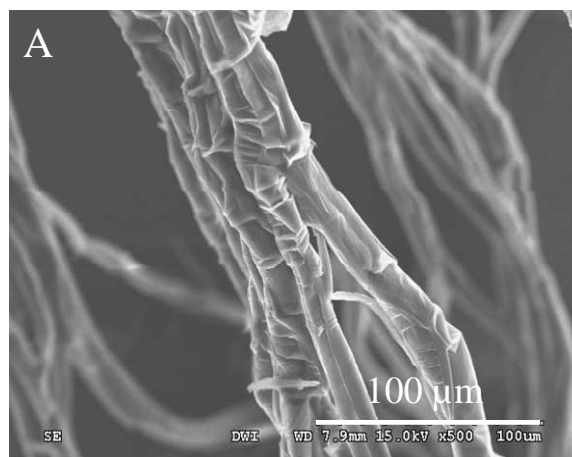


Figure 4-23: SEM graphs exhibits the relaxation morphology on the surface of fibers electrospun at electric field strength of 4.25 kV/cm, at the applied voltage of 17 kV and at the distance between electrodes of 4 cm. The fibers were collected on the cylindrical target with rotation speed of 850 RPM.

4 Summary

In this study the effect of ambient and processing parameters on the electrospun polypropylene fiber diameter and morphology was shown. It was observed that processing parameters such as presence of heat gradient between electrodes, electric field strength, flow rate of the polymer melt, distance between electrodes, needle diameter, polarity of electrodes, humidity and rotation speed of cylindrical targets have an influence on fiber diameter and homogeneity through increase the elongation of the polymer jet.

Inducing a heat gradient between electrodes combined with the elongation of the distance between them facilitates the formation of thin fiber diameters and induces the whipping instability. By increasing the distance between electrodes and optimizing the electric field strength, ultra-fine fibers in the range of 552 ± 260 nm were generated.

High rotation speeds of the cylindrical targets affect the aligning and the fiber diameter of the electrospun fibers. By removing of axial stresses on the electrospun fibers represented by fast rotation speeds, relaxed surface topography was detected.

5 References

1. Reneker, D.; Chun, I. Nanometre Diameter Fibres of Polymer, Produced by Electrospinning. *Nanotechnology* **1996**, *7*, 216-223.
2. Lyons, J.; Li, C.; Ko, F. Melt-Electrospinning Part I: Processing Parameters and Geometric Properties. *Polymer* **2004**, *45*, 7597-7603.
3. Lyons, J. Melt-Electrospinning of Thermoplastic Polymers : An Experimental and Theoretical Analysis. PhD. Thesis, Drexel University, Philadelphia, **2004**.
4. Lyons, J. Melt Electrospinning of Polymers: A Review. *Polymer News* **2005**, *30*, 170-178.
5. Dalton, P.; Grafahrend, D.; Klinkhammer, K.; Klee, D.; Möller, M. Electrospinning of Polymer Melts: Phenomenological Observations. *Polymer* **2007**, *48*, 6823-6833.
6. Ellison, C.; Phatak, A.; Giles, D.; Macosko, C.; Bates, F. Melt Blown Nanofibers: Fiber Diameter Distributions and Onset of Fiber Breakup. *Polymer* **2007**, *48*, 3306-3316.
7. Hassounah, I.; Thomas, H.; Moeller, M. Obtaining Poly(Propylene) Nanofibers by Melt Electrospinning through Additives, Second Aachen-Dresden International Textile Conference, Dresden, Germany, 26-27.11.2008.
8. Joo, Y. L.; Zhou, H. Apparatus and Method for Elevated Temperature Electrospinning. U.S. Patent 7,326,043 B2, 05.02.2008.
9. Teo, W. E.; Ramakrishna, S. A Review on Electrospinning Design and Nanofibre Assemblies. *Nanotechnology* **2006**, *17*, 89-106.
10. Reneker, D.; Haul, H.; Rangkupan, R.; Lennhoff, J. Electrospinning Polymer Nanofibers in a Vacuum. *Polymer Preprints* **2003**, *44*, 68-69.
11. Reznik, S.; Yarin, A.; Theron, A.; Zussman, E. Transient and Steady Shapes of Droplets Attached to a Surface in a Strong Electric Field. *J Fluid Mech* **2004**, *516*, 349-377.
12. Kanjanapongkul, K.; Wongsasulak, S.; Yoovidhya, T. Prediction of Clogging Time During Electrospinning of Zein Solution: Scaling Analysis and Experimental Verification. *Chem Eng Sci* **2010**, *65*, 5217-5225.
13. Huang, Z.-M.; Zhang, Y.-Z.; Kotaki, M.; Ramakrishna, S. A Review on Polymer Nanofibers by Electrospinning and Their Applications in Nanocomposites. *Compos Sci Technol* **2003**, *63*, 2223-2253.
14. He, J.-H.; Wan, Y.-Q.; Yu, J.-Y. Allometric Scaling and Instability in Electrospinning. *Int J Nonlinear Sci* **2004**, *5*, 243-252.

15. Subbiah, T.; Bhat, G.; Tock, R.; Parameswaran, S.; Ramkumar, S. Electrospinning of Nanofibers. *J Appl Polym Sci* **2005**, *96*, 557-569.
16. Ramakrishna, S.; Fujihara, K.; Teo, W.-E.; Lim, T.-C.; Ma, Z. *An Introduction to Electrospinning and Nanofibers*; World Scientific Printers, Singapore, **2005**, 425.
17. Larrondo, L.; Manley, R. Electrostatic Fiber Spinning from Polymer Melts. I. Experimental-Observations on Fiber Formation and Properties. *J Polym Sci Pol Phys* **1981**, *19*, 909-920.
18. Buchko, C.; Chen, L.; Shen, Y.; Martin, D. Processing and Microstructural Characterization of Porous Biocompatible Protein Polymer Thin Films. *Polymer* **1999**, *40*, 7397-7407.
19. Shin, Y. M.; Hohman, M. M.; Brenner, M. P.; Rutledge, G. C. Electrospinning: A Whipping Fluid Jet Generates Submicron Polymer Fibers. *Appl Phys Lett* **2001**, *78*, 1149-1151.
20. He, J.-H.; Wan, Y.-Q.; Yu, J.-Y. Application of Vibration Technology to Polymer Electrospinning. *Int J Nonlinear Sci* **2004**, *5*, 253-262.
21. Hohman, M.; Shin, M.; Rutledge, G.; Brenner, M. Experimental Characterization of Electrospinning: The Electrically Forced Jet and Instabilities. *Polymer* **2001**, *42*, 9955-9967.
22. Baumgart, P. Electrostatic Spinning of Acrylic Microfibers. *J Colloid Interf Sci* **1971**, *36*, 71-79.
23. Theron, S.; Yarin, A.; Zussman, E.; Kroll, E. Multiple Jets in Electrospinning: Experiment and Modeling. *Polymer* **2005**, *46*, 2889-2899.
24. Dalton, P. D.; Joergensen, N. T.; Groll, J.; Moeller, M. Patterned Melt Electrospun Substrates for Tissue Engineering. *Biomedical Materials* **2008**, *3*, 1-11.
25. Brandao, J.; Spieth, E.; Lekakou, C. Extrusion of Polypropylene. Part I: Melt Rheology. *Polym Eng Sci* **1996**, *36*, 49-55.

Chapter 5: Nucleation and crystallization of melt electrospun polypropylene fibers

1 Abstract

Degradation of polypropylene occurs normally by thermal degradation at long heating periods and high temperatures or by oxidative degradation due to the penetration of the oxygen molecules in the amorphous parts [1]. Generally, degradation is minimized by thermostabilizers, antioxidants or by increasing the degree of crystallization with nucleating agents [1]. Minimizing of oxidative degradation in polypropylene becomes an important issue in some applications as in filtration media, where hot air is passing through polypropylene webs and oxygen molecules start to oxidize the polypropylene at suitable thermal conditions. For this, it is important to use nucleating agents in order to reduce the amorphous fraction of the polymer, where oxygen diffusion is fast and oxidation processes occur preferably. In this chapter, three nucleating agents have been used to enhance the crystalline fraction of polypropylene nanofibers generated by melt electrospinning. Sodium stearate has been used as slipping agent to reduce the viscosity of the polyethylene melt [2]. Therefore, sodium stearate facilitates the formation of strands by applying an external electrical force. However, sodium stearate was found to reduce the degree of crystallization as it reduces the inner order and retards the packing of polymer chains close to each other. The generated fibers were characterized by scanning electron microscopy (SEM) to determine the fiber diameter and its diameter distribution. Dynamic scanning calorimetry (DSC) was used to measure the degree of crystallization.

2 Introduction

Stability of polymer melts in all processing stages is a crucial issue in polymer spinning processes. The properties of the produced fibers often depend to some extent on different processing parameters such as: extruder type, melt temperature, melt pressure, nozzle geometry, cooling and air flow, draft and drawing processes besides dyeing and postproduction processes [3]. Controlling and optimizing these process parameters, especially the processing temperature and shear rate, minimizes polymer degradation at elevated temperatures and in the presence of viscosity breaking agents (radical generators). Process control avoids the undesirable and unpredictable changes in tensile strength, color, shape or impact strength as results of uncontrolled polymer degradation [4]. Polypropylene is inherent sensitive to oxidative and UV degradation processes and the reduction of polymer chain length predominantly occurs by chain cleavage via β -scission in the presence of radicals [4, 5].

Although degradation processes are responsible for undesired fluctuations and property changes in the end products, it is a desirable and useful effect for recycling of polymer wastes or for the biodegradation of products in order to reduce environmental pollution [6].

Studying the degradation process of polypropylene in fiber production is essential due to the large surface area, which increases oxidative composition [1]. Due to the fact that the oxygen molecules cannot penetrate the crystalline structure easily and start the degradation process, it is important to increase the crystalline fraction and therefore minimize the overall oxidative degradation [1]. As the crystallinity of polypropylene depends mostly on the molecular structure of the polymer chains, the tacticity of polypropylene plays an important role for the crystallization process [1, 7]. The regularity of isotactic and syndiotactic polypropylene assists packing and crystallization of polypropylene chains, while in case of atactic polypropylene; the methylene groups are arranged randomly at the polypropylene backbone and reduce orientation. The steric hindrance limits polymer chain packing and crystallization, resulting in increased polymer degradation [5, 7].

Aim of this chapter was to generate polypropylene nanofibers by means of melt electrospinning with high degree of crystallization for filtration processes. The large crystalline fraction minimizes the thermooxidative degradation of polypropylene nonwovens

during their performance. As the nucleating agents cause fast solidification of the polymer melts and limit stretching during melt electrospinning, sodium stearate, which was used to reduce the melt viscosity and to facilitate electrospinning, in combination with nucleating agents were tested for their capacity to increase the crystalline fraction of the fibers. The effect of different types and concentration of nucleating agents as well as the effects of sodium stearate on the crystallization degree have been investigated.

2.1 Polypropylene degradation and polymer chain scission regulation

Thermal and oxidative degradation is a particular feature of polypropylene at elevated temperature. Radical attack to the polypropylene backbone results in chain scission and thus in reduction of melt viscosity [8]. The attack occurs preferably at the tertiary carbon atom followed by continuous scission of polymer chains forming shorter chains [5]. Hiltz et. al. showed this by using deuterated hydrogen atoms at tertiary carbons of polypropylene and found that the degradation process slows down with time [1].

Industrially, viscosity breaking agents as radical generators are used to regulate the melt viscosity of polypropylene. They lead to statistical cleavage of long polymer chains into shorter ones, Figure 5-1 [2]. This process is called viscosity breaking process. As a result of the viscosity breaking process, controlled rheology polypropylene (CRPP) is produced with a desired molecular weight, narrow molecular weight distribution, low melt viscosity and low elasticity [9, 10].

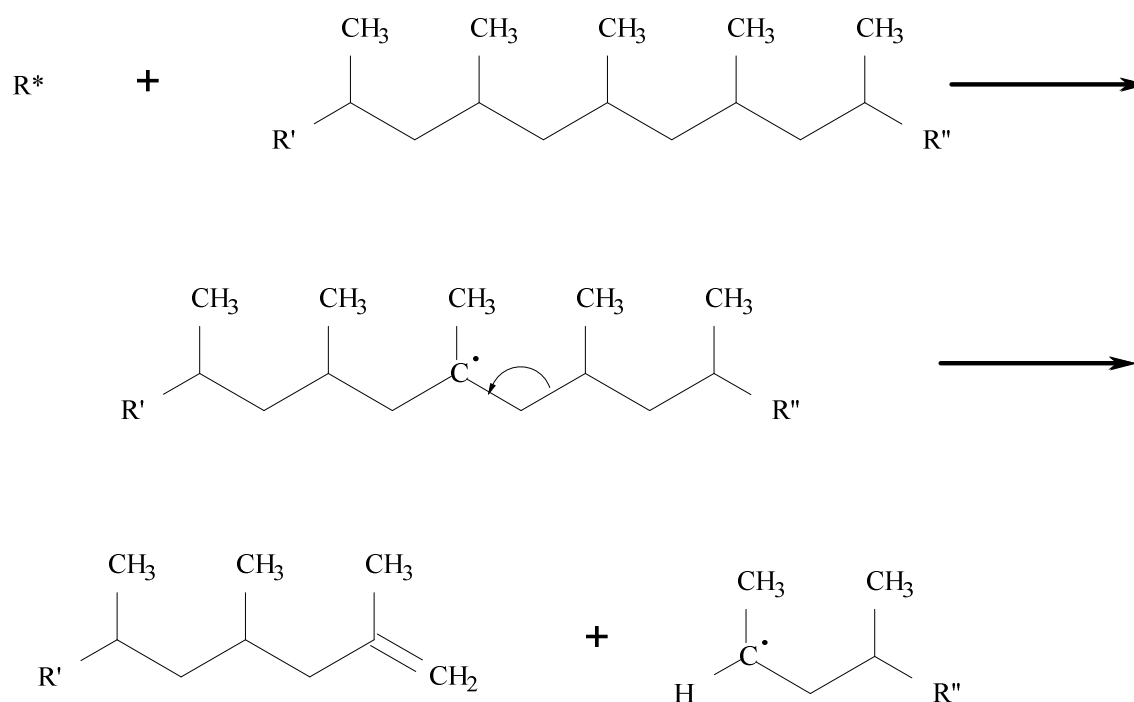


Figure 5-1: β -cleavage of polypropylene chains

The selection of a viscosity breaking agent has to be considered as it significantly affects the results and products [11]. Several criteria have to be taken into account for radical forming auxiliaries in order to be suitable for the viscosity breaking process [2, 11]:

- 1) Adequate reactivity at processing temperature,
- 2) Ease of accurate metering,
- 3) Avoidance of odor production or color change in the polymer,
- 4) Volatility of the compound-negligible losses due to vaporization or sublimation,
- 5) Low product toxicity, and
- 6) Complete inactivation of radicals at the proceeding temperature within the polymer.

High efficiency of CRPP is controlled by optimization of process parameters such as initiator concentration, temperature, screw rotation speed, ...etc [2, 11]

2.2 Nucleation and crystallization in polypropylene

Increasing the crystalline fraction of a polymer changes and improves its properties and in many cases enhances device performances.

Crystallization of a polymer describes the ability of polymer chains to assemble to a defined and well ordered structure. This exothermic process takes place in two stages: nucleation and crystal growth [12]. During nucleation, the polymer chains pack themselves, through primary and secondary nucleation processes, in lamellar structures with a specific gap length [12]. The nucleation is followed by crystal growth forming different crystal structures such as spherulite, lamellar or shish kebab depending on the chemical nature of the polymer and the interaction of the additives [12].

Polypropylene shows four different recognized crystal forms: Monoclinical α -form, hexagonal β -form, orthorhombic γ -form and a mesomorphic smectic form [3]. At normal conditions the monoclinical α -form is most stable [3]. Hexagonal β -form is achieved by using special nucleating agents [3]. α -form and hexagonal β -form exhibit different melting temperatures [13]. Behrendt et al. indicate two endothermal peaks with DSC: a low temperature peak at 149.9°C for β -form and a high temperature peak at 166.7°C for the α -form [13]. The orthorhombic γ -form is only found at high pressure and short isotactic polypropylene chains with less than 50 monomeric units [3]. Finally, the mesomorphic smectic form is achieved by fast melting or cooling rates and the predominant form observed in polypropylene fibers [3].

The nucleation process is enhanced by addition of nucleating agents which increase the cooling rate of polymer melts and reduce the production cycle [14]. Commercially, nucleating agents of polypropylene are classified according to melting range or reactivity. Within melting range, nucleating agents are classified as follows:

- 1) Melt sensitive nucleating agents that melt within the polymer melt temperature e.g.: phosphate based nucleating agent, and
- 2) Melt non-sensitive nucleating agents which do not melt within melt temperature of the polymer, e.g.: Benzoic acid [5].

According to their reactivity, they are divided into [15]:

- 1) Conventional nucleating agents e.g.: calcium carbonate and benzoic acid,
- 2) Advanced nucleating agents: give higher crystallization temperature and improve the stiffness of polypropylene e.g.: ester salts phosphate, and
- 3) Hyper nucleating agents: give higher crystallization temperature and more isotropic shrinkage than salts of carboxylic acids.

Following nucleation, crystallization starts by building a special lattice structure leading to an increase of the crystalline fraction. The crystalline fraction is influenced and controlled by addition of different types and amounts of nucleating agents which cause the properties of the end product. For instance, in fiber production, fast cooling caused by nucleating agents leads to vigorous increase of melt viscosity resulting in the formation of thick fibers due to formation of fibrillar structures in a three dimensional network [16].

Other possibility to influence the crystalline fraction is by an annealing process where the polymer is heated at a constant temperature for a certain period of time. Annealing allows polymer chains to align themselves and to form more ordered molecular structures [17].

3 Experimental

3.1 Electrospinning

The electrospinning device consists of a high voltage supply (Eltex KNH34 purchased from Eltex Elektrostatic GmbH, Weil am Rhein, Germany), a flat target, a syringe pump (type HA 11 plus Harvard Apparatus, purchased from Hugo-Sachs Elektronik GmbH, March-Hugstetten, Germany), a heating chamber (manufactured by DWI workshop) and a heat gun of the electron type (Leister, purchased from Klappenbach GmbH, Hagen, Germany). The collection distance was fixed at 80 mm. The flow rate was fixed at 0.2 mL/h and the electric field strength was altered from 3.13-3.75 kV/cm. Schematic illustration of the device is shown in Figure 5-2. The heat gradient was created by blowing a portion of a hot air blown by the heat gun through the lower orifice of the heating chamber as shown in Figure 5-2.

Polymer sticks were filled into 2 mL glass syringes, and melted at 220°C in the heating chamber by a heat gun as it is the suitable temperature to get low melt viscosities for electrospinning. The warm air-current provided a simple heat source and allows working with high melting polymers. The heating chamber allowed homogeneous distribution of the temperature around the syringe. A high positive voltage was applied to the spinneret and the fibers were collected on a grounded aluminum plate. The grounded aluminum plate is covered by aluminum foil.

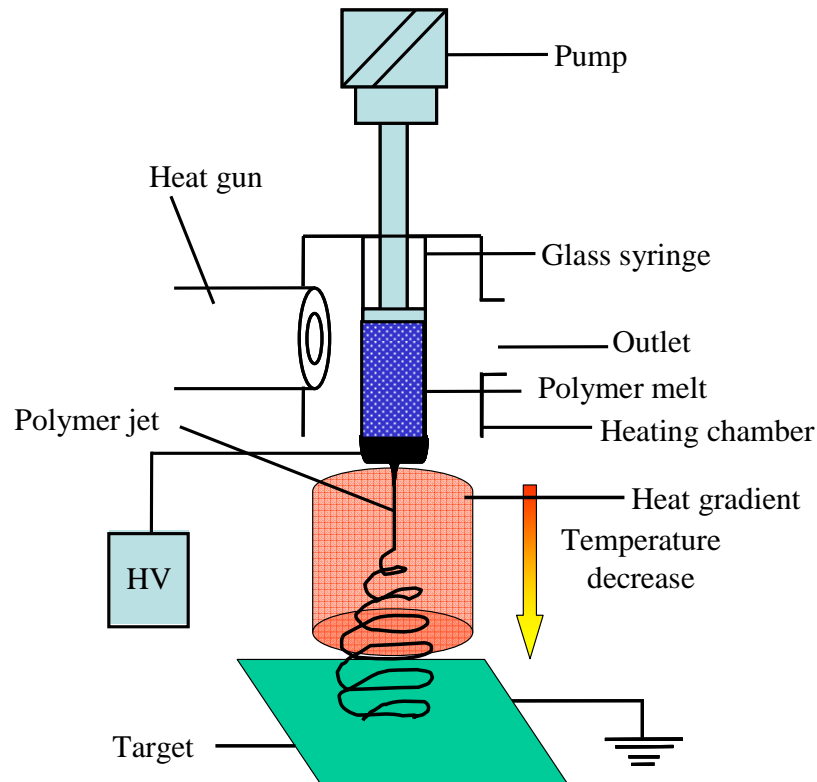


Figure 5-2: Schematic illustration of the setup of the electrospinning device using a flat aluminum plate as target for collection of non-wovens.

3.2 Materials

3.2.1 Polypropylene

Polypropylene with molecular weight of 190000 g/mol was purchased from Sigma-Aldrich (Taufkirchen, Germany) and HL 504 FB (polypropylene of molecular weight of 143000 g/mol) was purchased from Basell Polyolefine GmbH (Mainz, Germany).

3.2.2 Nucleating agents

Irgaclear DM (sorbitol based nucleating agent) was purchased from Ciba (Duluth, USA), Irgastab NA 11 (phosphate based nucleating agent) was purchased from Ciba (Lyon, France) and HPN-68 L (norborane acid based nucleating agent) was purchased from Milliken (Gent, Belgium). All nucleating agents were used as received.

3.2.3 Synthesis of sodium stearate

Sodium stearate was synthesized by esterification reaction using ethanol as solvent. Stearic acid and sodium hydroxide were purchased from Sigma Aldrich (Taufkirchen, Germany) and mixed after dissolving in ethanol. Sodium stearate was isolated by evaporation of ethanol using a rotary evaporator.

3.2.4 Preparation of the samples

The polypropylenes were used as received or blended with sodium stearate by twin screw extruder. The mixtures are prepared in the form of sticks by injection into a stick form mold.

3.3 Characterization methods

Fibers were characterized by scanning electron microscopy with a (SEM) Hitachi S-3000 N (Hitachi High-Technologies Europe GmbH, Krefeld, Germany). Therefore, the aluminum foil with the electrospun fibers was fixed onto an aluminum SEM stub and afterwards gold-coated and analyzed. An electron beam of 15 kV and working distance of 7-15 mm were used to image the electrospun material. The presented fiber diameters were measured using SEM (average numbers of 200 independent measurements). Representative images of the electrospun fibers are presented.

For thermal analysis, dynamic scanning calorimetry (DSC) measurements of produced fibers were performed by Perkin Elmer DSC. A sample of 7-10 mg were closed in an aluminum pan and measured at heating and cooling rates of 10°C/min from 50°C to 250°C and from 250°C to 50°C.

3.4 Results and discussion

3.4.1 Influence of nucleating agent

PP 190000 was mixed with 1 wt.-% HPN-68 L and electrospun with applied electric field strength of 3.13 kV/cm. SEM images in Figure 5-3 show that by addition of nucleating agents, a strong increase of fiber diameter occurred from $10.71 \pm 10.65 \mu\text{m}$ to $16.22 \pm 5.47 \mu\text{m}$. This is due to crystallization that accelerates the cooling of polypropylene melt. This results in an increase of the viscosity of the polymer jet which reduces the whipping and stretching deformation of fibers by electrical forces. Figure 5-4 shows that the crystallization

temperature increased from 100°C to 113°C by addition of 1 wt.-% HPN-68 L. The reduction of crystallization enthalpy is assumed to be a result of high concentration of HPN-68 L in the polypropylene matrix.

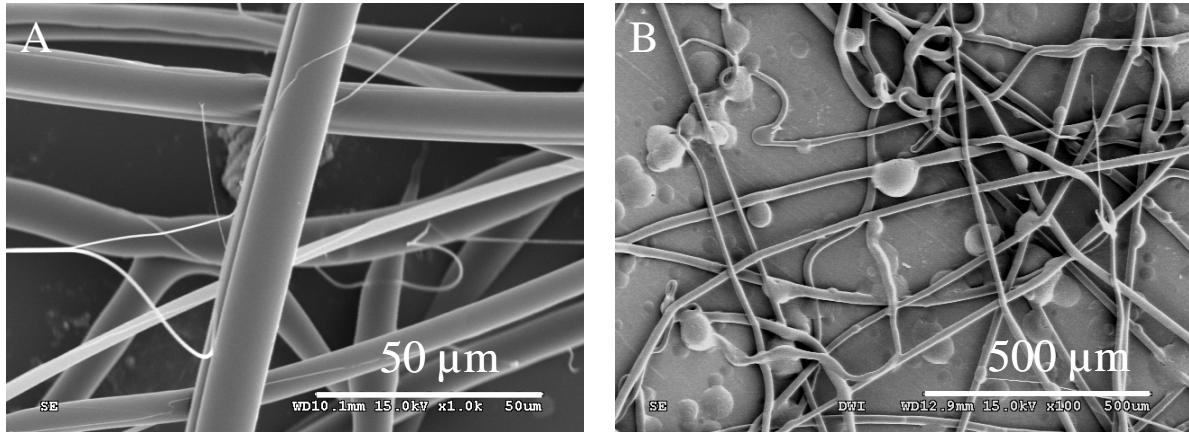


Figure 5-3: SEM graphs show polypropylene fibers containing HPN-68 L as nucleating agent and electrospun at electric field strength of 3.13 kV/cm at the distance between electrodes of 8 cm and the applied voltage of 25 kV. A: PP 190000, B: PP 190000 + 1 wt.-% HPN-68 L.

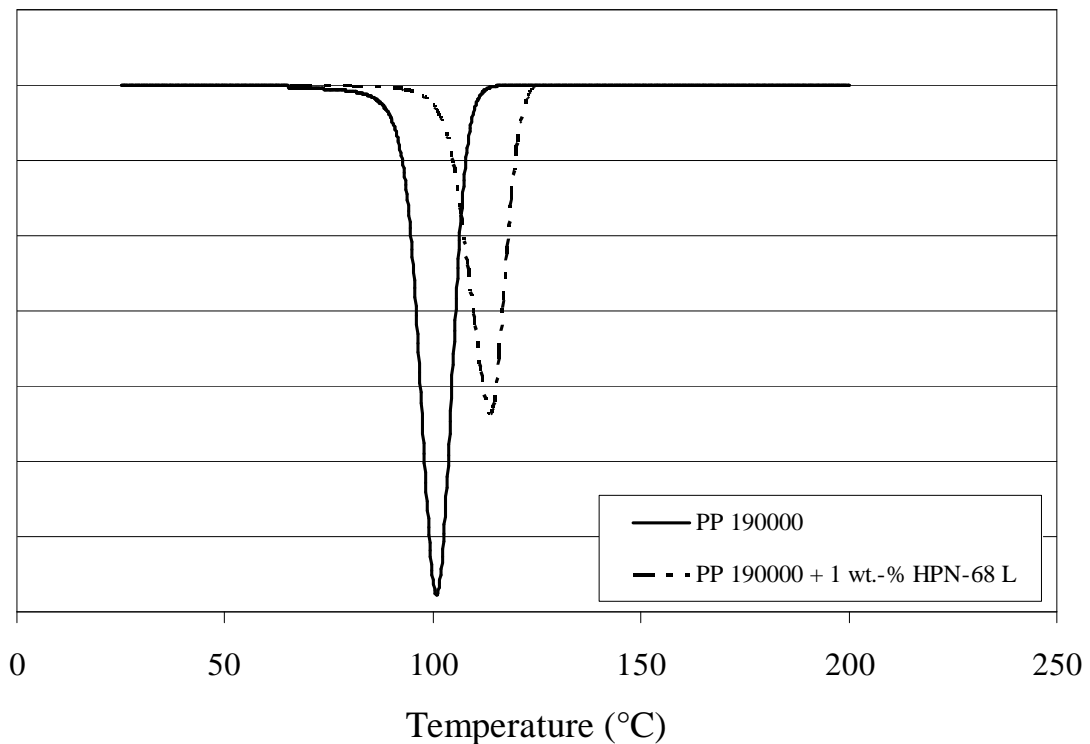


Figure 5-4: DSC cooling curves show the differences in crystallization points for PP 190000 containing HPN-68L (crystallization temperature: 113°C) and that one without HPN-68 L (crystallization temperature: 100°C). The cooling rate was 40°C/min.

Addition of sodium stearate causes a significant reduction of fiber diameter; however, this reduction in fiber diameter is combined with reduction of melt enthalpy represented by the area below the endothermic heating DSC curve, seen in Figure 5-5. The reduction of melt enthalpy is due to interference with stearates molecules. At high concentrations, sodium stearate is distributed in between polymer chains and reduces the packing of these chains close to each other and as a result, the formation of crystals is disturbed. Figure 5-5 shows that the melt enthalpy is reduced around 20% (from 115.61 J/g to 93.18 J/g) by addition of 5 wt.-% sodium stearate.

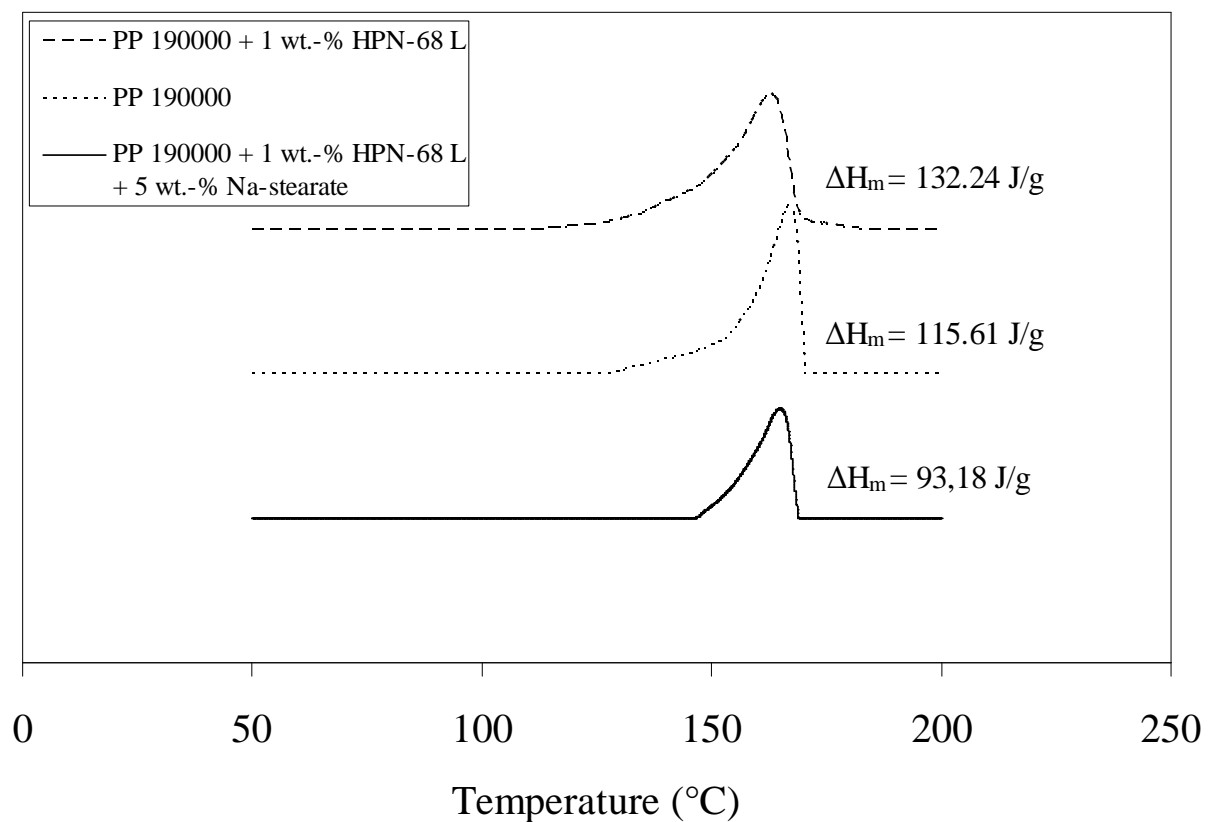


Figure 5-5: DSC curves show the difference in peak area in the heating cycle in polypropylene mixture containing HPN-68 L in the presence and absence of sodium stearate. The heating rate was 10°C/min.

The reduction of crystallinity of PP is essential for generating nano-scaled fibers. This can be seen in Figure 5-6. When the nucleating agent is added to the melt, the fiber diameter increased significantly to $16.22 \pm 5.47 \mu\text{m}$ from 10.71 ± 10.65 without HPN-68 L. Therefore, in order to generate ultra-fine fibers, polypropylene free of nucleating agents has to be chosen. The presence of traces of nucleating agents causes fast cooling of polymer jet and retards stretching of polymer jet to form fine fibers by electrical forces. Generation of polypropylene

nanofibers containing nucleating agent was possible at higher electric field strength 3.75 kV/cm in the presence of 5 wt.-% sodium stearate, Figure 5-7. The SEM graph in Figure 5-7 shows that the fiber diameter for polypropylene nanofibers is in the range $0.74 \pm 0.39 \mu\text{m}$.

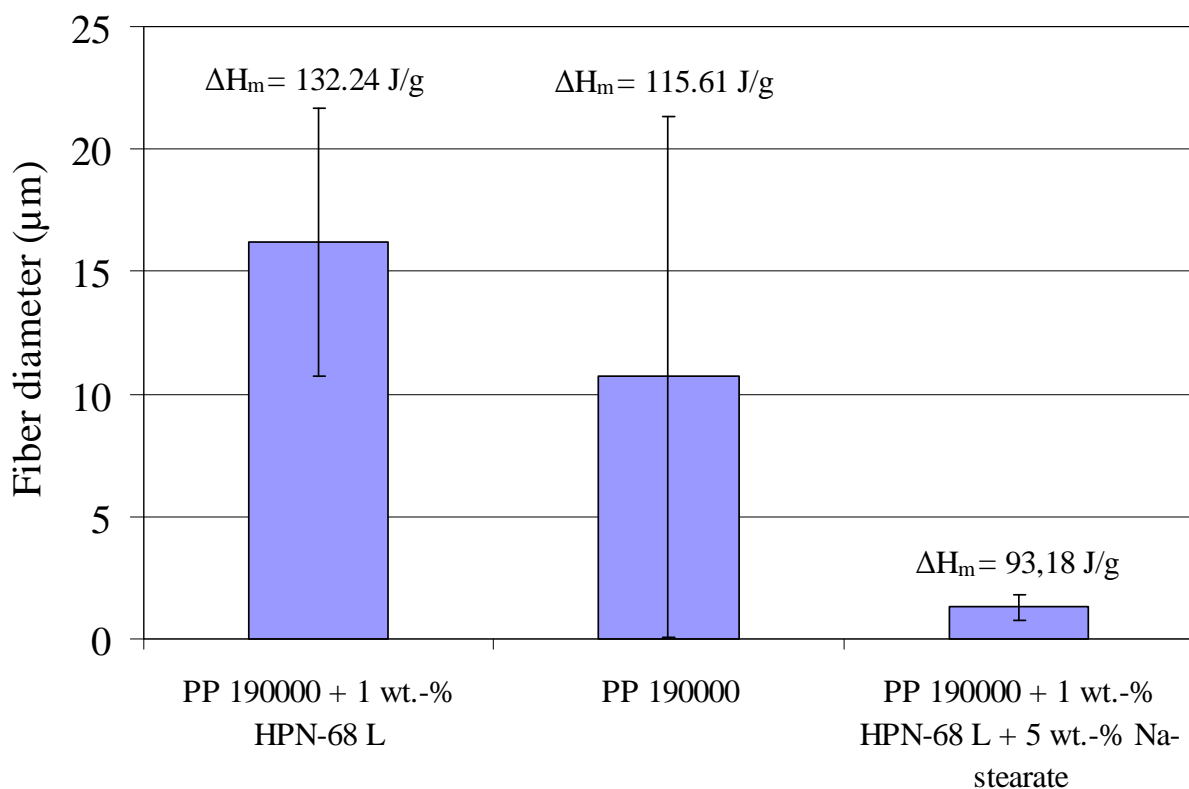


Figure 5-6: Histogram shows that the reductions of fiber diameter as a result of reduction of melt enthalpy by addition of sodium stearate.

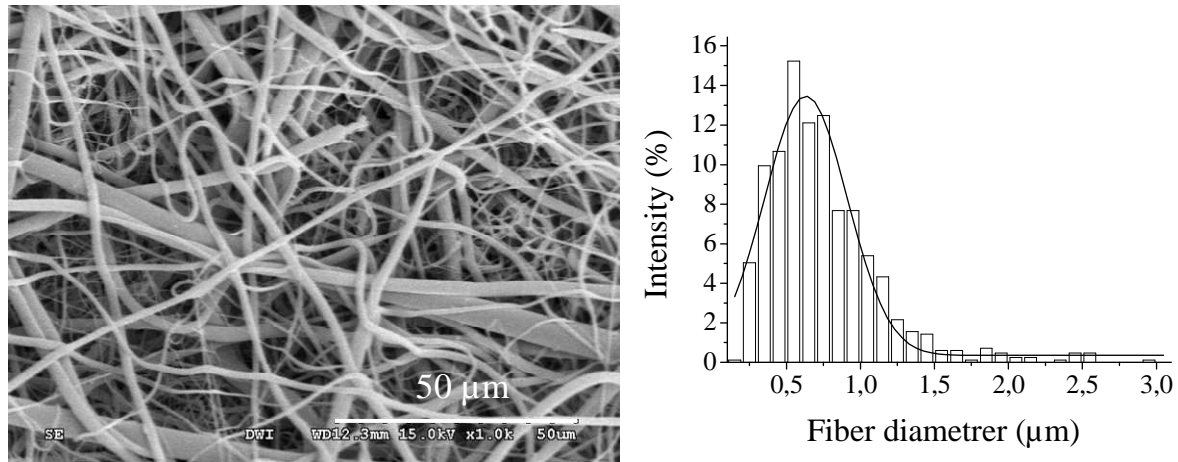


Figure 5-7: Left: SEM graph show the polypropylene nanofibers containing HPN-68 L and 5 wt.-% sodium stearate produced at electric field strength of 3.75 kV/cm at the distance between electrodes of 8 cm and the applied voltage of 30 kV/cm. Right: fiber diameter distribution shows that the produced fiber diameters are in the range $0.74 \pm 0.39 \mu\text{m}$.

3.4.2 Influence of nucleating agents concentration

PP 190000 was mixed with three different concentrations of HPN-68 L (0.1, 0.2 and 0.3 wt.-%) and 5 wt.-% sodium stearate. The produced mixtures were electrospun at applied electric field strength of 3.25 kV/cm and a distance of 8 cm between both electrodes. Afterwards, the electrospun fibers were thermally characterized by DSC to study the degree of crystallization.

It was observed that by increasing the concentration of HPN-68 L, the melt enthalpy was increased consequently due to increase number of crystals in the polypropylene bulk as shown in Figure 5-8. The melting temperature was slightly shifted to higher values by increasing the amount of HPN-68 L from 162.3 to 165.8°C. This is due to the higher energy consumption needed to breakdown the newly formed crystals.

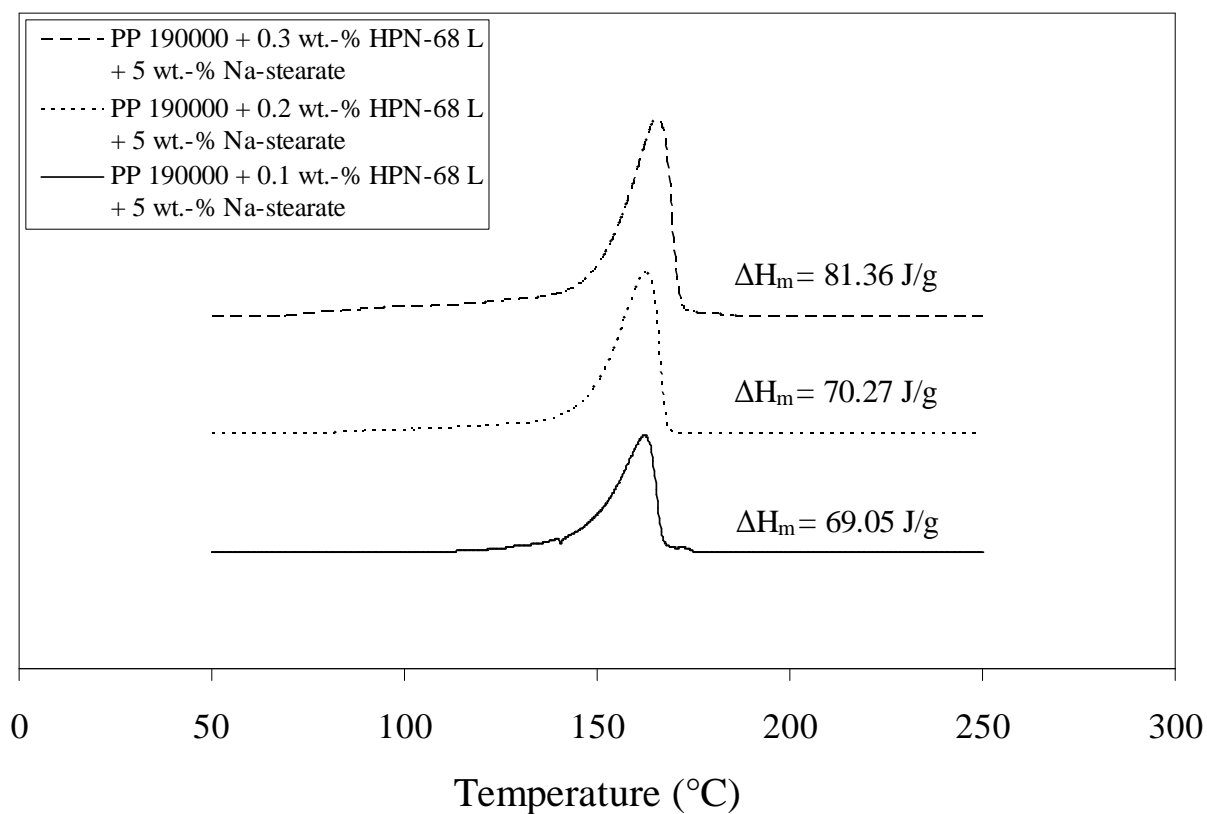


Figure 5-8: DSC endothermic heating curve for polypropylene/sodium stearate electrospun fibers containing different concentrations of HPN-68 L. The heating rate was 10°C/min.

During the cooling cycle, crystallization temperature was shifted to higher values with an increasing concentration of HPN-68 L, shown in Figure 5-9. The crystallization enthalpy was observed to be increased at high concentration of HPN-68 L, due to formation of more crystals. The crystallization temperature was increased from 118.1 to 120.4°C.

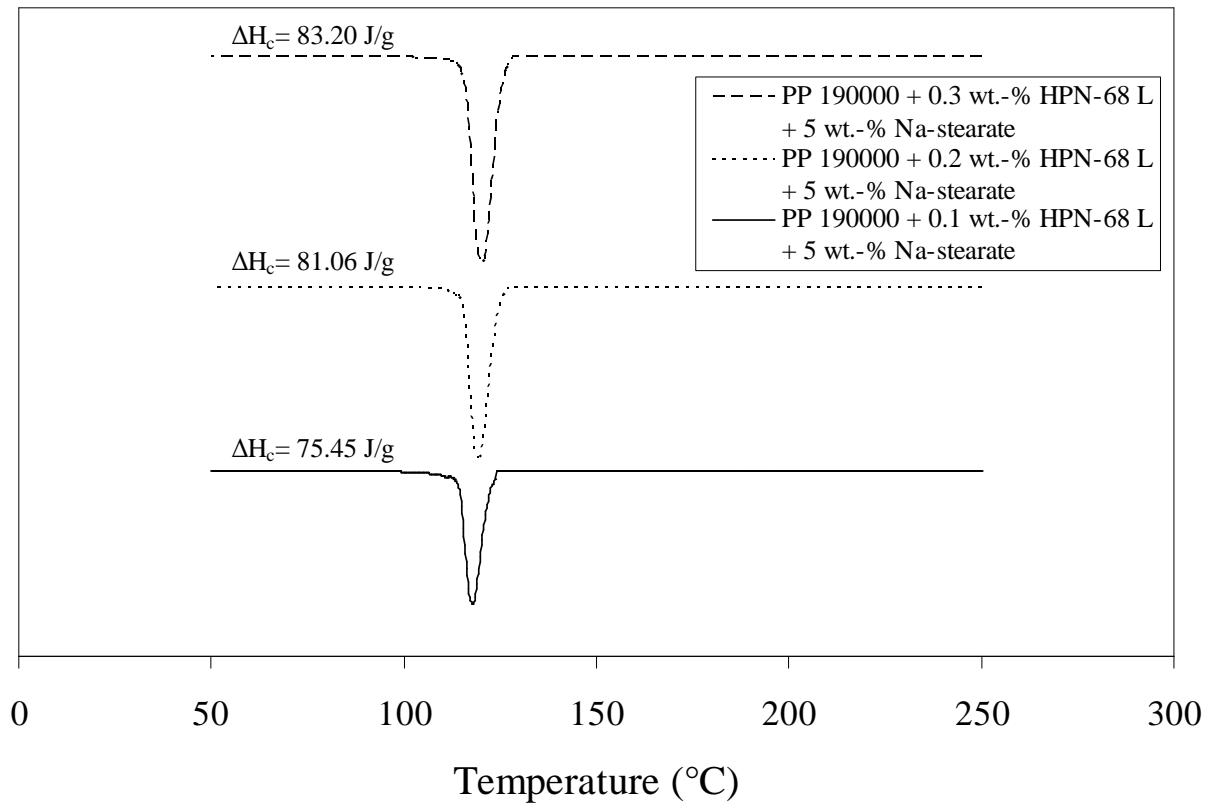


Figure 5-9: DSC exothermic cooling curves for polypropylene/sodium stearate electrospun fibers containing different concentrations of HPN-68 L. The cooling rate was 10°C/min.

SEM graphs of electrospun fibers containing HPN-68 L, Figure 5-10, show that the fiber diameter is reduced with increasing the concentration of HPN-68 L from 6.11 ± 3.21 μm for 0.1 wt.-% HPN-68 L to 1.58 ± 1.39 μm for 0.3 wt.-% HPN-68 L. This might be attributed to the smaller molecular weight and the higher mobility of shorter chains. Therefore, resulting in a more pronounced deformation at high electric field strength and leading to the formation of thin fibers with large degree of crystallization.

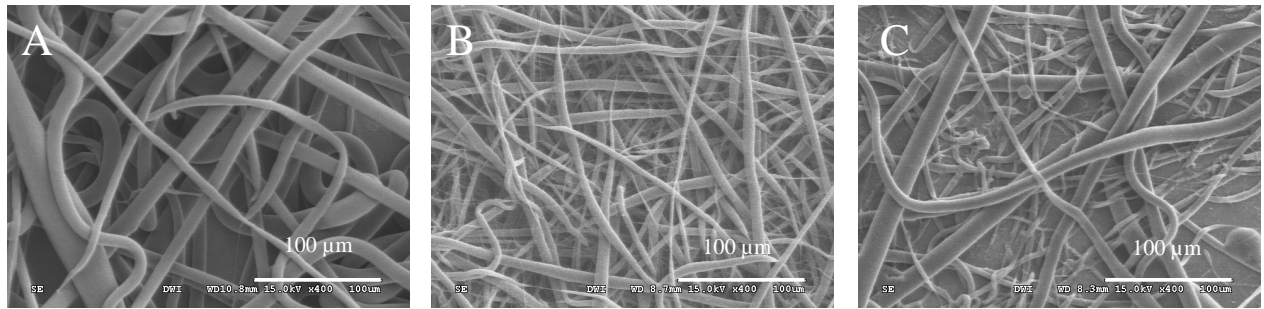


Figure 5-10: SEM graphs for polypropylene containing different concentrations of HPN-68 L electrospun at an electric field strength 3.75 kV/cm at the distance between electrodes of 8 cm and the applied voltage of 30 kV. A: PP 190000 + 0.1 wt.-% HPN-68 L (fiber diameter: $6.11 \pm 3.21 \mu\text{m}$), B: PP 190000 + 0.2 wt.-% HPN-68 L (fiber diameter: $3.81 \pm 2.23 \mu\text{m}$) and C: PP 190000 + 0.3 wt.-% HPN-68 L (fiber diameter: $1.85 \pm 1.39 \mu\text{m}$).

3.4.3 Influence of nucleating agent type

Polypropylene HL 504 FB containing 4 wt.-% sodium stearate was mixed with 0.2 wt.-% of Irgaclear DM, 0.2 wt.-% Irgastab NA 11 and 0.2 wt.-% HPN-68 L respectively. Polypropylene mixtures were electrospun at electric field strength of 3.75 kV/cm.

Thermal analysis of these mixtures showed that Irgaclear DM had higher melt enthalpy than HPN-68 L and Irgastab NA 11 respectively, Figure 5-11. This could be a result of chemical structure of sorbitol based nucleating agent that facilitates the formation of crystal structure.

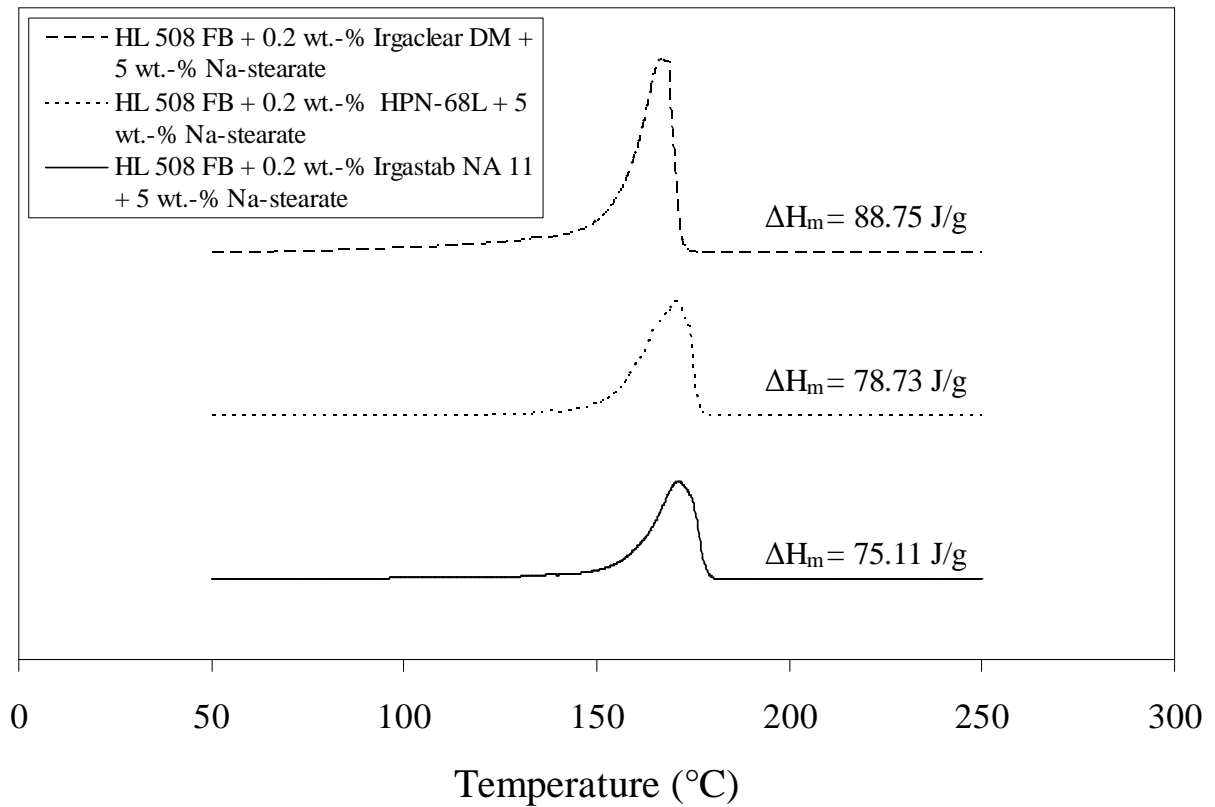


Figure 5-11: DSC endothermic heating curve for polypropylene/sodium stearate electrospun fibers containing different types of nucleating agents. The heating rate was 10°C/min.

The exothermic cooling curves are shown in Figure 5-12 indicating that the crystallization temperature was reduced from Irgastab NA 11 (128°C) to HPN-68 L (125.7°C) and finally to Irgaclear DM (120.5°C). This consequently showed an effect on the diameter of the produced fiber. In Figure 5-13, SEM graphs demonstrate that the fiber diameter of polypropylene containing Irgaclear DM was smaller than those fibers containing Irgastab NA 11 or HPN-68 L. Most probably, the low crystallization temperature of polypropylene containing Irgaclear DM resulted in further stretching of polymer jet by electrical forces.

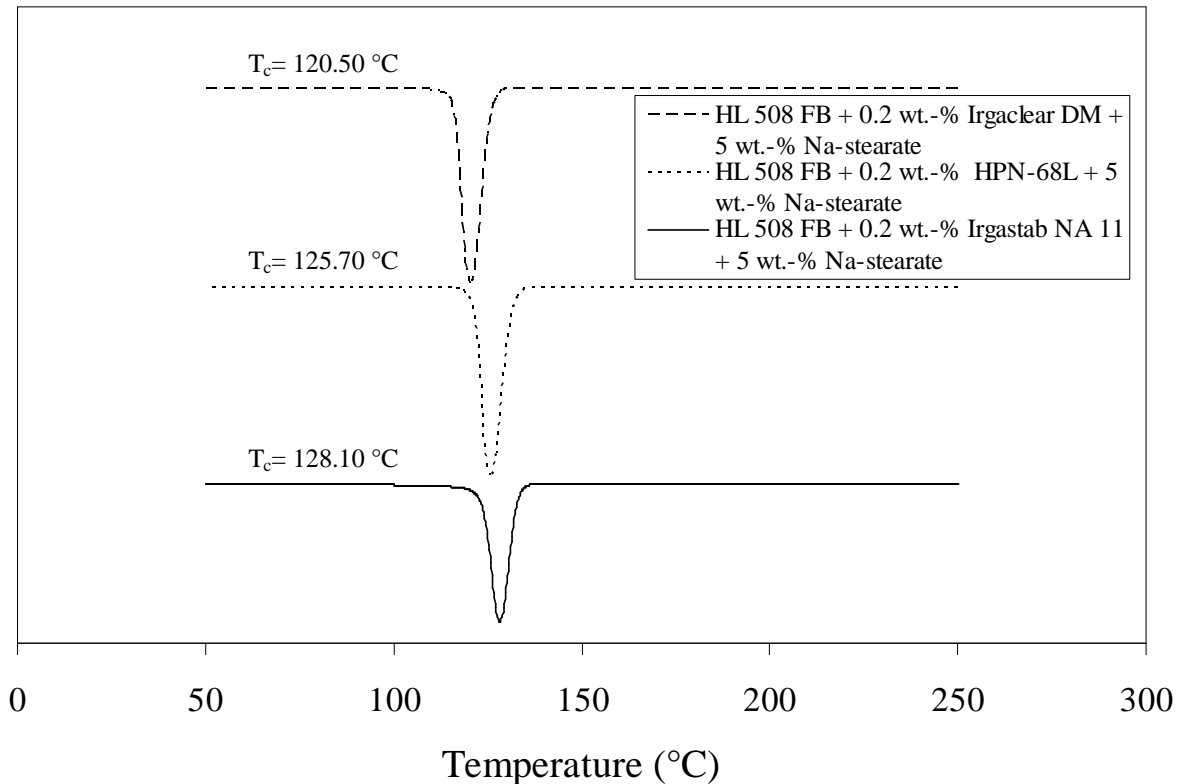


Figure 5-12: DSC exothermic cooling curves for polypropylene/sodium stearate electrospun fibers containing different types of nucleating agents. The cooling rate was $10\text{ }^\circ\text{C}/\text{min}$.



Figure 5-13: SEM graphs for polypropylene electrospun fibers containing different types of nucleating agents electrospun at electric field strength of $3.75\text{ kV}/\text{cm}$ at the applied voltage of 30 kV and the distance between electrodes was 8 cm . **A:** HL 504 FB + 0.2 wt.-% Irgastab NA 11 (Fiber diameter: $2.98 \pm 1.54\text{ }\mu\text{m}$), **B:** HL 504 FB + 0.2 wt.-% HPN-68L (Fiber diameter: $0.98 \pm 0.51\text{ }\mu\text{m}$) and **C:** HL 504 FB + 0.2 wt.-% Irgaclear DM (Fiber diameter: $1.52 \pm 0.70\text{ }\mu\text{m}$).

4 Summary

Stability of polypropylene melts and nanofibers is a crucial issue during melt electrospinning of nanofibers as it can change their mechanical properties of the final product such as fiber strength. Stability of the fibers can be achieved by addition of nucleating agents, which minimize the oxidative degradation, or by addition of thermostabilizer.

During melt electrospinning of polypropylene a slipping agent as sodium stearate was used to reduce the melt viscosity for fiber formation by electrical forces. However, sodium stearate in high concentrations also reduces the crystalline fraction due to the interference of the small molecules with the polymer chains. This limits the polymer chain packing and subsequent the formation of crystals. Therefore, nucleating agents are required as an additional component in order to increase the crystalline fraction again.

Use of nucleating agents has an influence on the diameter of the generated electrospun fibers, as faster cooling of the polymer jet is induced. This faster cooling retards the stretching of the polymer jet by electrical forces. However, small fiber diameters can be generated again at higher applied electric field strengths. It was shown that increasing amounts of HPN-68 L resulted in generation of small fibers at higher electric field strength. This might be attributed to the high electric field strength acting on the polymer jet, which compensates the effect of nucleating agents. As a consequence small fiber diameters close to 2 μm with larger crystalline fraction have been generated. For that, it is essential to reduce the crystallization in order to generate nanofibers. It was also found that blends of polypropylene containing sorbitol based nucleating agents as Irgaclear DM generated thin fibers by melt electrospinning with high crystalline fraction.

5 References

1. Hiltz, A. A.; Beck, D. L. Oxidative Degradation of Unstabilized Polypropylene. *Text Res J* **1965**, *35*, 716-724.
2. Zweifel, H. *Plastics Additives Handbook*; Hanser Publishers, Munich and Hanser Gardner Publications, Inc., Cincinnati, Munich, **2004**, 725-811.
3. Schmenk, B.; Meyer, R. M.; Steffens, M.; Wulfhorst, B.; Gleixner, G. Polypropylene Fiber Table. *Chem Fibers Int* **2000**, *50*, 233-253.
4. Ezrin, M. *Plastics Failure Guide: Cause and Prevention*; Hanser/Grandner Publication Inc, Cincinnati, **1996**, 473.
5. Moore, E. P. *Polypropylene Handbook*; Hanser/Gardner Publications, Inc. / Hanser Publishers, Munich, New York, Cincinnati, **1996**, 420.
6. Zlatkevich, L. *Polymer Degradation and Stability Research Developments*; Nova Science Publishers Inc., New York, **2007**, 315.
7. Lyons, J.; Li, C.; Ko, F. Melt-Electrospinning Part I: Processing Parameters and Geometric Properties. *Polymer* **2004**, *45*, 7597-7603.
8. Brandao, J.; Spieth, E.; Lekakou, C. Extrusion of Polypropylene. Part I: Melt Rheology. *Polym Eng Sci* **1996**, *36*, 49-55.
9. Psarreas, A. Nitroxide-Mediated Controlled Degradation of Polypropylene. Master Thesis, University of Waterloo, Waterloo, **2006**.
10. Psarreas, A.; Tzoganakis, C.; McManus, N.; Penlidis, A. Nitroxide-Mediated Controlled Degradation of Polypropylene. *Polym Eng Sci* **2007**, *47*, 2118-2123.
11. Coutinho, F.; Rocha, M.; Balke, S. Polypropylene (Controlled Degradation). In *The Polymeric Materials Encyclopedia*, CRC Press, Inc., Boca Raton, **1996**, 1-9.
12. Geankoplis, C. J. *Transport Processes and Separation Process Principles (Includes Unit Operations)*; Addison Wesley Pub Co Inc, Englewood Cliffs, **2003**, 1056.
13. Behrendt, N.; Mohmeyer, N.; Hillenbrand, J.; Klaiber, M.; Zhang, X.; Sessler, G.; Schmidt, H.-W.; Altstädt, V. Charge Storage Behavior of Isotropic and Biaxially-Oriented Polypropylene Films Containing Alpha- and Beta-Nucleating Agents. *J Appl Polym Sci* **2006**, *99*, 650-658.
14. Mohmeyer, N.; Mueller, B.; Behrendt, N.; Hillenbrand, J.; Klaiber, M.; Zhang, X.; Smith, P.; Altstaedt, V.; Sessler, G.; Schmidt, H.-W. Nucleation of Isotactic Polypropylene by Triphenylamine-Based Trisamide Derivatives and Their Influence on Charge-Storage Properties. *Polymer* **2004**, *45*, 6655-6663.
15. Halstead, A.; Jones, J. A New Look at Nucleating Agents for Use in Polypropylene Color Concentrates. http://www.packagingdigest.com/file/5421-More_consistent_par-

- [t dimensions and less warpage from pigments in polypropylene through the use of nucleating agents.pdf?force=true](#) (accessed 13.03.2012).
16. Hassounah, I.; Thomas, H.; Moeller, M. Obtaining Poly(Propylene) Nanofibers by Melt Electrospinning through Additives, Second Aachen-Dresden International Textile Conference, Dresden, Germany, 26-27.11.2008.
 17. Voigt, W. V. Water Stable, Antimicrobial Active Nanofibres Generated by Electrospinning from Aqueous Spinning Solutions. PhD. Thesis, RWTH Aachen, Aachen, **2009**.

Appendix

Work package with electrospinning machine

Appendix: Work package with electrospinning machine

1 Introduction

Altering the setup of the electrospinning device has a crucial influence on the properties of the generated fibers (e.g. fiber diameter, diameter distribution, morphology, porosity of the nonwoven, and fiber orientation). Minor changes in the design can alter the electric field, heat gradient or the area of collection on the target. For instance, changing the polarity of electrodes changes the minimal electric field strength required to stretch the polymer jet and initiate the spinning process.

In this appendix, a lab scaled electrospinning machine has been developed by the Institute for textile engineering at RWTH-Aachen, ITA (Figure 1), constructed and tested.



Figure 1: Electrospinning machine designed by ITA (Source: ITA, RWTH-Aachen, Dipl. Ing. Christoph Hacker, Dipl. Ing. Philip Jungbecker and Prof. Dr. Ing. Thomas Gries)

The electrospinning device consists of two heating elements, one controls the temperature of the syringe and a second controls the temperature of the needle. The difference in temperatures between reservoir/syringe and the nozzle/needle creates a temperature gradient in the melt and subsequently a viscosity gradient. Additionally, both heating elements keep the polymer melt in molten phase without significant degradation. This special set-up showed benefits for polymer mixtures containing viscosity breaking agents. The temperature of the syringe/reservoir can be kept underneath the degradation temperature of the polymer. Therefore, the time of exposure to critical temperatures has been minimized. On the other hand, the needle temperature can be regulated to the electrospinning temperature or the activation temperature of the viscosity breaking agent. This special design allows preventing breaking up of the polymer jet during the fast electrospinning process.

The main differences between the new built melt electrospinning machine and the heat chamber electrospinning system used in the previous chapters are:

1. The target is charged and the needle is grounded,
2. Electrical heating elements were used in order to guarantee a controlled and homogeneous heat distribution within the melt, and
3. The electric field strength is not disturbed by the presence of other constructive elements which can interfere.

With the aim to evaluate the suitability of the new design for nanofibers production, process parameters such as electric field strength, flow rate and distance between electrodes in both production systems (new electrospinning machine and the heat chamber electrospinning system) were studied, compared and discussed.

2 Experimental

2.1 Electrospinning

The new melt electrospinning device in lab scale, consists of a high voltage supply (Eltex KNH34, Eltex Elektrostatic GmbH, Weil am Rhein, Germany), a flat conductive target, a syringe pump (type HA 11 plus Harvard Apparatus, Hugo-Sachs Elektronik GmbH, March-Hugstetten, Germany), an electric hot coil heating element to control the temperature of the syringe, and an electrically controlled heating plate to heat the needle (designed by ITA and manufactured by DWI workshop). The collection distance was varied between 65 and 80 mm. The flow rate was varied between 0.1 and 1 mL/h, and the electric field strength was varied between 3.75 and 7 kV/cm.

Polymer sticks were filled into 2 mL glass syringes, and melted by the use of an electronically controlled heat gun (Leister, purchased from Klappenbach GmbH, Hagen, Germany) at 220°C in a heating chamber (manufactured by DWI workshop) as shown in Figure 2.

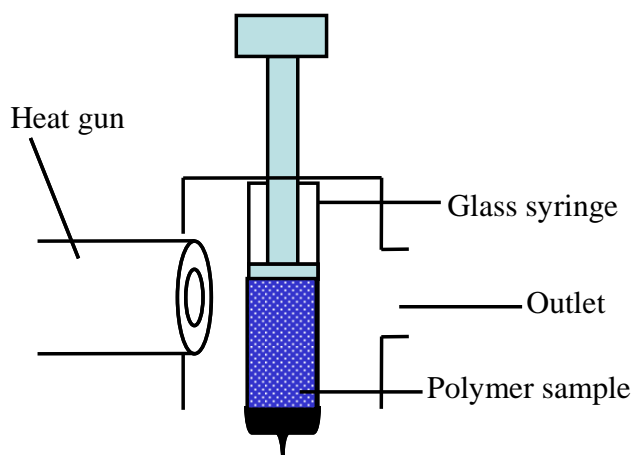


Figure 2: Schematic illustration of the heating chamber used for preparation of polymer samples for melt electrospinning.

The syringes containing polymer samples were cooled down and later transferred to the new electrospinning machine. The temperature of the hot coil was fixed at 260°C and the temperature at the needle was regulated to 290°C (a suitable temperature to maintain a steady jet). A positive voltage was applied to the target while the spinneret remained on ground potential. Fibers were collected on the charged target, which was covered with an aluminum foil.

A detailed description of the electrospinning device with heat chamber and hot air is described in the previous chapters.

2.2 Materials and preparation of the sample

Polypropylene with a molecular weight 190000 g/mol (PP 190000) (Sigma-Aldrich, Taufkirchen, Germany) containing 4 wt.-% sodium stearate was chosen as standard material for performing the electrospinning experiments. Using this material, small nanofibers were obtained with the heat chamber electrospinning set-up. Sodium stearate was synthesized by esterification, using ethanol as a solvent. Stearic acid and sodium hydroxide were purchased from Sigma Aldrich (Taufkirchen, Germany), dissolved in ethanol and mixed. Sodium stearate was isolated by evaporation of the ethanol using a rotary evaporator. Polypropylene was blended with sodium stearate using a twin screw extruder. The mixtures were prepared in the form of sticks by injection into corresponding molds.

2.3 Characterization methods

Fibers were characterized by scanning electron microscopy Hitachi S-3000 N (Hitachi High-Technologies Europe GmbH, Krefeld, Germany). Therefore, aluminum foil with the electrospun material was fixed onto an aluminum SEM stub. Afterwards, the sample was gold-coated and analyzed by SEM. An electron beam of 15 kV and a working distance of 7-15 mm were used to image the electrospun material. The presented fiber diameters were measured using SEM (average numbers of 200 independent measurements).

3 Results and discussion

3.1 Effect of electric field strength

The compounded polypropylene was electrospun with electric field strengths between 4 and 7.5 kV/cm, and an electrodes distance of 6.5 cm. The system requires high critical electric field strength to initiate the ejection of a polymer jet (compared to the heat chamber electrospinning system). The fast cooling of the melt, which is responsible for this effect, is attributed to the absence of a heating zone between both electrodes. Figure 3 shows the reduced fiber diameter. The diameter of the fibers was reduced from $21 \pm 5.11 \mu\text{m}$ to $9.17 \pm 3.40 \mu\text{m}$ by increasing the electric field strength. As the stretching forces increased, fiber diameter decreased. However, the heat chamber electrospinning set-up generated fibers at

larger distances between the two electrodes, lower electric field strengths and also required lower melt temperatures. The resulted fiber diameter generated by heat chamber electrospinning system is obviously lower than those produced by the electrospinning machine.

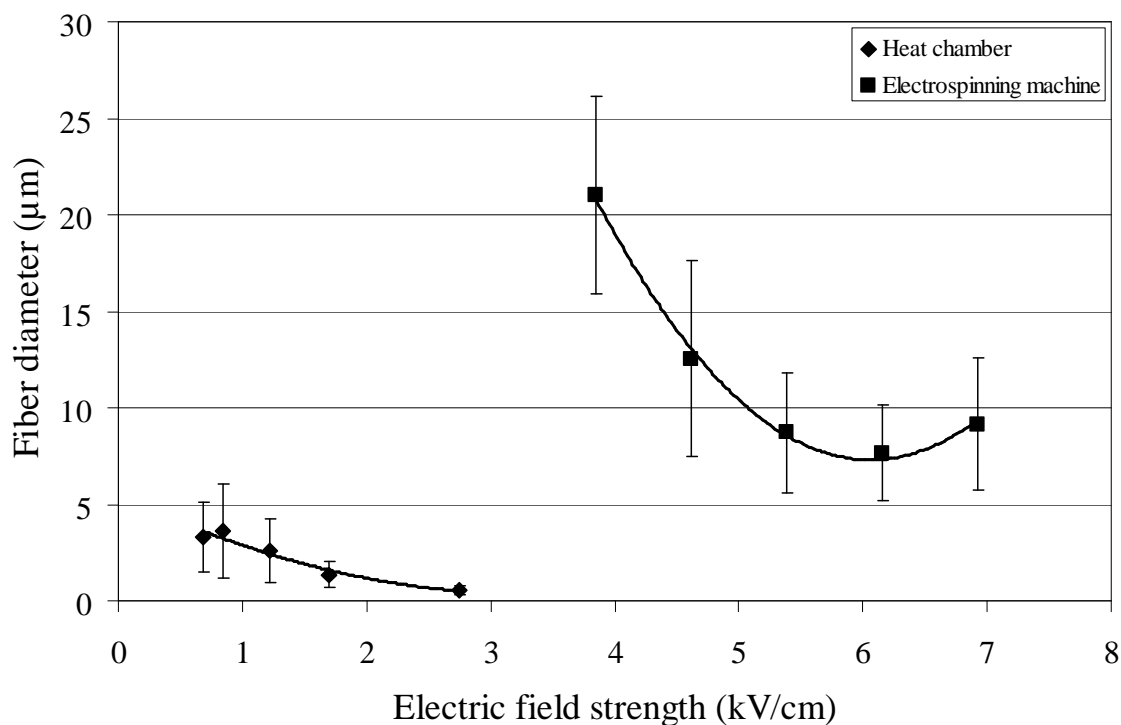


Figure 3: Graph shows the relation between electric field strength and fiber diameter of the fibers produced by the use of two different electrospinning systems.

3.2 Effect of flow rate

PP 190000 blended with 4 wt.-% sodium stearate was electrospun at 0.1, 0.3 and 1 mL/h, and a distance of 6.50 between both electrodes. However, the applied voltage was changed during the series of experiments. Figure 4 illustrates the increasing fiber diameters with flow rate. The increasing fiber diameter corresponds to more material which is drawn from the nozzle by the electrical forces.

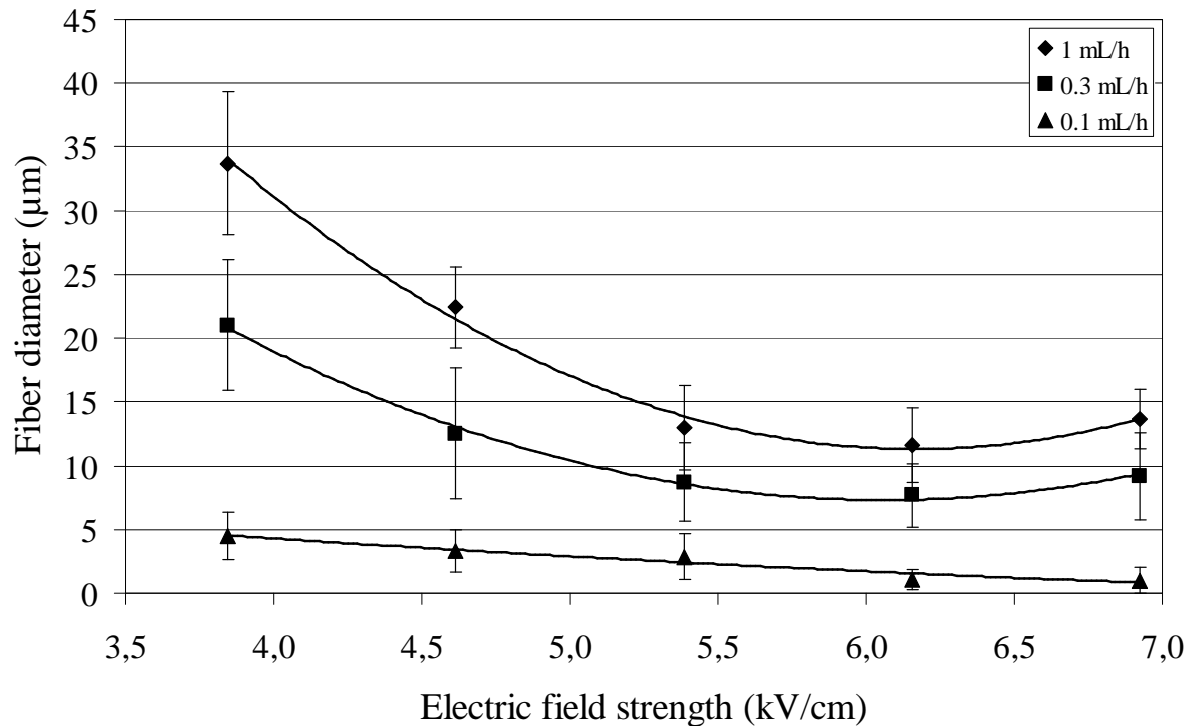


Figure 4: Graph shows the relation between electric field strength and fiber diameter for three different flow rates: 0.1, 0.3 and 1 mL/h by the use of the newly designed electrospinning machine.

Adjusting the flow rate resulted in fine fibers. The smallest fibers showed diameters in the range of $1 \pm 1.02 \mu\text{m}$ and 74 % of these were nanofibers. Figure 5 shows a SEM graph of polypropylene fibers produced and the diameter distribution at a flow rate of 0.1 ml/h and at electric field strength of 6 kV/cm.

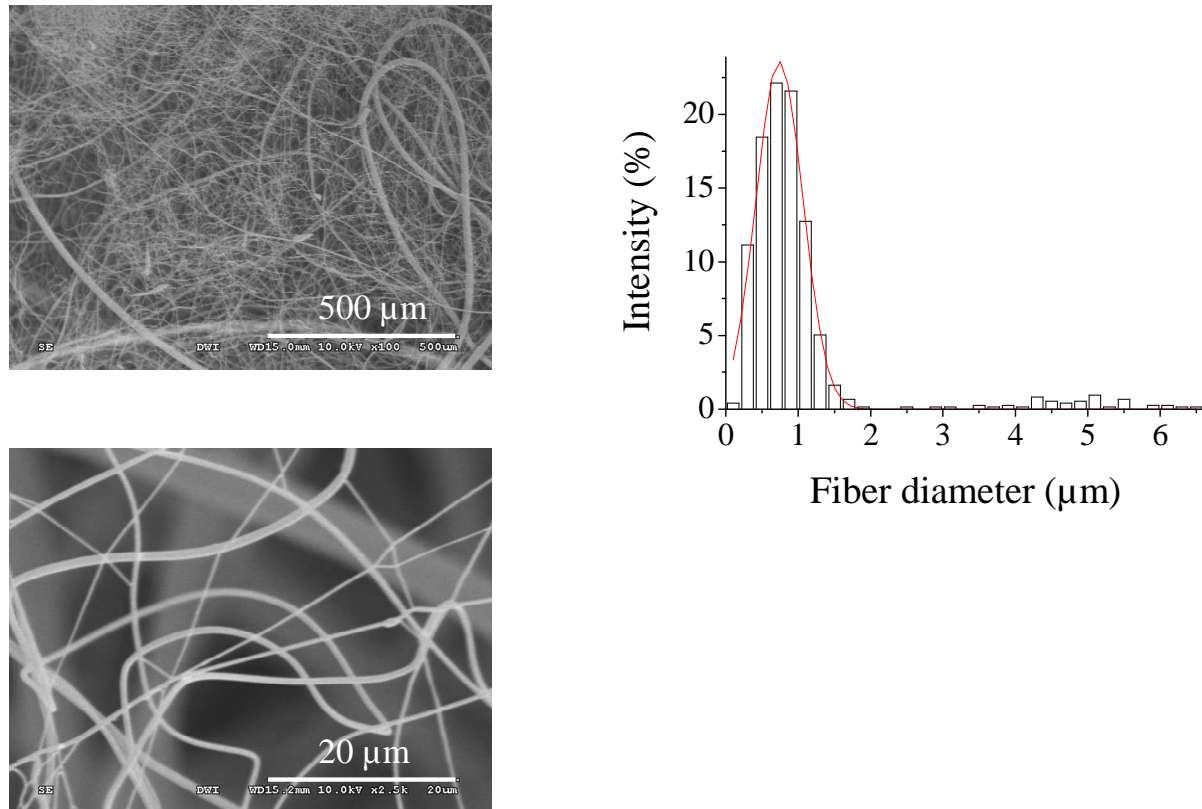


Figure 5: SEM graphs shows the electrospun polypropylene of molecular weight 190000 g/mol blended with 4 wt.-% sodium stearate electrospun at electric field strength 6 kV/cm by the use of electrospinning machine. The fiber diameter distribution shows that almost 74% of fibers lay in nanometer range. The average fiber diameter is $1 \pm 1.02 \mu\text{m}$.

Figure 6 A shows that, independently on the electrospinning systems, for certain electric field strengths the fiber diameter increases with the flow rate. Differences between fiber diameters generated at different electric field strength at low flow rate are smaller than those at high flow rates. This is caused by the ability of the polymer jet to form the cone-jet mode and its stability over certain time periods in the case of low flow rates. In the case of fast polymer flow, no steady-state jet is achieved. The droplet at the orifice changes constantly as the feed rate is faster than the ejection rate caused by electric forces. At a certain moment, when gravity assists the droplet to detach from the orifice, more material is ejected and the fiber diameter increases. Fast feeding of the polymer melt together with high electric field strength therefore results in the largest diameter variations. The similar relation between flow rate and fiber diameter at different electric field strength was observed with the heat chamber electrospinning system, Figure 6 B.

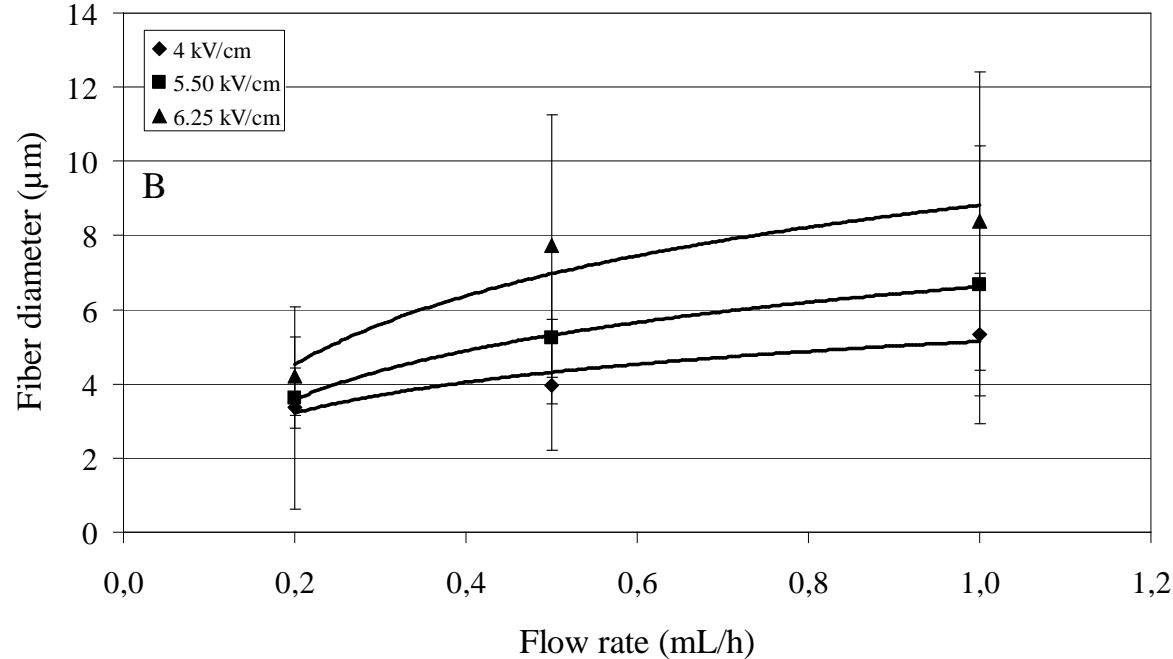
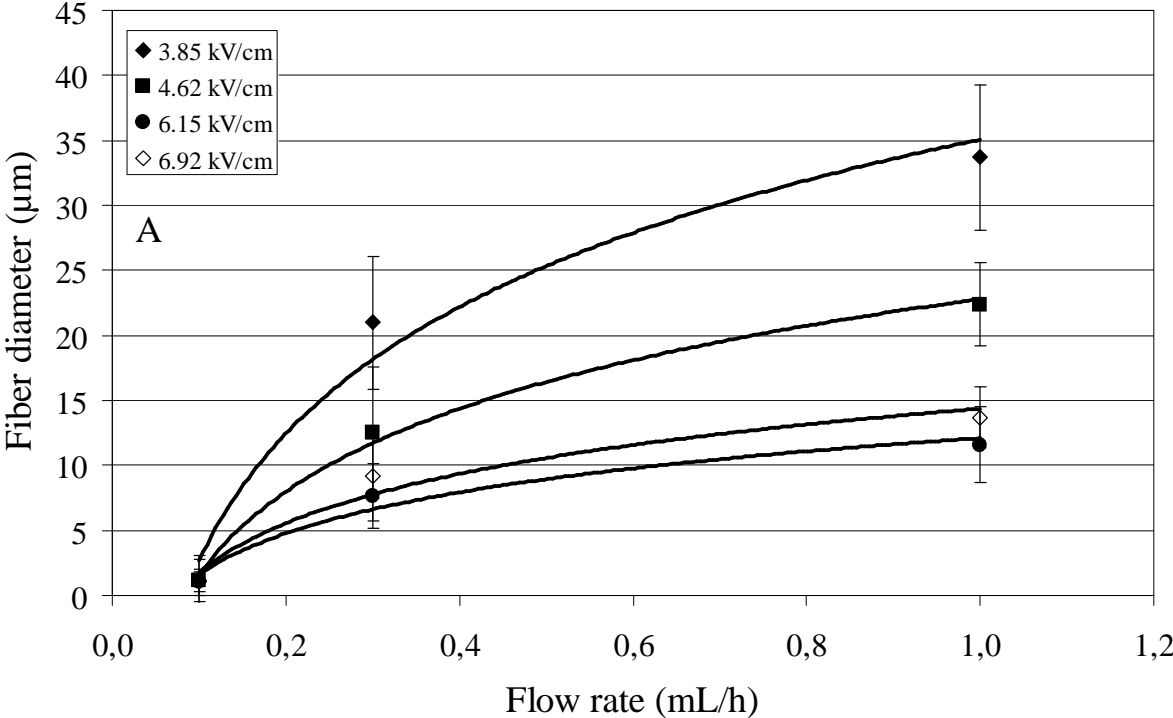


Figure 6: Graph shows the relation between flow rate and fiber diameter for PP 190000 containing 4 wt-% sodium stearate at different electric field strengths. A: Fibers generated by electrospinning machine, B: fibers generated by heating chamber.

3.3 Effect of distance between electrodes

In this part of research, polypropylene fibers containing 4 wt.-% sodium stearate were electrospun at a constant flow rate of 0.3 mL/h and at two different distances (6.5 and 8 cm) between both electrodes: Electrospinning at larger distances was not feasible as electrical forces were not capable of attracting the polymer jet. Distances below 6.5 cm resulted in discharge of electrodes due to the conductivity of air. Figure 7 shows the electric field strength versus fiber diameter for both distances between the electrodes.

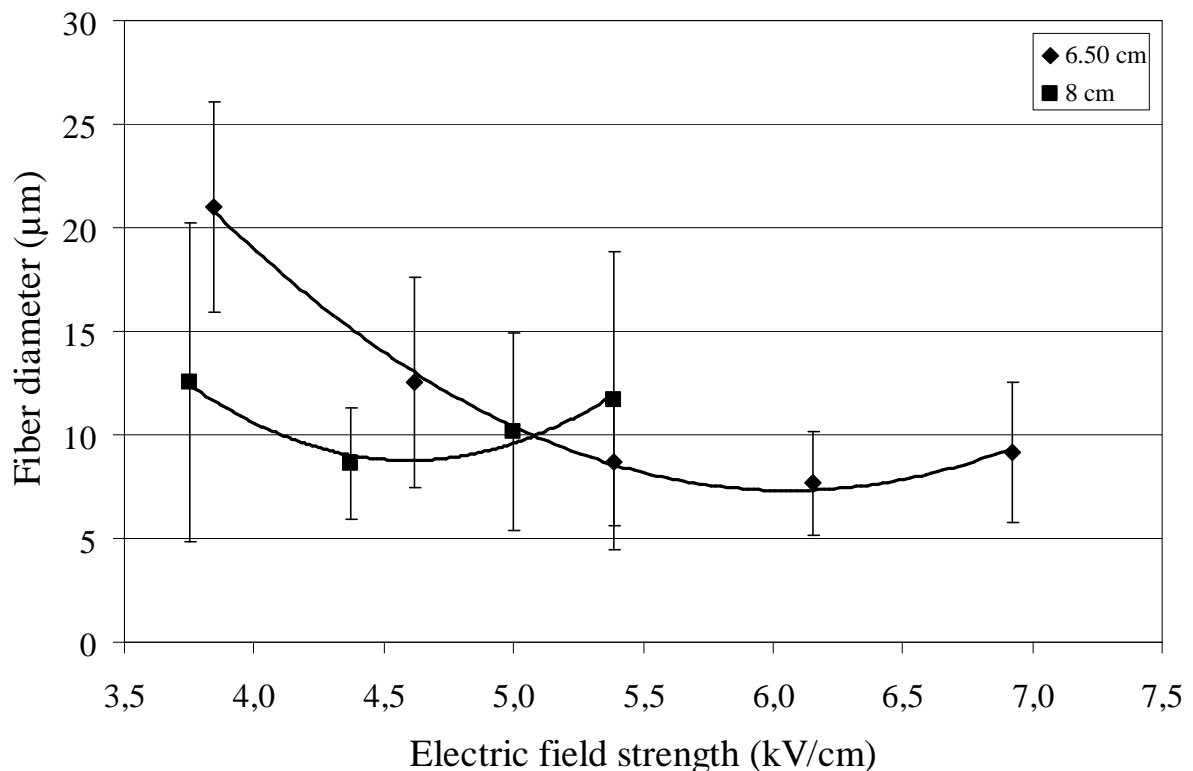


Figure 7: Graph shows the relation between the distance between electrodes and the produced fiber diameter of PP 190000 electrospun at a flow rate of 0.3 mL/h by the use of newly designed electrospinning machine.

With increasing distance between both electrodes the on-set of whipping instabilities was observed. However, due to the absence of a strong heat gradient the generated fiber diameters were thicker than those generated by the heat chamber set-up. Due to fast cooling of the polymer jet no further diameter reduction occurred by the action of the electrical forces. Figure 7 shows the fibers generated at 6.5 and 8 cm distance, no significant differences for the fiber diameters obtained at both distances were found. Using the heat chamber set-up allowed

Appendix: Work package with electrospinning machine: Effect of distance between 125 electrodes

us to electrospin pure PP 190000 at large distances between both electrodes (26 cm), a flow rate of 0.2 mL/h, and at an applied voltage of 25 kV. The relation between the generated fiber diameter and the distance between the electrodes is shown in Figure 8. The fiber diameters reduced with distance between the electrodes.

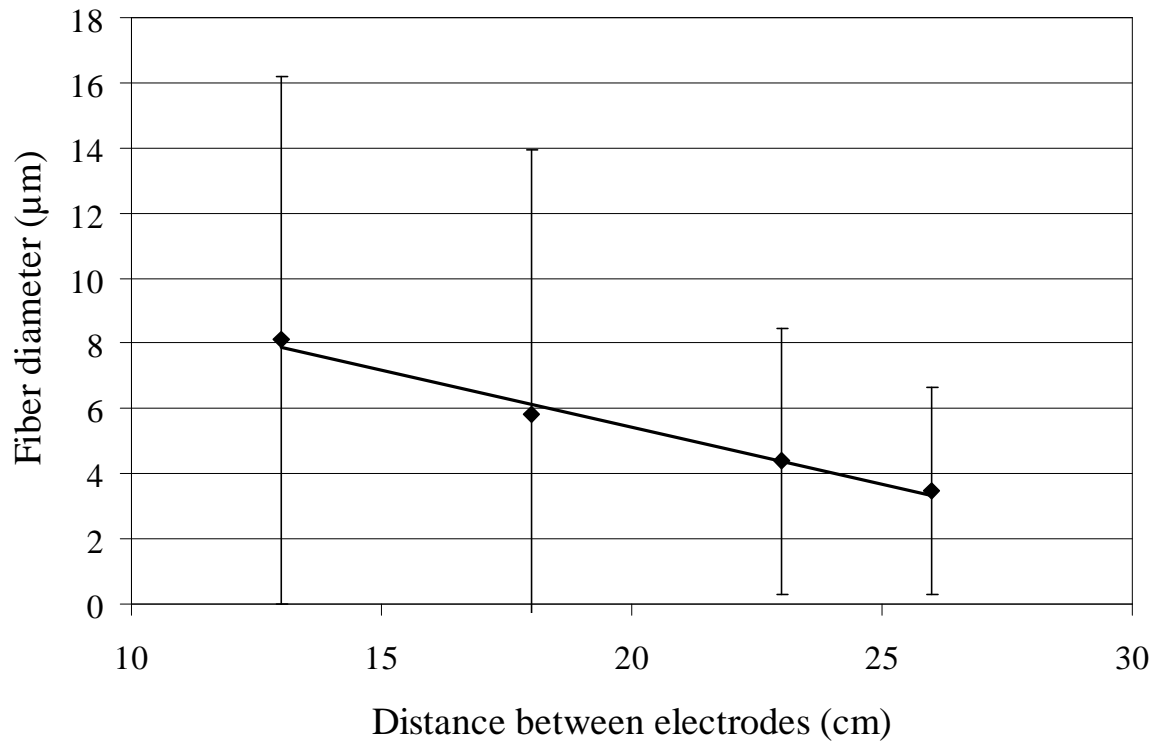


Figure 8: Curve shows the Relation between the distance between electrodes and the produced fiber diameter of PP 190000 electrospun by heat chamber electrospinning system with heat zone, the fibers were collected on the flat target and the applied voltage was 25 kV.

4 Summary

In this appendix, polypropylene containing sodium stearate was electrospun with a new electrospinning device. During electrospinning, relatively thick fibers were produced due to the absence of heat gradient between electrodes. This resulted in fast cooling and solidification and therefore limited stretching of the polymer jet.

Increasing the distance between electrodes did not result in any significant differences. Small fiber diameters were produced by optimizing the flow rate. The smallest fiber diameter obtained was in the range of $1 \pm 1.02 \mu\text{m}$. 74% nanofibers have been generated at a flow rate of 0.1 ml/h (lowest investigated flow rate) and electric field strength around 6 kV/cm. Discharges between both electrodes interrupted the electrospinning process. Therefore, such high voltages combined with the chosen distance were not suitable for a continuous process.

Due to the absence of the heat gradient between electrodes in the new design, higher electric field strength is required compared to a system with heating chamber. The fibers generated with the heat chamber electrospinning device were smaller in size and more homogeneous than fibers generated with the new electrospinning machine. These results again confirm the importance of existence the instabilities acting on the electrified jet for production of nanofibers by electrospinning.

Curriculum Vitae

Name Ibrahim Hassounah

Birth date 29 December 1980

Place of Birth Abu-Dhabi, U. A. E.

1986-1991 Rosary Primary School, Abu-Dhabi, U. A. E.

1992-1995 Zayed II Preparatory School, Abu-Dhabi, U. A. E.

1996-1998 Abu-Dhabi Secondary School, Abu-Dhabi, U. A. E.

1998-2002 Study of Chemistry and Microbiology at Ain-Shams University, Cairo, Egypt

2003-2006 Study of Master program 'Applied Polymer Science' at University of Halle-Wittenberg, Halle (Saale), Germany

2006-2010 Ph. D. work under the supervision of Prof. Dr. M. Möller: melt electrospinning of thermoplastic polymers at DWI at RWTH Aachen University, Aachen, Germany

2010-2012 Research Scientist at Elmarco s. r. o., Department of Technology, Liberec, Czech Republic

13.02.2012 Oral PhD examination (Tag der mündlichen Prüfung)